AD_____

GRANT NUMBER DAMD17-94-J-4319

TITLE: Analysis of Multistep Mammary Tumorigenesis in Wnt-1 Transgenic Mice

PRINCIPAL INVESTIGATOR: Deepa Shankar, M.D.

CONTRACTING ORGANIZATION: Children's Hospital of Los Angeles
Los Angeles, California 90027

REPORT DATE: September 1998

TYPE OF REPORT: Final

PREPARED FOR: Commander
U.S. Army Medical Research and Materiel Command
Fort Detrick, Frederick, Maryland 21702-5012

DISTRIBUTION STATEMENT: Approved for public release;
distribution unlimited

The views, opinions and/or findings contained in this report are those of the author(s) and should not be construed as an official Department of the Army position, policy or decision unless so designated by other documentation.

20010216 035

REPORT DOCUMENTATION PAGE

Form Approved
OMB No. 0704-0188

Public reporting burden for this collection of information is estimated to average 1 hour per response, including the time for reviewing instructions, searching existing data sources, gathering and maintaining the data needed, and completing and reviewing the collection of information. Send comments regarding this burden estimate or any other aspect of this collection of information, including suggestions for reducing this burden, to Washington Headquarters Services, Directorate for Information Operations and Reports, 1215 Jefferson Davis Highway, Suite 1204, Arlington, VA 22202-4302, and to the Office of Management and Budget, Paperwork Reduction Project (0704-0188), Washington, DC 20503.

1. AGENCY USE ONLY *(Leave blank)*

2. REPORT DATE
September 1998

3. REPORT TYPE AND DATES COVERED
Final (1 Sep 94 - 31 A 98)

4. TITLE AND SUBTITLE
Analysis of Multistep Mammary Tumorigenesis in Wnt-1 Transgenic Mice

5. FUNDING NUMBERS
DAMD17-94-J-4319

6. AUTHOR(S)
Deepa Shankar, M.D.

7. PERFORMING ORGANIZATION NAME(S) AND ADDRESS(ES)
Children's Hospital of Los Angeles
Los Angeles, California 90027

E*Mail: d.shankar@ucla.edu

8. PERFORMING ORGANIZATION REPORT NUMBER

9. SPONSORING/MONITORING AGENCY NAME(S) AND ADDRESS(ES)
Commander
U.S. Army Medical Research and Materiel Command
Fort Detrick, Frederick, Maryland 21702-5012

10. SPONSORING/MONITORING AGENCY REPORT NUMBER

11. SUPPLEMENTARY NOTES
Report contains colored photograph

12a. DISTRIBUTION / AVAILABILITY STATEMENT
Approved for public release; distribution unlimited

12b. DISTRIBUTION CODE

13. ABSTRACT *(Maximum 200*

Breast cancer like all cancers, is a multistep process involving the sequential acquisition of genetic alterations over a period of time. Studying this process in humans is a prolonged and arduous task; therefore, animal models are a desirable alternative. We have used a *Wnt1* transgenic mouse model to study the multiple genetic events in mammary cancer development. We infected these transgenic mice with the mouse mammary tumor virus (MMTV) to accelerate tumorigenesis and to molecularly tag proto-oncogenes that are activated in the resulting tumors and that cooperate with Wnt-1 in mammary tumorigenesis. By examination of the tumors that lack activation of genes that are usual targets of MMTV insertions, we identified a common insertion locus for MMTV and determined the activated gene in this locus to be another member of the FGF family, *Fgf8* . *Fgf8* is transcriptionaly activated in 50% of the tumors from infected *Wnt1* transgenic mice in comparison to the lack of *Fgf8* RNA in other tumors and mammary tissues, suggesting a strong oncogenic cooperation between *Fgf8* and *Wnt1* in mammary tumorigenesis. Fgf8 induced apoptosis of mammary epithelial cells as evidenced by by nuclear condensation and fragmentation and oligonucleosomal laddering. Overexpression of the anti-apoptotic gene *bcl2* in these cells transiently rescued or delayed the apoptosis induced by FGFs. These results describe a new property for FGFs and suggest that these growth factors play very important roles in regulating cell growth and death both in normal development as well as in pathological conditions like cancer.

14. SUBJECT TERMS
Breast Cancer
MMTV, WNT-1, Mammary Tumors, Transgenic Mice, Cooperating Oncogenes

15. NUMBER OF PAGES
44

16. PRICE CODE

17. SECURITY CLASSIFICATION OF REPORT	18. SECURITY CLASSIFICATION OF THIS PAGE	19. SECURITY CLASSIFICATION OF ABSTRACT	20. LIMITATION OF ABSTRACT
Unclassified	Unclassified	Unclassified	Unlimited

FOREWORD

Opinions, interpretations, conclusions and recommendations are those of the author and are not necessarily endorsed by the U.S. Army.

____ Where copyrighted material is quoted, permission has been obtained to use such material.

____ Where material from documents designated for limited distribution is quoted, permission has been obtained to use the material.

____ Citations of commercial organizations and trade names in this report do not constitute an official Department of Army endorsement or approval of the products or services of these organizations.

✓ In conducting research using animals, the investigator(s) adhered to the "Guide for the Care and Use of Laboratory Animals," prepared by the Committee on Care and Use of Laboratory Animals of the Institute of Laboratory Resources, National Research Council (NIH Publication No. 86-23, Revised 1985).

____ For the protection of human subjects, the investigator(s) adhered to policies of applicable Federal Law 45 CFR 46.

✓ In conducting research utilizing recombinant DNA technology, the investigator(s) adhered to current guidelines promulgated by the National Institutes of Health.

✓ In the conduct of research utilizing recombinant DNA, the investigator(s) adhered to the NIH Guidelines for Research Involving Recombinant DNA Molecules.

____ In the conduct of research involving hazardous organisms, the investigator(s) adhered to the CDC-NIH Guide for Biosafety in Microbiological and Biomedical Laboratories.

PI - Signature 2/11/99 Date

TABLE OF CONTENTS

PAGE	SECTION
1	FRONT COVER
2	SF298 REPORT DOCUMENTATION PAGE
3	FOREWORD
4	TABLE OF CONTENTS
5-6	INTRODUCTION
6-10	BODY OF REPORT
12-13	CONCLUSIONS
13-14	REFERENCES
15	BIBLIOGRAPHY
	APPENDIX

INTRODUCTION

Breast cancer, like other cancers, results primarily from accumulation of genetic mutations. Many of the identified mutations associated with cancer result in the activation of proto-oncogenes or inactivation of tumor suppressor genes. In most cases, a single chromosomal aberration is insufficient to cause carcinogenesis but rather mutations in two or more genes are required. In order to understand the development and progression to cancer, it is imperative to identify not only the single mutations involved, but also synergistically acting groups of cancer related genes.

The role of retroviruses in viral-induced cancers has been well established in mice. For example, MMTV has proven to be a powerful tool for studying murine mammary tumorigenesis. MMTV is a B type retrovirus that is known to cause mammary adenocarcinomas in certain inbred strains of mice (e.g. C3H, BR6, GR) (1, 2). The tumor inducing property of MMTV is intrinsically related to an obligatory step in its life cycle, the insertion of a proviral copy of its genome into host cellular DNA. The integration is a mutagenic event for the host cells and, as a consequence, may lead to the transcriptional activation of closely linked proto-oncogenes by the mechanism of insertional mutagenesis (3). The activation of the proto-oncogene by MMTV contributes to the transformation of the cell and development of a tumor. A number of proto-oncogenes activated by MMTV in mammary tumors have been identified. They are *Wnt1, Wnt3, Wnt10b, Int2/Fgf3, Fgf3, Fgf-4* and *Fgf8* (4,5,6,7,8,9,11,17).

While the structure of these genes is known, less is known about their function. A common factor among the MMTV activated genes is that they all appear to play key roles in early embryonic development (12). To prove the oncogenic potential of *Wnt1*, transgenic mice containing the *Wnt1* gene under the control of an MMTV enhancer were generated. Both male and female transgenics developed mammary adenocarcinomas following a generalized mammary hyperplasia (13). The median latency of mammary tumor formation was ~ 5 months in female mice. Males developed tumors less frequently and later in life. The generalized hyperplasia, coupled with the long latency and the sporadic nature of the tumor formation, suggest that *Wnt1* contributes to but is not sufficient for mammary tumorigenesis in these mice. Activation of *Wnt1* is probably an early event in the process of tumor formation; therefore other events, presumably genetic, are necessary for tumor progression.

In an attempt to identify genes acting in synergy in the multistep process of murine mammary tumorigenesis, these *Wnt1* transgenic mice were mutagenized by infection with MMTV (14,15). The strategy was that since MMTV transcriptionally activates proto-oncogenes by insertion of its own DNA near them (2), one could possibly identify additional oncogenes that oncogenically cooperate with *Wnt1* by tagging them with viral DNA. Activation of the cooperating oncogene would therefore confer a growth advantage and would presumably produce a tumor composed mainly of cells that are clonally derived from the cell bearing the proviral insertion. Implicit in this hypothesis was the expectation of a reduction in tumor latency. As predicted, in MMTV infected *Wnt1* transgenics the median latency of tumor formation decreased from ~5 months to 2.5 months and the number of tumors per mouse increased (15). Southern blot data reveal that most of these tumors contained clonal tumor-specific proviruses in addition to the endogenous proviruses found in laboratory mice (15). The advantage of this approach over other mutagenesis procedures is that tumors arising due to proviral insertions contain proviruses physically linked to the activated proto-oncogenes, forming a molecular tag, which permits easy identification, and cloning of the activated genes (2).

Analysis of the tumor DNAs derived from infected *Wnt1* transgenic mice by Southern blotting showed that at least 80 of 128 tumors (59%) contained clonal MMTV-specific

proviruses (15). These tumors were examined for the insertional activation of proto-oncogenes known to be activated by MMTV: *int2/Fgf3, hst/Fgf-4, int-3* and *Wnt-3* (2,5,7,8). Approximately 45% of these tumors contained insertionally activated *int2/Fgf3* and/or *hst* (15). These results show the cooperation of *int2/Fgf3* and *hst* with *Wnt-1*, which strongly corroborates prior findings indicating the same cooperation (16). I (in collaboration with a post-doctoral fellow Craig MacArthur) recently identified another member of the FGF family of growth factors that is insertionally activated by MMTV in 8 of 80 mammary tumors with clonal tumor-specific proviral insertions (17). This gene (*Fgf-8*) was cloned from one of the tumors that had a single tumor specific proviral insertion as described in the methods section. *Fgf8* is transcriptionally activated in the tumors from a silent state (17). This is the third member of the FGF family to be activated in this system, indicating that *Fgfs* and *Wnts* are strong collaborators in inducing mammary tumors.

As we have already demonstrated, this infected *Wnt1* transgenic system can be used to identify novel or/and unexpected oncogenes that are involved in mammary tumorigenesis, thereby demonstrating oncogenic cooperation with *Wnt1* and elucidating the multiple steps involved in murine mammary tumorigenesis. At the time of the original proposal, we still had ~ 55% of the mammary tumors from infected *Wnt1* transgenic mice with new proviral insertions in which the known targets of MMTV mutations are not affected.

My specific aims:

1. Isolation and identification of proto-oncogenes (novel and unexpected) insertionally activated by MMTV in tumors of infected *Wnt1* transgenic mice.
   - Identification of proviral-cellular junction fragments.
   - Clone cellular sequences flanking the proviral insertion
   - Locate and isolate the activated gene in the locus using Northern blot and exon trap strategies.
   - Determine the expression pattern of the gene in normal tissues and in tumors.

2. Characterization of the gene and analysis of the oncogenic potential of the identified proto-oncogene.
   - Demonstrate the oncogenic potential of the isolated proto-oncogene in cell culture transfection assays.
   - Demonstrate the gene's oncogenic potential *in vivo* using transgenic mice.

3. Demonstration of the cooperativity of *Wnt1* with the proto-oncogene that is activated by MMTV.
   - Demonstrate cooperativity by cotransfection of C57MG cells.
   - Obtain definite proof of cooperativity by generating bitransgenic mice.

BODY OF ANNUAL REPORT

Specific Aim 1. Isolation and identification of proto-oncogenes insertionally activated by MMTV in tumors of infected *Wnt1* transgenic mice.

Task-1: Cloning the junction fragment (s), and isolation of the gene (s) activated by MMTV insertions.

A proviral-cellular junction fragment from tumor #76 from infected Wnt-1 transgenic mice was identified and cloned. Screening of the tumor panel by Southern analysis using cellular probes derived from this cloned region detected insertions in 12 of 85 tumors within this locus indicating that this is a new common insertion locus for MMTV. Northern analysis and exon trapping procedures failed to identify any coding sequences within the cloned region.

Mapping of tumor 76 locus to mouse chromosome:

In the process of identifying the gene activated by proviral insertions in this locus, I decided to localize this locus to the mouse chromosome. I reasoned that this process would save time, provide reasonable determination if the cloned fragment was located near a previously identified MMTV insertion site, and/or indicate any probable "candidates" for MMTV activations. The locus was mapped to the chromosome using the Jackson laboratory Backcross DNA Panel Map service.

Briefly, a restriction length polymorphism (RFLP) was identified between the two mouse strains M.spretus and C57BL/6. This RFLP was traced through the entire BSS reciprocal cross panel by Southern analysis. The result from this analysis was sent to Jackson lab and, thorough analysis of the database mapped the locus very nicely to the distal region of mouse chromosome-7. This locus was linked to the *int-2/Fgf-3* locus unfortunately suggesting that this was probably the most likely candidate to be activated by MMTV proviral insertions. However, previous analysis of these tumors did not detect MMTV insertions within the int-2 locus (15). This suggests that either these insertions are not activating *int-2* but probably other genes that are linked to this locus, or that these insertions are long-range activations of *int-2*. I decided to address both possibilities.

Identification of the proto-oncogene activated by MMTV insertions in this locus:

To test if there were activations in other genes, I performed Southern analysis using DNAs from these tumors digested with several enzymes. Southern blots were hybridized to probes containing coding sequences of the following genes: *Cyclin D1, H-19, IGF-2.* and *hst.* These genes are located near *int-2* on mouse chromosome-7 and seemed to be good candidates for MMTV activations. *Cyclin D1* has been implicated in tumorigenesis and overexpression of *cyclinD1* in the mammary gland using a MMTV promoter results in hyperplasia and tumor formation (24). *H-19* has been shown to function as a tumor suppressor and therefore inactivation of the gene could result from MMTV insertions. *Hst/Fgf4* is a previously described target for MMTV activations (15).
Results from these experiments showed no rearrangements in any of the tumors , when probed with any of the genes.

Long range activations of genes by MMTV have been previously described by many investigators (5,10). Peters et al showed long range activations of *Int-2/Fgf-3* by MMTV insertions ~20kb upstream of the gene. Comparison of the restriction maps between my lambda clones and their published map showed that the new cluster of insertions that I identified maps to the same place as that previously published (10). This further supports the idea of long range activations. Northern analysis of some of the tumor RNAs probed with an *int-2* probe showed activation of the gene in the tumors and no expression in mammary gland controls, proving that *Int-2/Fgf-3* is the gene activated by MMTV in these tumors.

The Oncogenic potential of *int-2/Fgf-3* has already been demonstrated, and others & we have shown *int-2 /Fgf-3* to be a strong oncogenic collaborator of *Wnt-1* in promoting mammary carcinogenesis (7,11,15,16). Because of this fact, I slightly altered the focus of my proposal from that originally described. This change does not affect or change my primary goals towards identifying genes involved in the multistep process of mammary tumorigenesis, nor does it alter the specific aims and focus of research described in the original proposal. The only difference is

that further characterization of the identified gene int-2 was not performed, instead I pursued the characterization of a gene (Fgf-8) that I had previously identified to be frequently activated by MMTV proviral insertions in these infected Wnt-1 transgenic mice (17).

Prior to cloning the tumor 76 insertion, I had cloned another junction fragment from tumor 111 and identified (in collaboration with Craig MacArthur a fellow in the lab)the gene *Fgf-8* or *Androgen Induced growth factor (Aigf)* to be activated by MMTV proviral insertions in 10% of tumors from infected *Wnt-1* transgenic mice (17). Fgf-8 was the third member of the fibroblast family of growth factors to be activated in these tumors further supporting the evidence that Wnt and Fgf family of growth factors are strong oncogenic collaborators. I published these results as a co-author in the Journal of virology (17).

Specific Aim 2. Characterization of the gene and analysis of the oncogenic potential of the identified proto-oncogene.

Task-2a: Demonstration of the oncogenic potential of the isolated proto-oncogene in cell culture assays.

Fgf8 consists of at least six exons and codes for at least seven protein isoforms, due to alternative splicing of the primary transcript (17,18). We analyzed the oncogenic potentials and differences in the biological activities of three isoforms (8a, 8b, and 8c) in NIH3T3 cells and showed that the isoform Fgf8b was highly transforming in NIH3T3 cells and highly tumorigenic in nude mice, while the other two isoforms showed moderate to low transforming potentials (22).

Oncogenic potential of human *FGF8* isoforms;

Additionally, I also tested the human isoforms of FGF8 for their oncogenic capabilities (cDNAs obtained from Dr. P. Roy-Burman). The human isoforms of FGF8 were isolated by reverse transcription-polymerase chain reaction (RT-PCR) from a human prostate tumor cell line. Three different isoforms were isolated which correspond to the murine Fgf-8a, 8b and 8e isoforms. The human FGF8a and FGF8b exhibit identical amino acid sequences to their murine counterparts, while FGF8e shows a partial variation from the corresponding murine isoform in the additional exon found in both species (17,18).

To address the biological effect of specific isoform expression, the cDNAs corresponding to the different isoforms (*FGF8a, 8b, and 8c)* were cloned into the eukaryotic expression vector pcDNA (Invitrogen). The corresponding plasmids together with the empty vector control were transfected into NIH3T3 cells by Lipofectamine mediated transfection (GIBCO-BRL). Twenty-four hours after transfection, the cells were selected for stable transfectants with 400 μg/ml of Geneticin (G418, GIBCO-BRL). At least 60-70 colonies were pooled from each transfection to generate stable cell lines that were used for transformation and tumoriginicity assays.

The results from these analyses showed that, the cells expressing *FGF8b* cDNA exhibited marked morphological transformation from a flat uniform organization (vector controls) to a highly elongated, spindle shaped, refractile morphology. The cells expressing FGF8a and FGF8e cDNAs showed moderate degrees of transformation when compared tot the normal morphology of the control cells, but much less than FGF8b. The FGF8b cells also showed higher saturation densities at confluence when compared to the controls, indicating loss of contact inhibition (Figure 3). FGF8a and FGF8e cells also displayed loss of contact inhibition at confluence, but their saturation densities were lower than FGF8b. These results correspond closely to those we described previously for mouse Fgf8 isoforms (22). A manuscript describing these findings has been published in the journal *Cell, Growth, and Differentiation.* (29).

Task-2b: Confirmation of the oncogenic potential *in vivo* using transgenic mice.

The *Fgf8* transgene:

The transgene for the *Fgf8* transgenic mice was directly cloned from a tumor (tumor 86) that has an MMTV insertion very close to the 5' end of the *Fgf-8*. This particular insertion is in a "promoter insertion" orientation, i.e., it is upstream from the initiation codon in the same transcriptional orientation. The transgene contains the 3' MMTV LTR, and the entire genomic *Fgf8* gene in a single DNA fragment of ~13 Kb (Figure 1).

Fgf8 transgenic mice:

The founder animals generated were screened by Southern blots of the tail DNAs for the presence of the transgene. We had three transgenic founders that contain the MMTV/*Fgf8* transgene. These animals were bred to normal BALB/c mice to generate independent lines. Since the transgenic founders were poor mothers we were unable to establish independent lines from the female mice and the one we esatbklished from the male founder did not express the transgene. Mammary tumors started developing in the transgenic mice between 5-7 months. The tumors were resected from the animals and processed for histological and northern analyses.

Expression of the transgene in the mammary gland and tumors.

Very high expression of Fgf8b RNA was seen in the tumors. Expression was also detected in the mammary gland RNA and interestingly in the ovaries. Even though normal expression of Fgf8 can be found in adult ovaries. It could be detected only with a northern blot containing 20 μg of Poly(A) RNA (17), whereas I was able to see a signal with 10 μg of total RNA with 3 hrs exposure (Figure 2).

Histology of the tumors

The tumors were formalin fixed, paraffin embedded and sections were stained with Hematoxylin and Eosin. The stained sections were analyzed microscopically. The tumors from the transgenic animals were identified to be ductal adenocarcinomas with varying degrees of pathogenicity, ranging from benign adenomas to clearly invasive papillomas. In addition we also found mammary hyperplasia and hyperplasia of the ovarian stroma. (32) (Figure 3 & 4)

Biological effects of murine Fgf8 isoforms on mammary epithelial cells

In my previous report I had described an interesting property that I had discovered while analyzing the differences in the biological activities of the Fgf8b protein isoforms. I had found that mammary epithelial cells either over expressing Fgf8b or when treated with 8b protein containing conditioned medium, underwent apoptosis. I demonstrated that the cell death was indeed due to apoptosis by Hoescht staining and DNA ladder analyses. Since this was the first observation so far that Fgfs could cause apoptosis of mammary epithelial cells, to better test our results, we partially purified Fgf8b using a heparin sepharose affinity column and demonstrated induction of apoptosis by the partially purified Fgf8b protein.

In the last year I have done more experiments on this property of Fgf8b. I will describe the results in this report. Eventhough these experiments were not originally proposed, they are highly significant to my proposal, and also to the understanding of oncogenic cooperation in this system.

Induction of apoptosis by several members of the FGF family of growth factors.

To test if the phenomenon of apoptosis was specific to only Fgf-8b or was also seen with any other FGF family member(s), I used purified human FGF1,2,4,5,6,7,and 9 (R&Dsystems) to treat C57MG cells. 100ng/ml of the FGF proteins was added to the cells at 40%confluence with 0.1mg/ml of Heparin. NIH 3T3 cells were used as a control to assay the activity of the protein. Cells treated with FGF1, FGF2, FGF4, FGF6 and FGF9 showed morphological transformation and apoptotic cell death similar to Fgf8b. FGF2, FGF4 and FGF9 showed this effect even in the absence of heparin. FGF5 did not show any show any changes at concentrations of 200 ng/ml. Cells treated with 500 ng/ml of FGF5 showed moderate transformation but no apoptosis, and cells treated with 1mg/ml of the growth factor showed both transformation and apoptosis. The only growth factor that was tested but did not show any activity was FGF7. Even 1mg/ml of FGF7 did not show any changes in morphology.

Table 1. Apoptosis of mammary epithelial cells is induced by several members of the FGF family

FGF *	Transformation of NIH3T3 Cells	Apoptosis of C57MG cells
FGF1	+++	+++
FGF2	+++	+++
FGF4	+++	+++
FGF5	+++	+/– †
FGF6	+++	+++
FGF7	+++	– ‡
FGF8b	+++	+++
FGF9	+++	+++

* FGFs were added at 100 ng/ml final concentration and cells observed for four days.

† Apoptosis observed only at 1 μg/ml FGF5; transformation of C57MG but no apoptosis at 500 ng/ml; no effects at 200 ng/ml.

‡ No apoptosis or transformation at 1 μg/ml FGF7.

Neutralization experiments using a polyclonal antibody against human FGF2 completely blocked the apoptosis seen on treatment with FGF2 in C57MG cells (Figure 5). Cells treated with FGF2 showed transformation and apoptosis by days 3-4. However, the cells treated with FGF2 that was pre incubated with the antibody did not show any alteration in cellular and nuclear morphology, indicating that the apoptosis seen was indeed a result of treatment with FGF2/FGFs.

To address the possibility that this effect is not something specific to this cell line, we tested several other mammary cell lines (normal and tumor) for induction of apoptosis by FGF2, FGF4, FGF6 and FGF8. Three cell lines (C127I, BMG, GR) resembled C57MG in all respects; cellular transformation followed by apoptosis. HC11 cells showed some degree of apoptosis but cell death was not complete as seen in the other cell lines. The human breast carcinoma cell line MCF-7 when treated with the different FGFs did not undergo programmed cell death (Table 2). One explanation to this unresponsivenes to FGF signals is that MCF-7 cells are known to express high levels of the anti-apoptotic gene product Bcl-2. Therefore, Bcl-2 may be inhibiting or blocking the apoptotic signal provided by the FGF. Alternatively, MCF-7 being a carcinoma cell

line could have gone through several genetic alterations, some of them may result in providing survival functions for the cells.

Table 2. FGFs induce apoptosis of several mammary epithelial, but not fibroblast, cell lines *

Cell line	Apoptosis
Mammary epithelial cells	
C127I	+++
BMG	+++
GR	+++
HC11	+++/– †
MCF-7	–
S115 (negative control)	–
Fibroblasts	
NIH3T3	–
Rat-1	–

* Apoptosis was assessed using FGF2, FGF4, FGF6 and FGF8b at 100 ng/ml. All caused similar effects on an individual cell line.

† HC11 cells appeared to be composed of two cell populations, one that responded to FGFs with apoptosis and one which was nonresponsive

Inhibition of FGF induced programmed cell death by Bcl2

The Bcl2 protein is known to block apoptotic cell death induced by various agents (31). However, Bcl-2- independent apoptotic pathways are also known. We tested to see if Bcl-2 could inhibit FGF induced apoptosis of mammary epithelial cells. C57MG cells were transfected with an expression vector containing the *Bcl-2* cDNA. Stable clones expressing the Bcl-2 gene product were generated and treated with FGF2, FGF4 and FGF6. Stable clones expressing the vector alone was used as controls. The treated cells were observed for a period of 4 days. The control cells (clones transfected with vector alone) showed morphological changes within 12-16 hrs after treatment By 24 hr's many cells started dying and coming off the plate. By day 3 after treatment approximately 80% of the cells were apoptotic. In contrast, the Bcl-2 clones remained viable and were morphologically transformed from a flat cuboidal morphology to a more elongated spindle shaped appearance (Figure 6). No apoptosis was observed suggesting that Bcl-2 can block the apoptotic signal from FGF. However, on days 4 and 5, when the control cells were completely dead, the Bcl-2 clones started showing signs of apoptosis. This result could be explained by the possibility of transient expression of the protein from the vector or poor stability of the protein. It could also be possible that Bcl-2 does not completely inhibit apoptosis but delays the onset. This effect has been previously described for Bcl2 (31).

To test for deregulation of members of the Bcl2 family, FGF-treated mammary epithelial cells was assayed by northern and western analysis for upregulation of the proapoptotic genes like *Bax* and *Bik* and down regulation of anti-apoptotic genes like *Bcl2* and Bcl_xL. RNA and protein have been extracted from C57MG cells treated with FGF2, FGF4, FGF8 and controls, andiam in the process of generating northern and western blots which will be probed with *Bcl2*, Bcl_x *Bax,* and *Bik* cDNAs and antibodies (Calbiochem).

If down regulation of *Bcl2* or Bcl_xL is observed, then these genes will be overexpressed in C57MG cells using a retroviral (LNCX) or plasmid (pMIRB) expression vectors. Clones of

cells expressing the gene at high levels will be generated and then treated with FGFs to see if this can inhibit or suppress FGF mediated apoptosis thereby indicating that Bcl2 or Bcl_{XL} is involved in this pathway.

Specific Aim 3: Demonstration of the cooperativity of *Wnt1 with* the proto-oncogene that is activated by MMTV.

Task 3a:• Demonstrate cooperativity by cotransfection of C57MG cells.

Since Fgf8b by itself is highly transforming in NIH 3T3 cells, and induces apoptosis of C57MG mammary epithelial cells, It would not be possible to demonstrate oncogenic cooperativity as defined in the classical experiments. However, we could speculate that the cooperation may not be the synergistic action of two oncogenes, but maybe Wnt 1 provides survival signals to the cells, that have received the death signal from Fgf8b and hence cooperation towards cellular proliferation leading to transformation. To test this hypothesis, Wnt1 was expressed in C57MG cells by transfection of a retroviral expression vector carrying the *Wnt1* cDNA epitope tagged with HA (heme agglutinin) (LNCX-Wnt1HA). Stable clones were generated by selection in G418(Life technologies). Cells transfected with the vector containing the HA tag alone will serve as the controls. The clones generated are being tested for expression of Wnt1 at the RNA and protein levels. The Wnt1 clones with stable and high expression of the protein will be treated with FGF proteins (FGF2, FGF4 and FGF8) as described previously. The cells will be observed for transformation and apoptosis. Suppression of apoptosis if present will also be quantitatively determined in flow cytometry assays using Annexin V and propidium iodide staining. If Wnt1 can suppress apoptosis even partially it can be determined using this assay. An alternate approach would be to use soluble wingless (*drosophila*) as the source of Wnt protein and treat C57MG cells with wg and FGF, wg alone and FGF alone. If soluble wingless protein can be produced, we will perform this experiment to corroborate the Wnt1 cell clone approach.

Task 3b:• Obtain definite proof of cooperativity by generating bitransgenic mice.

Unfortunately we have had a severe set back in our experiments, because of our inability to generate Fgf8 transgenic lines. In addition since we discovered FGF induced apoptosis, we have concentrated on characterization of this finding and hence this specific aim could not be accomplished in the specified time frame.

CONCLUSIONS

A proviral-cellular junction fragment was identified and cloned form a tumor from infected Wnt1 transgenic mice. Twelve of eighty-five tumors tested had MMTV insertions within this locus. Analyses of these tumors showed that this newly identified cluster of MMTV insertions activate the previously characterized proto-oncogene *Fgf3,* over a long range (~20kb upstream of the gene). Since this gene has already been identified as an oncogenic collaborator of Wnt-1, I changed my focus to characterization of another gene *Fgf8* that I had previously cloned from a tumor from infected *Wnt1* transgenic mice, and identified to be activated from a silent state in 10 % if the tumors. This gene encodes at least seven different protein isoforms, three (Fgf8 a, b and c) of which were isolated in our lab.

Characterization of the biological activities of the different isoforms in mammary epithelial cells identified a new property (apoptosis) for the isoform Fgf8b. Stimulation of

C57MG cells by Fgf8b containing conditioned medium resulted in apoptotic cell death as shown by characteristic nuclear changes and DNA laddering. This finding was further proved by demonstration of apoptosis using partially purified Fgf8b protein (heparin sepharose affinity chromatography). This property was not confined to Fgf8b alone, but several other members of the FGF family of growth factors show the same effect. Apart from C57MG cells, other mammary epithelial cells also undergo apoptosis when induced by FGFs. Overexpression of Bcl2 in C57MG cells delayed the onset of apoptosis induced by FGFs.

To demonstrate the oncogenicity of Fgf8 in vivo, the mouse *Fgf8* transgene was cloned from a tumor with insertion in this locus (tumor 86). Three founders were obtained and unfortunately we were unable to establish any transgenic lines. We are currently injecting mouse embryos to generate more transgenic mice. The female founders developed tumors in 5-7 months. The tumors and surrounding mammary tissue highly expressed the transgene. The tumors were found to be ductal adenocarcinomas and stromal hyperplasia of the ovaries was also observed. In Summary, the results from this study has led to the discovery of a new property for fibroblast growth factors; induction of programmed cell death. Further characterization of this property and the signal transduction pathway could be of great help in the design of rational therapeutic interventions.

REFERENCES

1. Nandi, S and C.M. McGarth (1973). Mammary Neoplasia in Mice. Adv.Cancer Res. 17: 353-414.
2. Nusse, R.(1991) Insertional Mutagenesis in Mouse Mammary Tumorigenesis. Current Topics in Microbiology and Immunology. 171: 43-63.
3. Kung, H.J., Boerkoel, C., and T.H. Carter. (1991). Retroviral mutagenesis of cellular oncogenes: A review with insights into the mechanisms of insertional activation. Current Topics in Microbiology and Immunology. 171: 1-25.
4. Nusse, R. and H.E. Varmus (1982). Many tumors induced by mouse mammary tumor virus contain a provirus integrated in the same region of the host genome. Cell 31: 99-109.
5. Peters, G., S. Brookes, R. Smith, and C. Dickson (1983). Tumorigenesis by mouse mammary tumor virus: evidence for a common region for provirus integration in mammary tumors. Cell 33: 369-377.
6. Roelink, H.E. Wagenaar, S. Lopes Da Silva, and R. Nusse (1990). *Wnt-3* , a gene activated by proviral insertion in mouse mammary tumors is homologous to *int-1/Wnt-1* and is normally expressed in mouse embryos and adult brain. Proc. Natl. Acad. Sci. USA 87: 4519-4523.
7. Peters, G., S. Brookes, R. Smith, and C. Dickson (1989). The mouse homolog of the *hst/k-Fgf* gene is adjacent to *int-2* and is activated by proviral insertion in some virally induced tumors. Proc. Natl. Acad. Sci.USA. 86: 5678-5682.
8. Gallahan, D., C. Kozak, and R. Callahan (1987). A new integration region (*int-3)* for mouse mammary tumor virus on chromosome 17. J Virol. 61: 218-220.
9. Robbins, J., B.J. Blondel, D. Gallahan, and R. Callahan (1992). Mouse mammary tumor gene *int-3:* a member of the notch gene family transforms mammary epithelial cells. J. Virol. 66: 2594-2599.
10. Peters.G., Brooks,S., Placzek,M., Schuermann, M., Michalides,R., and C. Dickson (1989). A putative *int* domain for mammary tumor virus on mouse chromosome 7 is a 5' extension of *int-2.* J Virol. 63: 1448-1450.
11. Lee, F.S., Lane, T., Kuo,A., Shackleford, G.M., and P. Leder (1995). Insertional mutagenesis identifies a member of the *Wnt* gene family as a candidate oncogene in the mammary epithelium of *int2/fgf3* transgenic mice .Proc.Natl.Acad.Sci. 92: 2268-2272.
12. Nusse, R. and Varmus, H.E (1992). *Wnt* genes. Cell 69: 1073-1087.
13. Tsukamoto, A.S., R. Grosschedl, R.C. Guzman, T. Parslow, and H.E. Varmus (1988). Expression of the *int-1* gene in transgenic mice is associated with mammary gland hyperplasia and adenocarcinomas in male and female mice. Cell 55: 619-625.

14. Shackleford, G, M., and H. E. Varmus.(1987) Construction of a clonable, infectious and tumorigenic mouse mammary tumor virus provirus and a derivative vector. Proc. Natl. Acad. Sci.USA.85:9655-9659.
15. Shackleford, G.M., C.A. MacArthur, H.C. Kwan, and H.E. Varmus. (1993). Mouse mammary tumor virus infection accelerates mammary carcinogenesis in *Wnt-1* transgenic mice by insertional activation of *int-2/ Fgf-3* and *hst/Fgf-4*. Proc. Natl. Acad. Sci.USA. 90: 740-744.
16. Kwan H. C., V. Pecenka, A. Tsukamoto, T.G. Parslow, R.Guzman, Lin, T.P., W.J. Muller, F.S. Lee, P. Leder, and H. E.Varmus (1992). Transgenes expressing the *Wnt-1* and *int-2* proto-oncogenes cooperate during mammary carcinogenesis in doubly transgenic mice. Mol. Cell. Biol. 12: 147-154.
17. MacArthur, C.A., D.B. Shankar, and Shackleford, G.M (1995). *Fgf-8*, activated by proviral nsertion, cooperates with a *Wnt-1* transgene in mouse mammary tumorigenesis. J.Virol, 69: 2501-1507
18. Crossley, P.H., and G.R. Martin (1995). The mouse Fgf8 gene encodes a family of polypeptides and is expressed in regions that direct outgrowth and patterning in the developing embryo. Development. 121: 439-451
19. MacArthur, C.M., Lawshe, A., Xu, J., Santos-ocampo,S., Heikeinheimo, M., Chellaiah, A.T., and D.Ornitz (1995). Fgf8 isoforms activate receptor splice forms that are expressed in mesenchymal regions of mouse development. Development. 121: 3603-3613
20. Nonomura, N., Nakamura, N., Uchida, N., Noguchi,S., Sato, B., Sonoda, T., and K. Matsumoto (1988) Growth-stimulatory effect of androgen-induced autocrine growth factor(s) secreted from shionogi carcinoma 115 cells on androgen-unresponsive cancer cells in a paracrine mechanism. Cancer Research. 48: 4904-4908
21. Sambrook,J.,E.F. Fritsch and T . Maniatis (1989). Molecular cloning: A laboratory manuel, 2nd edition, (C, Nolen, ed.), Cold spring harbor laboratory press, Cold spring harbor, NY.
22. MacArthur,C.M.,Lawshe,A., Shankar,D.B., Heikinheimo.M., and G. Shackleford (1995) FGF-8 isoforms differ in NIH3T3 Cell Transforming Potential. Cell,Growth and Differ. 6; 817-825
23. Rowe, L.B., Nadeau, J.H., Turner, R., Frankel, W.N., Letts, V.A., Eppig, J.T., Ko, M.S.H., .Thurston, S.J., and E.H. Birkenmeir (1994). Maps from two interspecific backcross DNA panels available as a community genetic mapping resource. Mammalian Genome, 5,
24. Wang, T.C., Cardiff, R.D., Zukerberg,L., Lees,E., Arnold, A., and E. V.Schmidt (1994).. Mammary hyperplasia and carcinoma in MMTV-cyclin D1 transgenic mice. Nature 34. 669-671.
25. Hao,Y., Crenshaw, T, Moulton, T., Newcomb, E., and B. Tycko (1993). Tumour suppressor activity of H19 RNA. Nature 365, 764-767.
26. Zemel, S., Bartolomei, M.S., and S.M. Tilghman (1992). Physical linkage of two mammalian imprinted genes, H19 and insulin-like growth factor 2. Nature genetics. 40., 61-65
27. Vaux,D.L., and A. Strasser (1996). The molecular biology of apoptosis. Proc.Natl.Acad.Sci 93;2239-2244.
28. Hoffman,B., and D. Libermann (1994). Molecular controls of Apoptosis: Differentiation/growth arrest primary response cells, proto-oncogenes, and tumor suppressor genes as positive and negative modualtors. Oncogene 9; 1807-1812.
29. Ghosh, A., Shankar, D.B., Shackleford, G.M., Wu, K., T'Ang, A., Miller, G., Zheng, J., and P. Roy-Burman (1996). Molecular cloning and characterzation of human *FGF8* alternative messenger RNA forms. Cell, Growth and Diff. 7., 1425-1434.
30. Chomczynski, P. and N. Sacchi. 1987. Single-step method of RNA isolation by acid guanidinium thiocyanate-phenol-chloroform extraction. Anal. Biochem. 162:156-159.
31. Hockenbery, D.M., Zutter, M., Hickey W., Nahm,M., and S.J. Korsmeyer (1991). BCL2 protein is topographically restricted in tissued characterised by apoptotic cell death. PNAS., 88, 6961-6965.
32. . Daphna-Iken, D., **Shankar, D.B.**, Lawshé, A., Ornitz, D.M., Shackleford, G.M. and MacArthur, C.A. (1998). MMTV-*Fgf8* transgenic mice develop mammary and salivary gland neoplasia and ovarian stromal hyperplasia. *Oncogene* **17**: 2711-2717.

Bibliography

PUBLICATIONS

MacArthur, C.A*., **Shankar, D.B***., Shackleford, G.M. (1995). *Fgf-8*, activated by proviral insertion, cooperates with the *Wnt-1* transgene in murine mammary tumorigenesis. *J. Virol.,* **69**:2501-2507. (* Both authors contributed equally to this work)

MacArthur, C.A., Lawshe, A., **Shankar, D.B.**, Heikinheimo,M., and Shackleford G.M. (1995). FGF-8 isoforms differ in NIH3T3 cell transforming potential. *Cell,Growth and Differ.*, **6**:817-825

Ghosh, A.K., **Shankar, D.B.**, Shackleford G.M., Wu, K., T'ang, A., Miller, G.J., Zheng, J.P., and Roy-Burman, P. (1996) Molecular cloning and characterization of human FGF8 alternative messenger RNA forms. *Cell, Growth and Differ.,* **12:** 1425-1434.

Daphna-Iken, D., Shankar, D.B., Lawshé, A., Ornitz, D.M., Shackleford, G.M. and MacArthur, C.A. (1998). MMTV-*Fgf8* transgenic mice develop mammary and salivary gland neoplasia and ovarian stromal hyperplasia. *Oncogene* **17**: 2711-2717.

Shankar, D.B., and Shackleford G.M. Apoptosis of mammary epithelial cells induced by fibroblast growth factors. (manuscript in preparation)

ABSTRACTS AND PRESENTATIONS

October 1997: Era of Hope, The Dept. of Defense breast cancer research program meeting (poster). Proceedings, Volume II, page 391.

February 1995: The Wnt meeting, NIH, Bethesda. Multistep mammary tumorigenesis in transgenic mice (speaker).

January 1995: Oncogenes Revisted, Keystone, CO. FGF-8 protein isoforms differ in oncogenic potential (poster). *J of Cellular Biochemistry,* 19A; 22.

October 1994: The First West Coast Retroviral Meeting, Newport beach, CA. MMTV proviral insertions identify *Fgf-8* as an oncogenic collaborator of *Wnt-1* (Speaker). Abstract Book, page 42.

June 1994: Breast cancer, Keystone, CO. Multistep mamary carcinogenesis-Identification of cooperating proto-oncogenes (*Wnt-1 and Aigf/Fgf-8*) by retroviral insertion in transgenic mice (poster). *J of Cellular Biochemistry*, 18D; 234.

June 1993: Ninth annual meeting on Oncogenes, Fredrick,MD; Frequent MMTV proviral insertions near *Aigf/Fgf-8* in mammary tumors from Wnt-1 transgenic mice (Poster). Foundation for advanced cancer studies, Abstract 135.

October 1990: The XIV National Congress of the Indian Association of Medical Microbiologists, India; Immunological status of children with Persistent Diarrhoea (poster).

Personnel. Deepa B. Shankar, 100% effort.

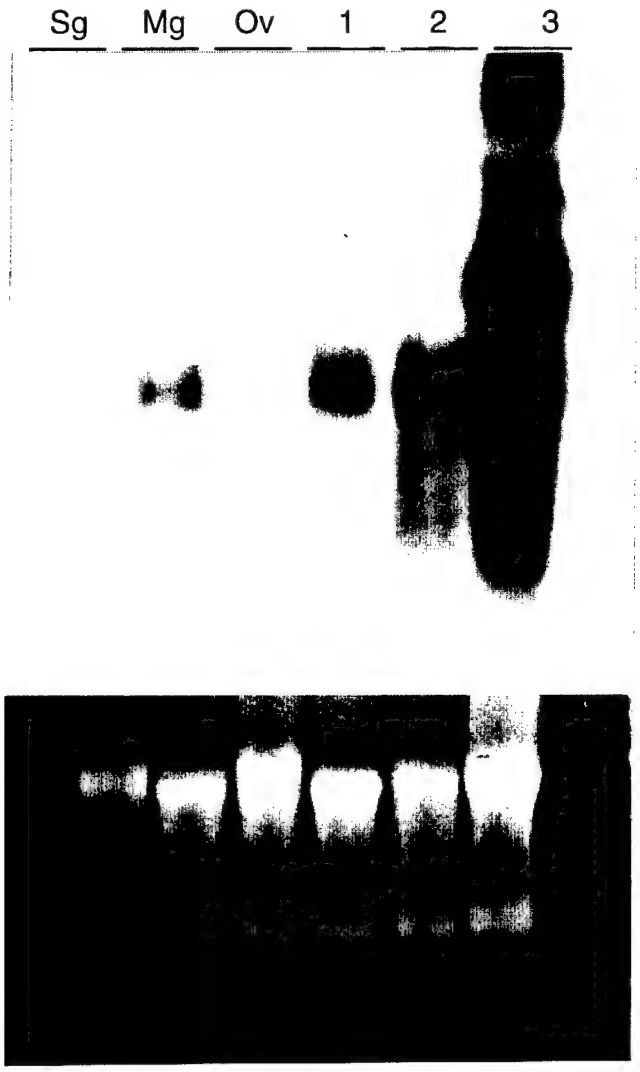

***Figure 1*. Expression of the *Fgf8* transgene in mammary tumors and some adult mouse tissues .** Northern blot of total cellular RNA (10 mg) from three normal tissues (salivary gand (Sg, mammary gland (Mg), and ovary (Ov), and three tumors from *Fgf8* transgenic mice (1, 2, & 3). The blot was probed with a full length *Fgf8b* cDNA (upper panel). Ethidium bromide stained photograph of the RNAs (lower panel).

Figure 2

MMTV-Fgf8 Transgene

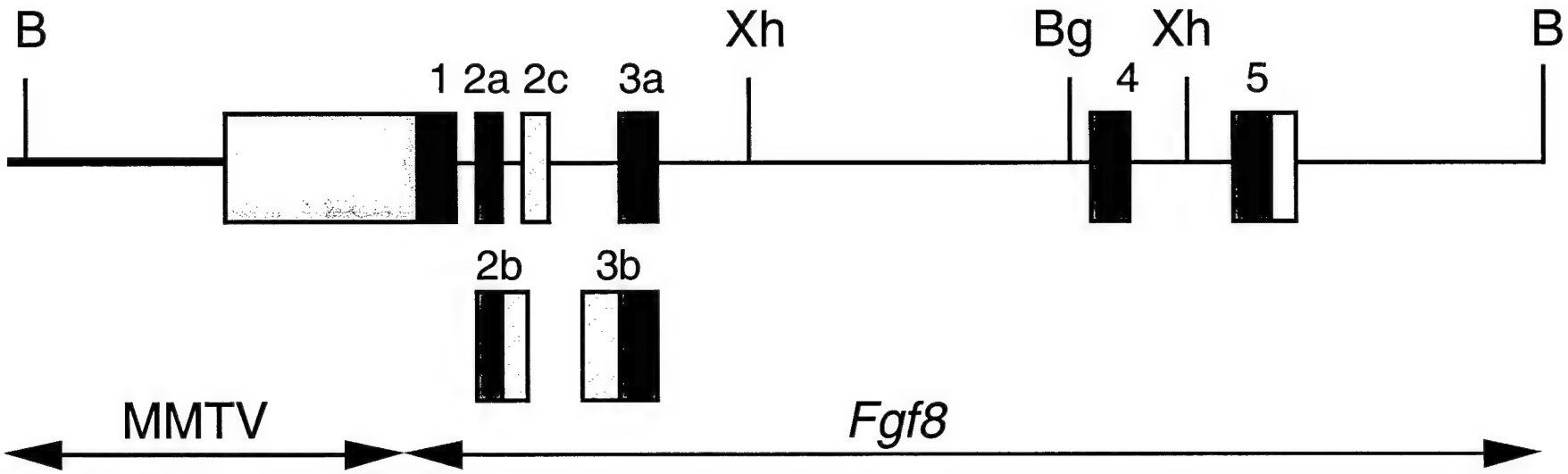

A

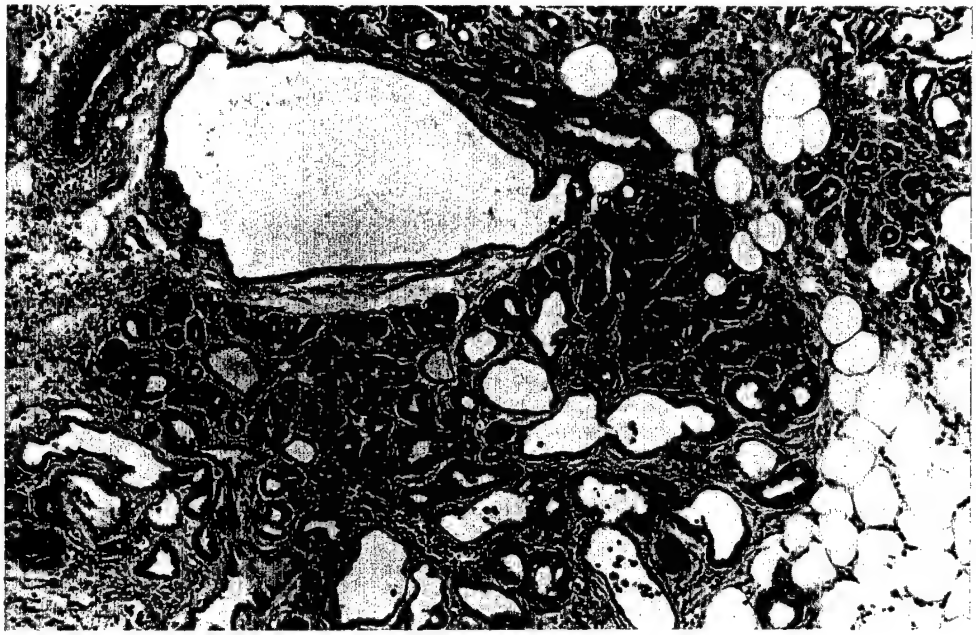

B

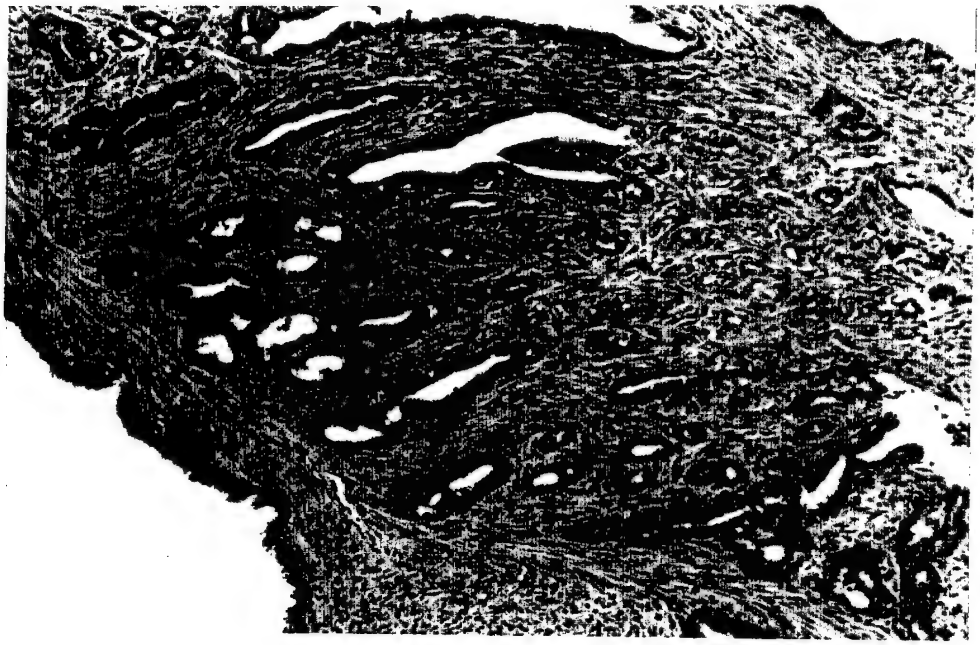

Figure 3. **Histopathology of the MMTV-*Fgf8* mammary tumors.** Histological section through fixed mammary gland tumors from MMTV-*Fgf8* transgenic mice. A. benign adenoma (100x), B. invasive adenocarcinoma (100x). The sections were stained with hematoxylin and eosin.

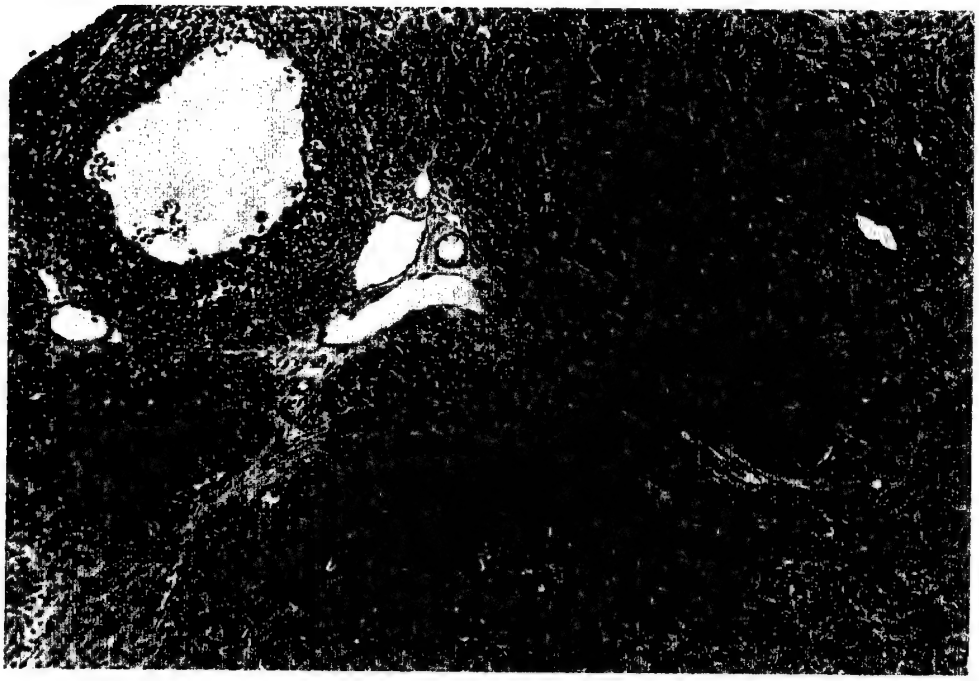

***Figure 4*. Pathology of the ovaries from MMTV-*Fgf8* transgenic mice.** Histological section of an ovary from *Fgf8* transgenic mouse showing extensive stromal hyperplasia (100x magnification). The sections were stained with hematoxylin and eosin.

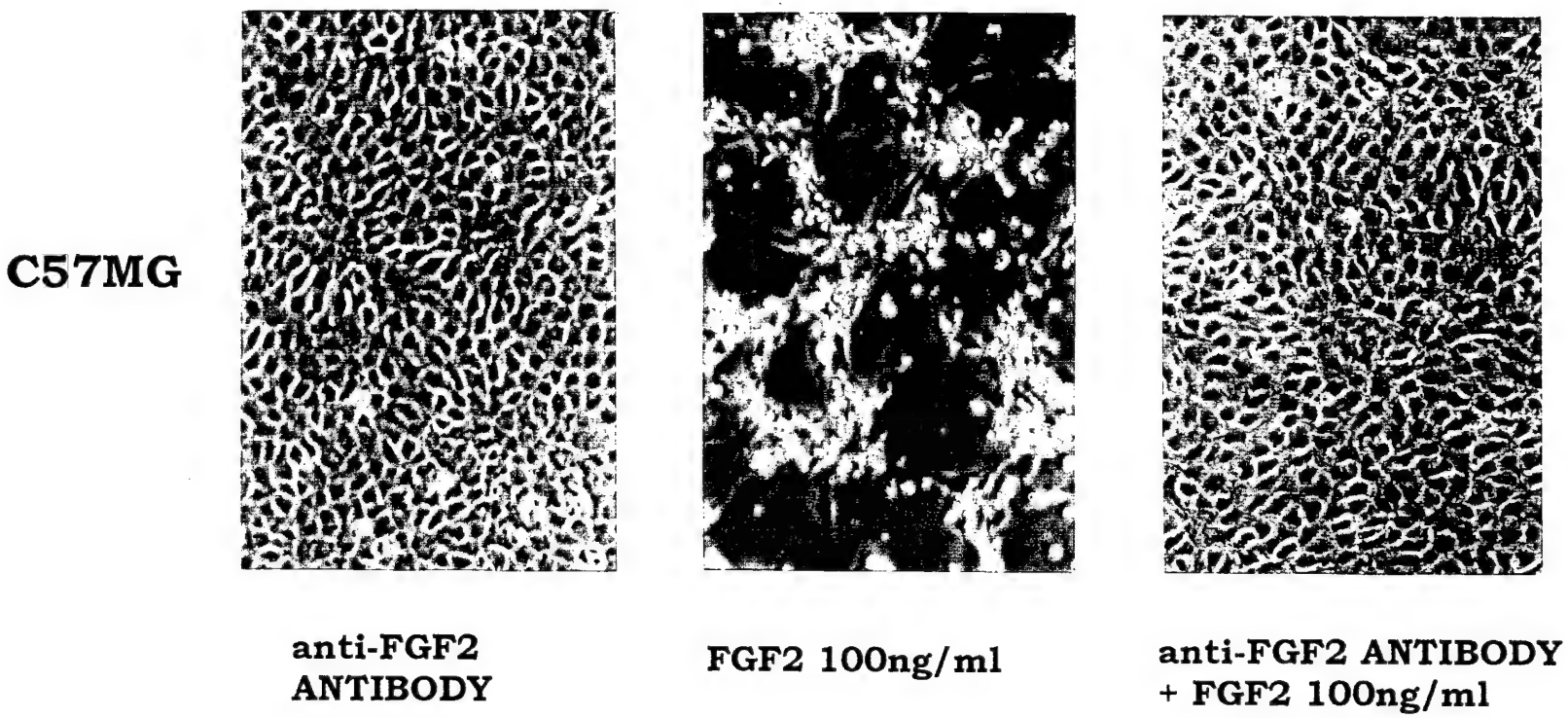

Figure 5 **Neutralization of FGF2 induced apoptosis of mammary epithelial cells by an anti-human FGF2 antibody.** C57MG cells were treated with FGF2 protein, anti-FGF2 antibody, or FGF2 protein preincubated with the FGF2 antibody. The cells treated with the neutralized protein showed no evidence of transformation or apoptosis in contrast to the cells treated with the FGF2 protein alone.

Figure 6

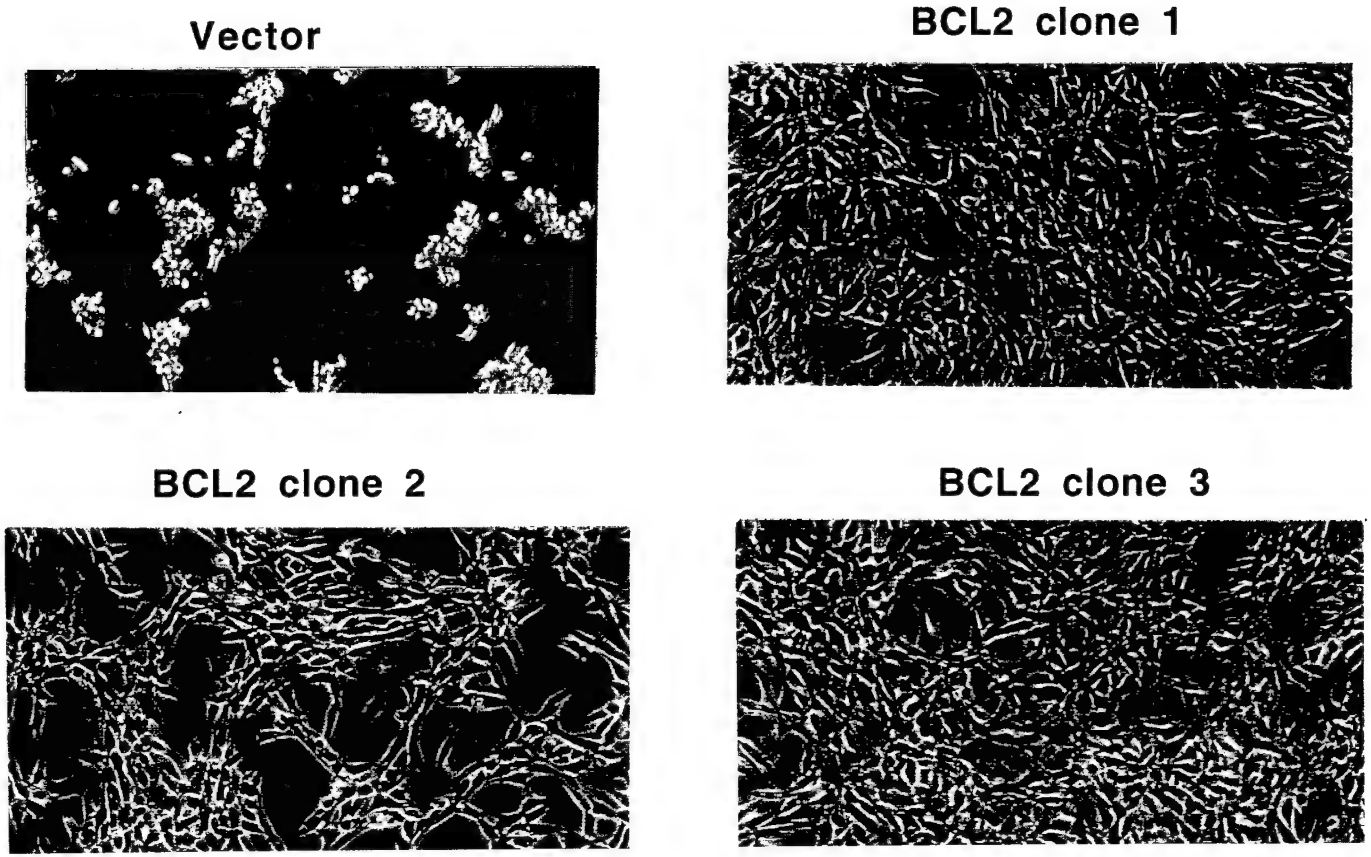

Oncogene (1998) 17, 2711–2717
© 1998 Stockton Press All rights reserved 0950–9232/98 $12.00
http://www.stockton-press.co.uk/onc

MMTV-*Fgf8* transgenic mice develop mammary and salivary gland neoplasia and ovarian stromal hyperplasia

D Daphna-Iken[1], DB Shankar[2], A Lawshé[1], DM Ornitz[3], GM Shackleford[2] and CA MacArthur[1]

[1]*Departments of Pediatrics and Pathology, Washington University School of Medicine, St. Louis, Missouri 63110;* [2]*Division of Hematology-Oncology, Children's Hospital Los Angeles and Departments of Pediatrics and Microbiology, University of Southern California School of Medicine, Los Angeles, California 90027;* [3]*Department of Molecular Biology and Pharmacology, Washington University School of Medicine, St Louis, Missouri 63110, USA*

Prior studies have identified Fibroblast Growth Factor-8 (*Fgf8*) as a possible proto-oncogene in mouse mammary tumorigenesis. We now report on the generation of two types of *Fgf8* transgenic mice that each utilize the mouse mammary tumor virus (MMTV) promoter. The first transgene (MMTV-*Fgf8b*) results in the overexpression of the FGF8b isoform exclusively. Male and female MMTV-*Fgf8b* transgenic mice are viable and fertile. RNA for FGF8b is detected in mammary gland and salivary gland tissues of transgenic mice by Northern blot analysis. Nearly 85% of breeding transgenic female mice developed mammary lobular adenocarcinomas by 12 months of age, while no tumors developed in non-transgenic littermates. Salivary gland tumors occurred in some animals, always in association with mammary tumors. Several MMTV-*Fgf8b* transgenic mice had lung metastases at necropsy. The second transgene (MMTV-*Fgf8*) uses the entire *Fgf8* gene and potentially encodes all FGF8 isoforms. *Fgf8* is expressed by this transgene in several tissues in addition to those described above, notably the ovaries. The two MMTV-*Fgf8* founders developed mammary ductal adenocarcinomas at five and eight months of age, and both displayed ovarian stromal hyperplasia. The founders expressing either transgene did not successfully nurse their pups. These results demonstrate that production of FGF8b, and possibly other FGF8 isoforms, in the mammary and salivary glands contributes to oncogenesis, and that ovarian expression results in stromal hyperplasia.

Keywords: Fibroblast Growth Factor; FGF8; *Fgf8*; mammary tumorigenesis; oncogenesis; breast cancer

Introduction

Most carcinogenic processes are multi-step, and understanding the multiple genetic events involved in mammary carcinogenesis may lead to rational interventional strategies (Harris *et al.*, 1992a,b). As one of these potential steps, alterations and/or over-expression of members of the Fibroblast Growth Factor (FGF) family and their receptors have been described in human breast cancers (Jaakkola *et al.*, 1993; Jacquemier *et al.*, 1994; Penault-Llorca *et al.*, 1995; Payson *et al.*, 1996; Bansal *et al.*, 1997; Yiangou *et al.*, 1997). FGFs are secreted peptide growth factors that are thought to have most of their biological effect by binding to membrane receptor tyrosine kinases that transmit intracellular signals that ultimately affect cellular growth and/or differentiation programs (Basilico and Moscatelli, 1992; Johnson and Williams, 1993; Ornitz *et al.*, 1996).

As human carcinogenic processes are temporally long and have limited potential for experimental exploitation, animal models of mammary gland carcinogenesis are necessary to rapidly advance our knowledge and our potential for intervention (Harris *et al.*, 1992a,b). Few mouse models of FGF in mammary gland cancer exist. Insertional activation of *Fgf3/int-2* (Dickson *et al.*, 1984), *Fgf4/hst* (Peters *et al.*, 1989), and *Fgf8* (MacArthur *et al.*, 1995c; Kapoun and Shackleford, 1997) by mouse mammary tumor virus (MMTV) in murine mammary cancers have been described. Female MMTV-*Fgf3* transgenic mice develop mammary gland cancer after several months of epithelial hyperplasia, while male MMTV-*Fgf3* mice develop prostatic hypertrophy (Muller *et al.*, 1990; Ornitz *et al.*, 1991) Similarly, MMTV-*Fgf7* transgenic mice develop the same phenotype as MMTV-*Fgf3* transgenic mice (Kitsberg and Leder, 1996). Both FGF3 and FGF7 proteins activate the KGF receptor (FGFR2b) (Miki *et al.*, 1991; Mathieu *et al.*, 1995), so it is not surprising that these FGFs, when over-expressed in the mammary gland as transgenes, result in similar mammary cancer phenotypes. Cooperativity of FGFs with *Wnt* genes in mammary gland cancer development has been demonstrated by two approaches: (1) more rapid tumorigenesis by insertional activation following MMTV infection of transgenic mice (Shackleford *et al.*, 1993; Lee *et al.*, 1995; MacArthur *et al.*, 1995c; Kapoun and Shackleford, 1997); and (2) more rapid tumorigenesis in bitransgenic *Fgf3/Wnt1* mice compared to the single transgenic mice (Kwan *et al.*, 1992).

Fgf8 was originally identified as a gene encoding an androgen inducible growth factor (Tanaka *et al.*, 1992). We identified *Fgf8* as a gene that is frequently activated by MMTV insertion in MMTV-*Wnt1* transgenic mice (MacArthur *et al.*, 1995c; Kapoun and Shackleford, 1997). *Fgf8* encodes multiple protein isoforms by alternative splicing at the 5′ end of the gene (Crossley and Martin, 1995; MacArthur *et al.*, 1995c), and these protein isoforms activate FGFR2c, FGFR3c, and FGFR4 (MacArthur *et al.*, 1995b; Blunt *et al.*, 1997). Normal functions of *Fgf8* are thought to include paracrine signaling during gastrulation, limb and central nervous system development (Crossley and Martin, 1995; Crossley *et al.*, 1996a,b; Meyers *et al.*,

Correspondence: CA MacArthur
Received 3 April 1998; revised 12 June 1998; accepted 12 June 1998

1998). FGF8b protein can transform NIH3T3 cells, demonstrating an oncogenic potential for at least one of the FGF8 isoforms (Kouhara *et al.*, 1994; MacArthur *et al.*, 1995a). *FGF8* expression has been described in human breast cancer samples (Tanaka *et al.*, 1995; Payson *et al.*, 1996). Here, we demonstrate that overexpression of FGF8b, and possibly other isoforms, in the mammary gland results in mammary tumorigenesis, confirming that overexpression of one or more isoforms of *Fgf8* is oncogenic for the mammary gland.

Results

Generation of MMTV-Fgf8 transgenic mice

To determine the mammary oncogenicity of *Fgf8*, we produced two transgenes under the control of the MMTV LTR (Figure 1). The MMTV-*Fgf8b* transgene contains the *Fgf8b* cDNA and encodes only the FGF8b protein isoform (Figure 1a). The MMTV-*Fgf8* transgene (Figure 1c) was cloned from genomic DNA from a previously described mammary tumor possessing a MMTV insertion into the *Fgf8* gene (tumor 86, (MacArthur *et al.*, 1995c)). PCR analysis of tail DNA from potential MMTV-*Fgf8b* founder transgenic animals revealed three founder animals that possessed the 179 bp amplified fragment (Figure 1b). The lower molecular weight fragment in Figure 1b likely represents a 'primer-dimer' artifact, since it is observed when the primers are added and independent of whether template DNA is present (data not shown). Mouse #4 was a male that never transmitted the transgene to any of his 70 offspring (data not shown). Mouse #14 was a female that transmitted the transgene to her offspring, but none of the offspring expressed the transgene (data not shown). Mouse #16 (8b-16) was a female whose first two litters died within 48 h of birth; all offspring appeared normal at birth. Subsequent litters were rescued with foster mothers, and the transgene was found to be transmitted and expressed. Although the offspring from 8b-16 required rescue by foster mothers, subsequent generations of this transgenic line did not require foster mother rescue. Southern blot analysis of potential founders of the MMTV-*Fgf8* transgene revealed two female founders (Mouse #3 and #17, Figure 1d). Both MMTV-*Fgf8* transgenic animals produced pups that died within 48 h of birth, possibly due to an inability to deliver milk.

Expression of MMTV-Fgf8 transgenes

Northern blot analysis of tissue RNAs from the 8b-16 transgenic line demonstrated strong expression of the transgene in normal parous mammary tissue and in mammary tumors with weaker expression in salivary glands (Figure 2a).

The MMTV-*Fgf8* transgenic founder #17 expressed the transgene in a somewhat different pattern, with highest levels of *Fgf8* RNA in mammary tumor, parous mammary glands, lung and ovary, and lower level in kidneys, salivary gland and spleen (Figure 2b). The MMTV-*Fgf8* transgenic founder #3 also expressed high levels of *Fgf8* RNA in mammary tumor and parous mammary glands (Figure 2b). A direct comparison showed that the extent of expression of the MMTV-*Fgf8* transgene was very similar to that of the MMTV-*Fgf8b* transgene in mammary glands and mammary tumors (Figure 2b).

To further identify the cells responsible for transgene expression, we employed *in situ* hybridization of frozen tissue sections, using an anti-sense *Fgf8b* riboprobe (Heikinheimo *et al.*, 1994). We observed weak expression of the MMTV-*Fgf8b* transgene in the ductal epithelium of the mammary gland (Figure

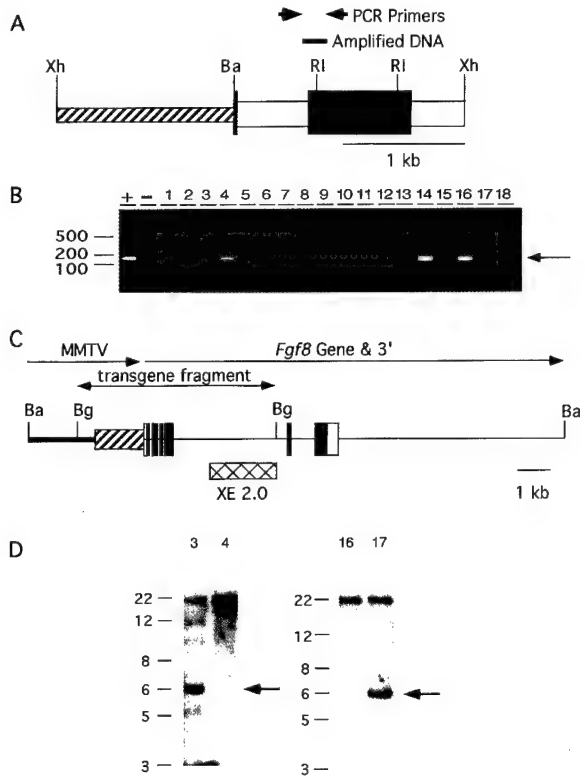

Figure 1 MMTV-*Fgf8* transgene constructs. Graphical representation of the MMTV-FGF8b (**a**) and MMTV-*Fgf8* (**c**) transgenes. Both transgenes are under the transcriptional control of the MMTV LTR (▨) in the same orientation as the *Fgf8* construct. In MMTV-*Fgf8b* (**a**), the *Fgf8b* cDNA is indicated by (▒), and as are rabbit β-globin exon (■) and intron (□) sequences of the MMTV-*Fgf8b* transgene. In the MMTV-*Fgf8b* transgene (**a**) translation starts and stops with the authentic *Fgf8* sites. Animals derived from the MMTV-*Fgf8b* transgene were screened by PCR methods with primers shown in (**a**). The expected amplified band was 179 bp (**b**). In (**b**), (+) is the positive control, (−) is the negative control, the numbers over the lanes represent potential MMTV-*Fgf8b* transgenic mice, and numbers at left indicate the molecular weight markers in basepairs (bp). Animals #4, 14, and 16 were positive for the MMTV-*Fgf8b* transgene (**b**). In the MMTV-*Fgf8* transgene (**c**), the entire *Fgf8* gene is present. The 15.5 kb transgene contains 12 kb of *Fgf8* sequence with 3.5 kb of the 3′ end of an inserted MMTV provirus. In (**c**), *Fgf8* exons that encode protein in all isoforms are designated by (■), alternatively spliced exons that encode protein in some isoforms are depicted by (▒), and non-coding exons are depicted by (□). The XE 2.0 probe (▩) used for Southern blot screening of *Bgl*II (Bg) digested tail DNA is indicated below the transgene. In (**d**), a Southern blot of tail DNA digested with *Bgl*II and hybridized to probe XE 2.0 is shown. The transgene fragment is a 6 kb band with these conditions (**c** and **d**), while the wild type *Fgf8* gene gives a 22 kb band under the same conditions (**c** and **d**). Note that the numbers in (**b**) and (**d**) refer to different animals and transgenes

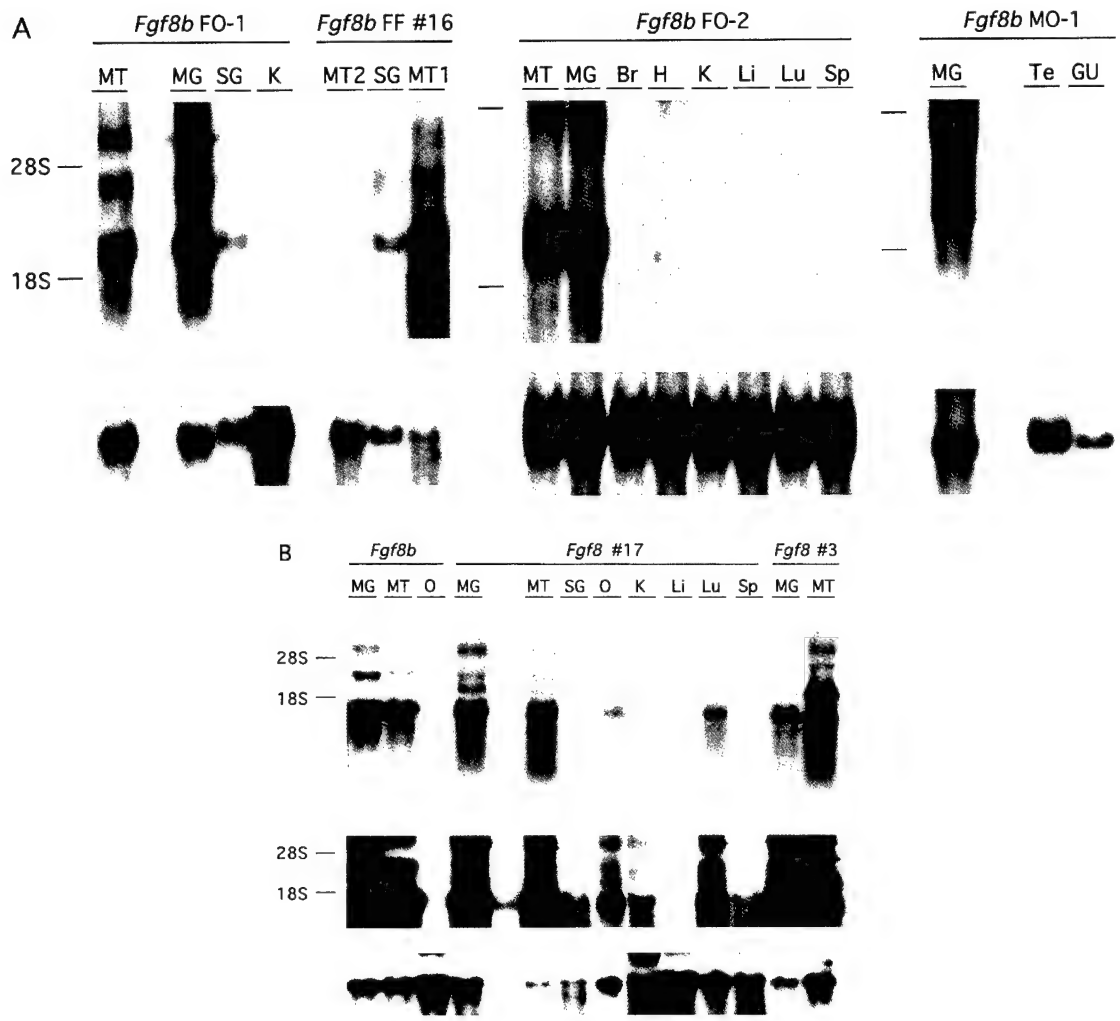

Figure 2 Northern blot analysis of MMTV-*Fgf8b* and MMTV-*Fgf8* transgene expression. (**a**) Upper panels: hybridized to murine *Fgf8b* cDNA. Lower panels: hybridized with rat GAPDH cDNA. RNAs were prepared from brain (Br), heart (H), kidney (K), liver (Li), lung (Lu), mammary tumors (MT), mammary glands (MG), ovary (O), salivary glands (SG), spleen (Sp), seminal vesicle/prostate (GU), and testis (Te), The 28S and 18S markers are indicated to the left of the blots. FO-1 and FO-2 refer to two female offspring of the founder female (FF #16) of the MMTV-*Fgf8b* transgenic line. MO-1 refers to a male offspring of FF #16. (**b**) Upper and middle panels: hybridized to murine *Fgf8b* cDNA. Middle exposure is approximately 10 times longer than upper exposure. Lower panel: hybridized to rat GAPDH cDNA. *Fgf8b* refers to the FO-1 animal in (**a**), the MMTV-*Fgf8b* transgenic line. *Fgf8* #3 and #17 are the founder transgenic mice for MMTV-*Fgf8* transgene

3a,b). In contrast, expression of the MMTV-*Fgf8b* transgene in lobular carcinomas from breeding animals was much higher (Figure 3a,b). No expression of the MMTV-*Fgf8b* transgene was detected in kidney (Figure 3c,d) or normal lung (Figure 3e,f). These *in situ* results (Figure 3) confirm the expression of the MMTV-FGF8b transgene in the 8b-16 transgenic line observed by Northern blot analysis (Figure 2) and localize its expression to the epithelial component of the hyperplastic and malignant mammary glands, as in MMTV-*Fgf3* and MMTV-*Fgf7* transgenic mice (Muller *et al.*, 1990; Ornitz *et al.*, 1991; Kitsberg and Leder, 1996).

Tumor incidence in MMTV-Fgf8 transgenic mice.

Forty-two transgenic females, 20 transgenic males, and 20 non-transgenic littermates (10 males and 10 females) from the MMTV-*Fgf8b* transgenic line 8b-16 were followed for the development of tumors (Figure 4). The transgenic females were separated into two groups: one group remained virgins (23 mice), and the other group was allowed to breed (19 mice). None of the 20 non-transgenic control littermates developed any type of tumor in the one year they were followed (Figure 4). Breeding transgenic females developed mammary gland tumors with a several month latency (Figure 4). The majority of tumors in this breeding cohort developed after six months of age and after multiple pregnancies (average number of pregnancies was six). Four virgin transgenic females developed fairly rapid tumors (all less than 4 months of age), but the remainder of the virgin transgenic mice did not develop tumors after one year (Figure 4). One transgenic male developed a mammary gland tumor (Figure 4). Salivary gland tumors were seen in three mice, all of which had

coincidental mammary gland tumors. The two actively breeding MMTV-*Fgf8* transgenic founder animals (Mice #3 and #17, Figure 1d) developed mammary tumors at a similar rate, showing tumors at five and eight months of age.

Histopathology of MMTV-Fgf8 transgenic mice

Histopathological analysis of tissues from MMTV-*Fgf8b* transgenic mice (line 8b-16) demonstrated ductal hyperplasia in the breeding females (Figure 5a), which preceded tumor development. The mammary tumors in this MMTV-*Fgf8b* transgenic line were lobular carcinomas in all cases (including the transgenic male) (Figure 5b,c, and data not shown). In eight of 20 of these MMTV-*Fgf8b* transgenic mice with mammary tumors, pleural-based metastases in the lungs were observed both grossly (data not shown) and microscopically (Figure 5d). Three animals with mammary tumors also had coincidental salivary gland tumors. These salivary gland tumors were adenocarcinomas that were well-circumscribed in all cases (Figure 5e).

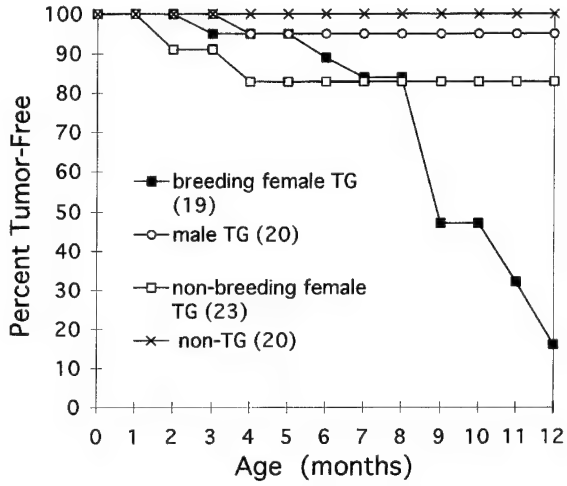

Figure 4 Tumor incidence versus age in MMTV-*Fgf8b* transgenic mice. The percentage of animals that remained tumor-free at each age in months is plotted. Female transgenic mice were split into 2 groups: breeding females (■) and virgin females (□). Non-transgenic littermates (10 male, 10 female) are indicated by (×), and transgenic males are indicated by (○). The total number of animals followed in each group are indicate in parentheses. The animals were followed for a maximum of 12 months

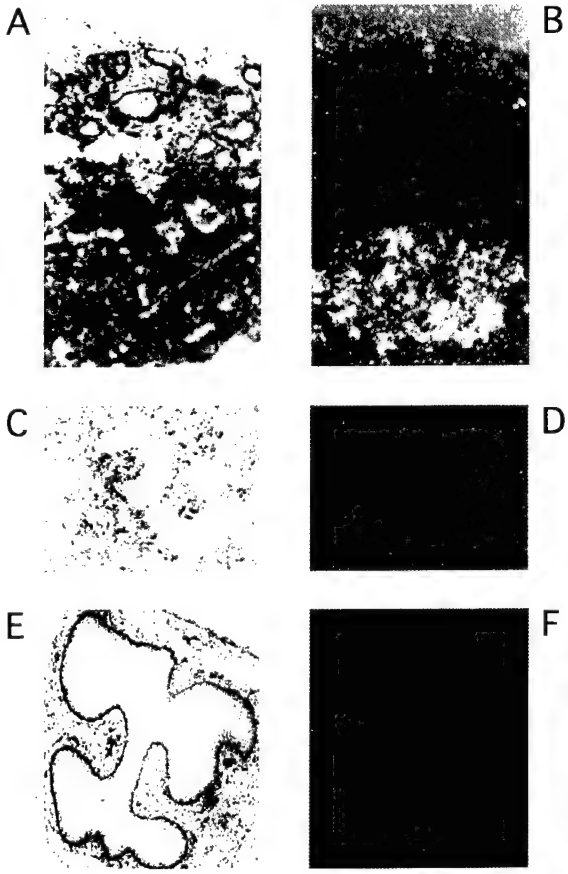

Figure 3 *In situ* hybridization analysis of MMTV-*Fgf8b* transgene expression. Bright field (**a, c, e**) and dark field (**b, d, f**) views of sections of frozen tissues derived from MMTV-*Fgf8b* transgenic mice (100×), hybridized to anti-sense FGF8b cDNA and stained with hematoxylin and eosin. (**a,b**), mammary gland containing normal (top) and tumor (lower) tissue, with expression of the transgene being higher in the tumor tissue; (**c,d**), kidney, with no transgene expression; and (**e,f**), lung/bronchus, with no transgene expression

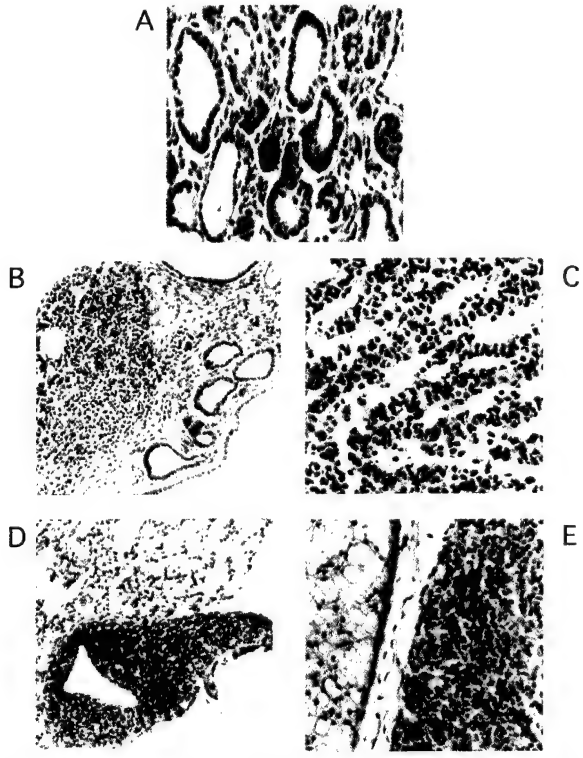

Figure 5 Histopathology of MMTV-*Fgf8b* transgenic mice. (**a**) Ductal hyperplasia in a mammary gland from a breeding female (400×). (**b**) Invasive lobular carcinoma in a mammary gland from a virgin female (100×). (**c**) Invasive lobular carcinoma in a mammary gland from a breeding female (400×). (**d**) Lung metastasis in a breeding female with an invasive lobular carcinoma (100×). (**e**) Salivary gland tumor (right) with adjacent normal salivary gland (left) (200×)

In the MMTV-*Fgf8* founder animals, ductal hyperplasia (Figure 6a) was seen in most non-tumorous mammary glands, and an adenoma (Figure 6b) was present in one of the mammary glands of these animals at the time of the development of infiltrating ductal adenocarcinomas (Figure 6c). Metastases were not observed in these two animals. Interestingly, these two animals were observed to have ovarian enlargement at necropsy, and histological examination of ovarian sections revealed stromal hyperplasia (Figure 6d), presumably as a direct result of transgene expression in this tissue (Figure 2b).

Discussion

Prior studies suggested that activation and inappropriate expression of *Fgf8* by MMTV insertion might be involved in mammary gland cancer development in mice (MacArthur *et al.*, 1995c; Kapoun and Shackleford, 1997). *FGF8* expression has been observed in human breast cancer cell lines (Payson *et al.*, 1996; Wu *et al.*, 1997), and the FGF8b protein isoform has been shown to transform NIH3T3 cells (Kouhara *et al.*, 1994; MacArthur *et al.*, 1995a). We now demonstrate that overexpression of the FGF8b isoform in the mammary and salivary glands (Figures 2 and 3), under the control of the MMTV LTR, results in the development of carcinomas of both tissues (Figure 5). Similarly, a transgene capable of overexpressing all of the FGF8 protein isoforms in several tissues results in the development of carcinomas of the mammary gland and ovarian stromal hyperplasia (Figure 6). Mammary ductal hyperplasia was seen in both transgenic lines, preceding the development of mammary adenocarcinomas in these transgenic lines (Figures 5 and 6). Although only one line of MMTV-*Fgf8b* transgenic mice was obtained, the expression patterns of the transgene, the corresponding phenotypes in the expressing tissues, and the similarity to the MMTV-*Fgf8* transgenic mice all strongly suggest that the observed phenotypes are due to the MMTV-*Fgf8b* transgene and not to insertion site effects.

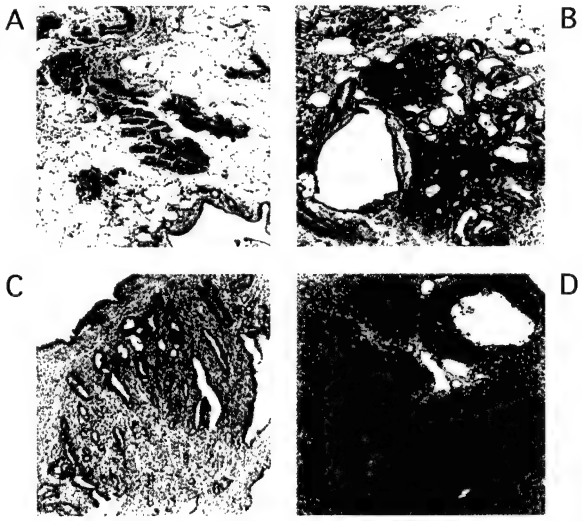

Figure 6 Histopathology of MMTV-*Fgf8* transgenic mice. (**a**) Non-neoplastic mammary gland (100×). (**b**) Adenoma of mammary gland (100×). (**c**) Invasive ductal carcinoma of the mammary gland (100×). (**d**) Stromal hyperplasia of ovary (100×)

In both MMTV-*Fgf8* transgenic lines, the development of most of the mammary adenocarcinomas was prolonged (Figure 4) and preceded by mammary ductal hyperplasia in the female mice (Figures 5 and 6). Only one tumor was seen in a male animal, and only four tumors in virgin females (Figure 4). The increased incidence of tumors in breeding females is likely due to higher expression of the transgene in the mammary glands with hormonal effects on the MMTV LTR (Haraguchi *et al.*, 1992; Le Ricousse *et al.*, 1996; Haraguchi *et al.*, 1997), together with the cell proliferation induced by cycles of pregnancy. The prolonged tumor latency indicates that additional genetic events are necessary for tumor development. Activated *Wnt* genes are likely candidates for one of these events in these tumors, given the strong oncogenic cooperation between FGFs and Wnts (Kwan *et al.*, 1992; Shackleford *et al.*, 1993; Lee *et al.*, 1995; Kapoun and Shackleford, 1997).

Although mammary adenocarcinomas developed in both MMTV-*Fgf8* transgenic lines, the histology was different in the two transgenic lines. MMTV-*Fgf8b* mice developed lobular adenocarcinomas (Figure 5) and MMTV-*Fgf8* mice developed ductal carcinomas (Figure 6). Possible explanations for this difference in mammary gland cancer histology between these two *Fgf8* transgenes include: (1) different levels of transgene expression; (2) different spatial or temporal expression of the transgenes in the mammary gland; and (3) effects of heterodimerization of FGF8 isoforms. Different quantitative levels of expression are possible, due to differences in transgene copy number, or insertion site. However, we did not detect significant differences in expression of the transgenes, as detected by Northern blot (Figure 2b). Different spatial or temporal expression patterns in the mammary gland of the two transgenes might be due to differences in the transgene insertion sites, or perhaps more likely to enhancers present in the MMTV-*Fgf8* transgene that are not present in the MMTV-*Fgf8b* transgene. We have previously demonstrated that the different FGF8 isoforms interact with the different FGFRs in a redundant fashion, with FGF8b activating FGFR2c, FGFR3c, and FGFR4 (MacArthur *et al.*, 1995b; Blunt *et al.*, 1997). Our work did not address the possibility that different FGF8 isoforms might heterodimerize and interact in a quantitatively or qualitatively different fashion with the known FGFRs (McKeehan and Kan, 1994). Thus it is possible that quantitatively or qualitatively different interactions due to potential heterodimerization of FGF8 isoforms present in the MMTV-*Fgf8* transgenic mammary gland might be responsible for the ductal tumor histology observed in this line.

Another intriguing difference between the two transgenic lines produced here is the ovarian stromal hyperplasia of the MMTV-*Fgf8* transgenic mice (Figure 6). This phenotype is rare, if not unique, among mice generated using MMTV LTR-driven transgenes. Since both MMTV-*Fgf8* transgenic founders of this transgene displayed the ovarian hyperplasia, it seems probable that the transgene, which consists of the entire *Fgf8* gene and at least 6 kb of downstream

genomic sequences, contains enhancers that promote expression in ovarian tissue. Indeed, the ovary is one of the few sites of normal *Fgf8* expression in the adult mouse, suggesting that the *Fgf8* gene contains such ovary-specific enhancers (MacArthur *et al.*, 1995c).

FGF8b is known to be produced by epithelial cells, and to activate in a paracrine manner FGFR2c, FGFR3c, and FGFR4, which are primarily located in mesenchymal locations (MacArthur *et al.*, 1995b; Ornitz *et al.*, 1996; Blunt *et al.*, 1997). We demonstrate expression of the MMTV-*Fgf8b* transgene in the epithelial compartment of the mammary tumors (Figure 3). Given the observed FGF8b interactions with FGFRs, we would not expect FGF8b to act in an autocrine manner to stimulate mammary epithelial growth and tumorigenesis directly. FGF7 is known to be produced by mesenchymal cells and to interact with epithelially localized FGFR2b, in a paracrine fashion (Rubin *et al.*, 1995; Ornitz *et al.*, 1996). FGF7 is a physiological stimulus for mammary epithelial growth (Coleman-Krnacik and Rosen, 1994; Imagawa *et al.*, 1994; Ulich *et al.*, 1994). Furthermore, MMTV-*Fgf7* transgenic mice develop mammary adenocarcinomas with lung metastases (Kitsberg and Leder, 1996), similar to our MMTV-*Fgf8b* transgenic mice. On the basis of these findings, we speculate that overexpression of FGF8b in the epithelial compartment results in the up-regulation of FGF7, or another epithelial growth factor(s), in the mesenchymal compartment of the mammary gland, which then provides the stimulus for mammary epithelial growth, and ultimately ductal hyperplasia and adenocarcinomas. This coupled paracrine stimulation occurs in vertebrate limb development, where FGF10 (an FGF closely related to FGF7) in the limb mesenchyme induces expression of FGF8 in the apical ectodermal ridge, and FGF8 expression in the apical ectodermal ridge maintains FGF10 expression in the mesenchyme (Ohuchi *et al.*, 1997).

The MMTV-*Fgf8b* transgenic line displayed a metastatic phenotype, similar to MMTV-*Fgf7* transgenic mice (Kitsberg and Leder, 1996), with several of our animals becoming ill-appearing during the development of the tumors. This is an uncommon phenotype for mouse models of mammary gland cancer. The similarities in the MMTV-*Fgf7* and MMTV-*Fgf8b* transgenic mouse phenotypes, and the possible cross-paracrine interactions between FGF7 and FGF8b make it difficult to sort out which FGF, if either, might be primarily responsible for the metastatic phenotype. Future work looking at the expression differences in hyperplastic mammary glands, primary tumors, and metastatic lesions from these mice might elucidate unique metastatic genes.

Materials and methods

*Preparation of MMTV-*Fgf8 *transgenes*

The MMTV-*Fgf8b* transgene was prepared by inserting the murine *Fgf8b* cDNA (MacArthur *et al.*, 1995c) into the *Eco*RI site of pMMTV-TGFα (Matsui *et al.*, 1990), thereby replacing TGFα with FGF8b. The pMMTV-*Fgf8b* plasmid was digested with *Afl*III (New England Biolabs) and *Xho*I (Promega), and the 3.4 kb MMTV-*Fgf8b* transgene (Figure 1a) was purified by low melting agarose gel electrophoresis (Life Sciences Tech.), followed by treatment with β-Agarase (New England Biolabs), and ethanol precipitation.

The MMTV-*Fgf8* transgene was obtained by cloning the 15.5 kb *Bam*HI fragment, containing the *env* gene 3′ of the *Bam*HI site in MMTV, the 3′ LTR, and 12 kb of genomic sequence containing *Fgf8*, from mammary tumor 86 DNA (Figure 1c) (MacArthur *et al.*, 1995c). This cloning was accomplished by digesting tumor 86 DNA with *Bam*HI, size selecting the DNA on a low-melting agarose gel and purifying the DNA with β-Agarase. The *Bam*HI-digested DNA was ligated into λ-Dash II (Stratagene), packaged into phage, and the resulting phage library screened for the correct insert with the genomic fragment, XE 2.0 (Figure 1c), and with a MMTV-*env* fragment, EB 0.9 (data not shown). The 15.5 kb MMTV-*Fgf8* insert from the correct phage was isolated by digestion with *Bam*HI, size selection in a 0.5% agarose gel, and purified using beads from the Lambda Quick Kit (BIO 101, Inc.) and ethanol precipitation.

*Generation of MMTV-*FGF8 *transgenic mice*

Pronuclear injection of the MMTV-*Fgf8b* transgene into C57BL/6 × SJL F1 hybrid embryos, followed by insertion of the embryos into pseudo-pregnant females, was performed at the NICHD Transgenic Development Facility at the University of Alabama, Birmingham, USA. Potential founder animals were analysed by PCR of tail DNA (1 μg), using a forward primer in the rabbit β-globin intron 2 (5′-GGCAACGTGCTGGTTATTGTG-3′) and a reverse primer in the FGF8b cDNA (5′-TCTGCTCCCTCACATGCTGTG-3′). PCR conditions were as follows: 95°C for 3 min, then 35 cycles of 94°C for 30 s, 57°C for 30 s, and 72°C for 30 s. Three of 18 potential founders were positive for the 179 bp amplified fragment, signifying possession of the MMTV-*Fgf8b* transgene (Figure 1b). The founder mice were bred to FVB mice, and offspring were analysed by the PCR methods above.

MMTV-*Fgf8* transgenic mice were prepared by pronuclear injection of the transgene into C57BL/6 × SJL F1 hybrid fertilized eggs, followed by placement of the embryos into pseudo-pregnant females at the Norris Cancer Center Transgenic Mouse Core Facility of the University of Southern California. Potential founder animals were screened by Southern blot analysis using Bgl II digestion of the DNA and the XE 2.0 probe. Southern blotting was performed as described (MacArthur *et al.*, 1995c) on 10 μg of tail DNA. The normal *Fgf8* genomic fragment is 22 kb in size with *Bgl*II digestion and XE 2.0 as the probe; the MMTV-*Fgf8* transgene fragment is 6 kb in size (Figures 1c and 1d).

Analysis of transgene expression

Total RNA was prepared from tissues from transgenic mice by the guanidium isothiocyanate/acid phenol method (Chomczynski and Sacchi, 1987). RNAs (10–20 μg) were denatured in formaldehyde/HEPES-Acetate-EDTA with 50% formamide, and electrophoresed in 1% agarose/formaldehyde/HEPES-Acetate-EDTA gels as described (MacArthur *et al.*, 1995c). Capillary blotting, UV-cross-linking, hybridization to random primed labeled DNA probes, washing and exposure to x-ray film was as described (MacArthur *et al.*, 1995c).

Histological sections of MMTV-*Fgf8b* transgenic animals were prepared from tissues either fixed in 4% paraformaldehyde, or snap frozen in liquid nitrogen. Following fixation or freezing, the sections were cut by the Washington University Department of Molecular Biology and Pharmacology Histology Core Facility. Fixed sections were stained with

hematoxylin and eosin, and photographed with an Olympus BX60 microscope and a Olympus PM-30 automatic photomicrographic system. Frozen sections were subjected to *in situ* hybridization with 1×10^6 counts/min. of ^{33}P-labeled antisense or sense riboprobes to the FGF8b cDNA, as described (Wilkinson, 1992). Bright-field and dark-field photomicroscopy was performed with an Olympus BX60 microscope and a Olympus PM-30 automatic photomicrographic system.

MMTV-*Fgf8* transgenic tissues were prepared for histology by fixing in 10% formalin. Paraffin-embedded sections were cut, stained in hematoxylin and eosin, and photographed by the Children's Hospital Los Angeles Pathology Core Facility.

Acknowledgements
We would like to thank Dr B Hogan for providing the MMTV-TGFα plasmid, and R Lopez-Diego and M Wuerffel for technical assistance. The MMTV-*Fgf8b* mice were created at the NICHD Transgenic Mouse Development Facility at the University of Alabama, Birmingham, USA, under the direction of Dr C Pinkert (N01-HD-5-3229). This work was funded by NIH grants R01 CA 70106 (to CAM) and R01 CA 60673 (to DMO), as well as grants from the Edward Mallinckrodt, Jr., Foundation (to CAM), the University of California Breast Cancer Research Program, 1RB-0484 (to GMS), and the Department of Defense Breast Cancer Research Program, DAMD17-96-1-6039 (to GMS), and DAMD17-94-J-4319 (to DBS).

References

Bansal GS, Cox HC, Marsh S, Gomm J, Yiangou C, Luqmani Y, Coombes RC and Johnston CL. (1997). *Br. J. Cancer*, **75**, 1567–1574.
Basilico C and Moscatelli D. (1992). *Adv. Cancer Res.*, **59**, 115–165.
Blunt AG, Lawshé A, Cunningham ML, Seto ML, Ornitz DM and MacArthur CA. (1997). *J. Biol. Chem.*, **272**, 3733–3738.
Chomczynski P and Sacchi N. (1987). *Anal. Biochem.*, **162**, 156–159.
Coleman-Krnacik S and Rosen JM. (1994). *Mol. Endocrinol.*, **8**, 218–29.
Crossley PH and Martin GR. (1995). *Development*, **121**, 439–451.
Crossley PH, Martinez S and Martin GR. (1996a). *Nature*, **380**, 66–68.
Crossley PH, Minowada G, MacArthur CA and Martin GR. (1996b). *Cell*, **84**, 127–136.
Dickson C, Smith R, Brookes S and Peters G. (1984). *Cell*, **37**, 529–536.
Haraguchi S, Good RA, Engelman RW and Day NK. (1992). *Int. J. Cancer*, **52**, 928–33.
Haraguchi S, Good RA, Engelman RW, Greene S and Day NK. (1997). *Mol. Cell. Endocrinol.*, **129**, 145–55.
Harris JR, Lippman ME, Veronesi U and Willett W. (1992a). *New Engl. J. Med.*, **327**, 319–328.
Harris JR, Lippman ME, Veronesi U and Willett W. (1992b). *New Engl. J. Med.*, **327**, 473–480.
Heikinheimo M, Lawshé A, Shackleford GM, Wilson DB and MacArthur CA. (1994). *Mech. Dev.*, **48**, 129–138.
Imagawa W, Cunha GR, Young P and Nandi S. (1994). *Biochem. Biophys. Res. Comm.*, **204**, 1165–1169.
Jaakkola S, Salmikangas P, Nylund S, Partanen J, Armstrong E, Pyrhonen S, Lehtovitra P and Nevanlinna H. (1993). *Int. J. Cancer*, **54**, 378–382.
Jacquemier J, Adelaide J, Parc P, Penault-Llorca F, Planche J, DeLapeyriere O and Birnbaum D. (1994). *Int. J. Cancer*, **59**, 373–378.
Johnson DE and Williams LT. (1993). *Adv. Cancer Res.*, **60**, 1–41.
Kapoun AM and Shackleford GM. (1997). *Oncogene*, **14**, 2985–2989.
Kitsberg DI and Leder P. (1996). *Oncogene*, **13**, 2507–2515.
Kouhara H, Koga M, Kasayama S, Tanaka A, Kishimoto T and Sato B. (1994). *Oncogene*, **9**, 455–462.
Kwan HC, Pecenka V, Tsukamoto AS, Parslow TG, Guzman R, Lin TP, Muller WJ, Lee FS, Leder P and Varmus HE. (1992). *Mol. Cell Biol.*, **12**, 147–154.
Le Ricousse S, Gouilleux F, Fortin D, Joulin V and Richard-Foy H. (1996). *Proc. Natl. Acad. Sci. USA*, **93**, 5072–7.
Lee FS, Lane TF, Kuo A, Shackleford GM and Leder P. (1995). *Proc. Natl. Acad. Sci. USA*, **92**, 2268–72.
MacArthur CA, Lawshé A, Shankar DB, Heikinheimo M and Shackleford GM. (1995a). *Cell Growth Diff.*, **6**, 817–825.
MacArthur CA, Lawshe A, Xu JS, Santos-Ocampo S, Heikinheimo M, Chellaiah AT and Ornitz DM. (1995b). *Development*, **121**, 3603–3613.
MacArthur CA, Shankar DB and Shackleford GM. (1995c). *J. Virol.*, **69**, 2501–2507.
Mathieu M, Chatelain E, Ornitz D, Bresnick J, Mason I, Kiefer P and Dickson C. (1995). *J. Biol. Chem.*, **270**, 24197–24203.
Matsui Y, Halter SA, Holt JT, Hogan BL and Coffey RJ. (1990). *Cell*, **61**, 1147–55.
McKeehan WL and Kan M. (1994). *Mol. Reproduct. Dev.*, **39**, 69–82.
Meyers EN, Lewandoski M and Martin GR. (1998). *Nature Genet.*, **18**, 136–141.
Miki T, Fleming TP, Bottaro DP, Rubin JS, Ron D and Aaronson SA. (1991). *Science*, **251**, 72–75.
Muller WJ, Lee FS, Dickson C, Peters G, Pattengale P and Leder P. (1990). *EMBO J.*, **9**, 907–13.
Ohuchi H, Nakagawa T, Yamamoto A, Araga A, Ohata T, Ishimaru Y, Yoshioka H, Kuwana T, Nohno T, Yamasaki M, Itoh N and Noji S. (1997). *Development*, **124**, 2235–2244.
Ornitz DM, Moreadith RW and Leder P. (1991). *Proc. Natl. Acad. Sci. USA*, **88**, 698–702.
Ornitz DM, Xu JS, Colvin JS, McEwen DG, MacArthur CA, Coulier F, Gao GX and Goldfarb M. (1996). *J. Biol. Chem.*, **271**, 15292–15297.
Payson RA, Wu J, Liu Y and Chiu IM. (1996). *Oncogene*, **13**, 47–53.
Penault-Llorca F, Bertucci F, Adelaide J, Parc P, Coulier F, Jacquemier J, Birnbaum D and deLapeyriere O. (1995). *Int. J. Cancer*, **61**, 170–176.
Peters G, Brookes S, Smith R, Placzek M and Dickson C. (1989). *Proc. Natl. Acad. Sci. USA*, **86**, 5678–5682.
Rubin JS, Bottaro DP, Chedid M, Miki T, Ron D, Cheon G, Taylor WG, Fortney E, Sakata H, Finch PW *et al.* (1995). *Cell Biol. Int.*, **19**, 399–411.
Shackleford GM, MacArthur CA, Kwan HC and Varmus HE. (1993). *Proc. Natl. Acad. Sci., USA*, **90**, 740–744.
Tanaka A, Miyamoto K, Matsuo H, Matsumoto K and Yoshida H. (1995). *FEBS Letters*, **363**, 226–230.
Tanaka A, Miyamoto K, Minamino N, Takeda M, Sato B, Matsuo H and Matsumoto K. (1992). *Proc. Natl. Acad. Sci., USA*, **89**, 8928–8932.
Ulich TR, Yi ES, Cardiff R, Yin SM, Bikhazi N, Biltz R, Morris CF and Pierce GF. (1994). *Am. J. Pathol.*, **144**, 862–868.
Wilkinson DG. (1992). *In Situ hybridization – a practical approach*. IRL Press, Oxford.
Wu J, Payson RA, Lang JC and Chiu IM. (1997). *J. Steroid Biochem. Mol. Biol.*, **62**, 1–10.
Yiangou C, Gomm JJ, Coope RC, Law M, Luqmani YA, Shousha S, Coombes RC and Johnston CL. (1997). *Br. J. Cancer*, **75**, 28–33.

FGF-8 Isoforms Differ in NIH3T3 Cell Transforming Potential[1]

Craig A. MacArthur,[2] Avril Lawshé, Deepa B. Shankar, Markku Heikinheimo, and Gregory M. Shackleford

Department of Pediatrics, Washington University School of Medicine, St. Louis, Missouri 63110 [C. A. M., A. L., M. H.]; Departments of Molecular Microbiology and Immunology [D. B. S., G. M. S.] and Pediatrics [G. M. S.], University of Southern California School of Medicine, Division of Hematology-Oncology, Childrens Hospital Los Angeles, Los Angeles, California 90027; and Children's Hospital, University of Helsinki, 00290 Helsinki, Finland [M. H.]

Abstract

We previously identified *Fgf-8* as a frequently activated gene in tumors from mouse mammary tumor virus-infected *Wnt-1* transgenic mice, suggesting that *Fgf-8* is a proto-oncogene. We further determined that multiple, secreted protein isoforms that differ at their mature amino termini are encoded by alternatively spliced mRNAs transcribed from the gene. We now present evidence that there are differences in the potency of NIH3T3 cell transformation displayed by three of the FGF (fibroblast growth factor)-8 isoforms. We find that stable transfection of a cDNA for the FGF-8b isoform leads to marked morphological transformation of NIH3T3 cells and rapid tumorigenicity of the transfected cells in nude mice. In contrast, transfection of a cDNA for the FGF-8a or FGF-8c isoform results in moderate morphological changes in the NIH3T3 cells, and the transfected cells are weakly tumorigenic in nude mice. All three transfections result in cells that express comparable amounts of *Fgf-8* mRNA and that produce the FGF-8 protein isoforms. The morphological changes observed in NIH3T3 cells can be reproduced by the addition of recombinant FGF-8 protein isoforms to the culture medium. Therefore, these results indicate that there are differences in the potency of transformation of NIH3T3 cells by FGF-8 protein isoforms and suggest that these FGF-8 isoforms may have different *in vivo* functions.

Introduction

Oncogenesis is a multistep process involving the sequential acquisition of multiple genetic alterations. Because this process is prolonged and complicated in humans (1), animal models to study the process of oncogenesis are desirable. We have used a *Wnt-1* transgenic mouse model to study breast cancer development (2). We infected *Wnt-1* transgenic mice with mouse mammary tumor virus to accelerate tumorigenesis and to "molecularly tag" proto-oncogenes that are activated in the resulting tumors and that cooperate with *Wnt-1* in mammary tumorigenesis (3, 4). Using this approach, we identified *Fgf-3* and *Fgf-4* as *Wnt-1*-collaborating proto-oncogenes (3) and subsequently cloned a genomic locus that contained MMTV insertions in the DNA from several mammary tumors of MMTV-infected *Wnt-1* transgenic mice (4). We determined that the activated gene in this locus was also a member of the FGF[3] family, *Fgf-8*, previously described as androgen-induced growth factor (5).

FGFs are a family of growth factors, related by amino acid sequence similarity, that are encoded by at least nine genes in mammals (5–7). They are mitogenic for a variety of cell types, although their physiological roles *in vivo* may be in wound healing and embryonic development (reviewed in Ref. 8). FGFs are thought to elicit their effects by binding to high affinity tyrosine kinase receptors on the cell surface, encoded by a family of at least four genes (*Fgfr1–4*) in mammals (9–15). Heparan sulfate proteoglycans are low affinity cell surface receptors important for FGF effects (16, 17), although heparin can substitute for these receptors *in vitro* (18). In addition, a cysteine-rich transmembrane receptor for FGFs exists, but its significance to FGF effects is unknown (19). Most *Fgf* genes code for single proteins (6), but different isoforms of FGF-2 and FGF-3 exist and have different cellular locations, due to alternative translation initiation (20–23).

Fgf-8 consists of at least six exons and codes for at least seven protein isoforms, due to alternative splicing of the primary transcript (4, 5, 24). RNAs for the FGF-8 isoforms are present during murine embryogenesis (4, 24–26) and are detectable only in gonadal tissue of adult mice at low levels (4). These results and the insertional activation of *Fgf-8* described above suggest that *Fgf-8* is a normal embryonic gene that is oncogenic when overexpressed in adult mammary tissue. The significance of the different FGF-8 isoforms is not known; however, we hypothesize that their existence suggests that they have different biological properties.

Overexpression of FGF-3 (27), FGF-4 (28), FGF-5 (29), FGF-6 (30), and at least one FGF-8 isoform, FGF-8b (pSC17) (5, 31), can transform NIH3T3 cells. Given the ability to observe a phenotype in NIH3T3 cells in response to FGFs, we decided to test the hypothesis that the FGF-8 isoforms might possess different biological properties by stably transfecting NIH3T3 cells with cDNAs for the three FGF-8 isoforms we identified previously (4). We confirm previous findings that transfection and expression of the *Fgf-8b* cDNA in NIH3T3 cells strongly transforms them, such that they become altered morphologically, clonagenic in soft agar, and tumorigenic in nude mice (31). In contrast, trans-

Received 1/25/95; revised 4/7/95; accepted 4/28/95.

[1] This work was supported by NIH Grant R01CA58412 (to G. M. S.), research grants to C. A. M. from the Elsa U. Pardee Foundation and the Edward Mallinckrodt, Jr. Foundation. C. A. M. is supported by an American Society of Clinical Oncology Young Investigator Award (sponsored by the Don Shula Foundation), an Intramural Research Grant from the American Cancer Society, and NIH Training Award 5K12CA0170403. G. M. S. is supported by a Junior Faculty Research Award from the American Cancer Society. D. B. S. is supported by a predoctoral fellowship for breast cancer research (DAMD17–94-J-4319) from the Department of the Army. M. H. is supported by the Finnish Cultural Foundation and the Paulo Foundation.

[2] To whom requests for reprints should be addressed.

[3] The abbreviations used are: FGF, fibroblast growth factor; FGFR, FGF receptor; rFGF-8, recombinant FGF-8; G418^r, G418 resistant; DMEM-FCS, DMEM supplemented with 10% FCS, 2 mM L-glutamine, 100 units/ml penicillin, and 100 μg/ml streptomycin; HRP, horseradish peroxidase; PBS-Ca, PBS with 1 mM $CaCl_2$; nt, nucleotides.

fection and expression of the *Fgf-8a* or the *Fgf-8c* cDNA in NIH3T3 cells lead to more subtle morphological changes. The morphological changes in all cases can be produced by adding the rFGF-8 isoform to the culture medium. NIH3T3 cells producing FGF-8a or FGF-8c are not clonagenic in soft agar and are less tumorigenic than FGF-8b-producing cells, despite similar amounts of FGF-8 isoform RNA and protein being made. These results indicate that the FGF-8 isoforms have different potencies for transformation of NIH3T3 cells and suggest that they may have different functions *in vivo*.

Results

NIH3T3 Cells Transfected with Different *Fgf-8* cDNAs Display Different Morphologies. We have identified three FGF-8 isoforms in our prior work (4) and hypothesize that they have different biological properties. To begin to test this hypothesis, we subcloned the cDNAs encoding the three FGF-8 isoform cDNAs into the expression vector pMIRB (Fig. 1). The majority of the amino acids encoded by these three FGF-8 isoform cDNAs are identical, but they differ in the region immediately following the signal peptide, *i.e.*, the amino terminal portions of the mature secreted proteins (4, 5). The resulting vectors were used in transfection experiments of NIH3T3 cells, and stable cell lines were selected with G418. We chose to pool the selected G418^r cells rather than individually clone them, so as to preclude inaccuracies due to clonal variation. The expression vector used, pMIRB, allowed this approach, since virtually all selected G418^r cells would express the FGF-8 isoform (Fig. 1).

NIH3T3 cells transfected with expression vectors coding for the FGF-8 isoforms and selected for G418 resistance display different morphologies (Fig. 2). In agreement with previous results (31), cells transfected with pMIRB containing the *Fgf-8b* cDNA (hereafter called 8B cells) displayed marked morphological transformation with an elongated, spindle-like shape (Fig. 2). In contrast, cells transfected with pMIRB containing the *Fgf-8a* cDNA (hereafter called 8A cells) or with pMIRB containing the *Fgf-8c* cDNA (hereafter called 8C cells) displayed modest morphological transformation and a flatter morphology (Fig. 2). NIH3T3 cells transfected with the pMIRB vector alone (no *Fgf-8* cDNA, called MIRB cells hereafter) were morphologically identical to nontransfected NIH3T3 cells (Fig. 2). We have observed variability in the degree of morphological transformation observed in 8A cells, ranging from morphologies like MIRB cells to morphologies like 8C cells, which we suspect may be due to different levels of FGF-8a (data not shown). These results suggest that the different FGF-8 isoforms have different potencies with respect to morphological transformation of NIH3T3 cells.

Transfected NIH3T3 Cells Express the *Fgf-8* cDNAs. To demonstrate expression of the transfected cDNAs, we prepared total RNAs from pools of G418^r NIH3T3 cells that were transfected with the *Fgf-8* cDNA (and control) vectors described above. We analyzed RNAs from the cell lines using an antisense 5′ *Fgf-8b* riboprobe in an RNase protection assay (25). The antisense *Fgf-8b* riboprobe is 317 nt in length and is digested to 153 nt when protected by *Fgf-8a* RNA, 222 nt when protected by *Fgf-8b* RNA, and 157 nt when protected by *Fgf-8c* RNA. We observed the correct size-protected fragment in each of the 8A, 8B, and 8C cell lines but did not observe any protected fragments in the MIRB line (Fig. 3). These results confirm that the correct

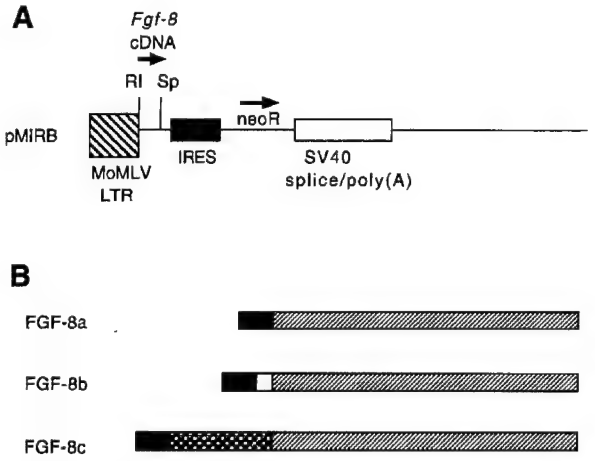

Fig. 1. Schematic representation of FGF-8 protein isoforms and plasmids used for transfection. *A*, representation of the expression vector, pMIRB. Transcription from the Moloney murine leukemia virus long terminal repeat (*MoMLV LTR*, ▧) of the transfected plasmid results in a single transcript that uses SV40 splicing and polyadenylation sequences (□). An internal ribosome entry site (■, *IRES*) allows eukaryotic ribosomes to initiate translation of the sequences coding for G418 resistance (*neoR*). The *Fgf-8* cDNAs were directionally cloned into the *Eco*RI (*RI*) and blunted *Spe*I (*Sp*) restriction sites. Translation start and stop codons and the sequence encoding the signal peptide for the FGF-8 isoforms were present in the *Fgf-8* cDNAs. The plasmid base for pMIRB is pBluescript II KS– (Stratagene). *B*, representation of the pre-FGF-8a, FGF-8b, and FGF-8c protein isoforms, depicted amino terminus (*left*) to carboxy terminus (*right*) ▨, common carboxyl region of the FGF-8 isoforms; □ and ▩, the unique amino terminal extensions for FGF-8b and FGF-8c, respectively; ■, the common signal peptide, which is not part of the mature FGF-8 isoforms.

FGF-8 isoform mRNA was produced by the 8A, 8B, and 8C cell lines.

To control for differences in RNA loading and to confirm the integrity of the RNAs, we performed a RNase protection assay with an antisense β-actin riboprobe. This riboprobe is 300 nt in length and is digested to 250 nt when protected by β-actin mRNA. All four cell lines protected a 250-nt fragment (Fig. 3). The resulting gels were quantitatively imaged and analyzed as described in "Materials and Methods." The cell lines make comparable amounts of *Fgf-8* RNA (Fig. 3). The 8B cells, which have the most dramatic morphology, actually produce less *Fgf-8* RNA than the 8A and 8C cell lines, indicating that the weaker biological responses of 8A and 8C cells cannot be explained by low expression levels.

The Transfected NIH3T3 Cells Produce FGF-8 Protein. Although the RNase protection assays in Fig. 3 show that the 8A, 8B, and 8C cell lines appropriately expressed the transfected *Fgf-8* cDNAs, it is formally possible that one or more of the FGF-8 isoform proteins might not be produced or may be rapidly degraded. To address this question, we prepared an affinity-purified polyclonal antibody to FGF-8a (anti-mouse FGF-8) that should theoretically bind the three FGF-8 isoforms. The affinity-purified anti-mouse FGF-8 was tested in Western blot analysis of rFGF-8 isoform proteins and bound the three rFGF-8 isoforms (Fig. 4). FGF-8 isoforms were not readily detected in the conditioned medium from these cell lines by immunoblotting, possibly due to FGF-8 binding to cell surface heparan-sulfated proteoglycans (16, 17).

To demonstrate the production of FGF-8 isoforms in these cells, we performed immunohistochemical staining of the

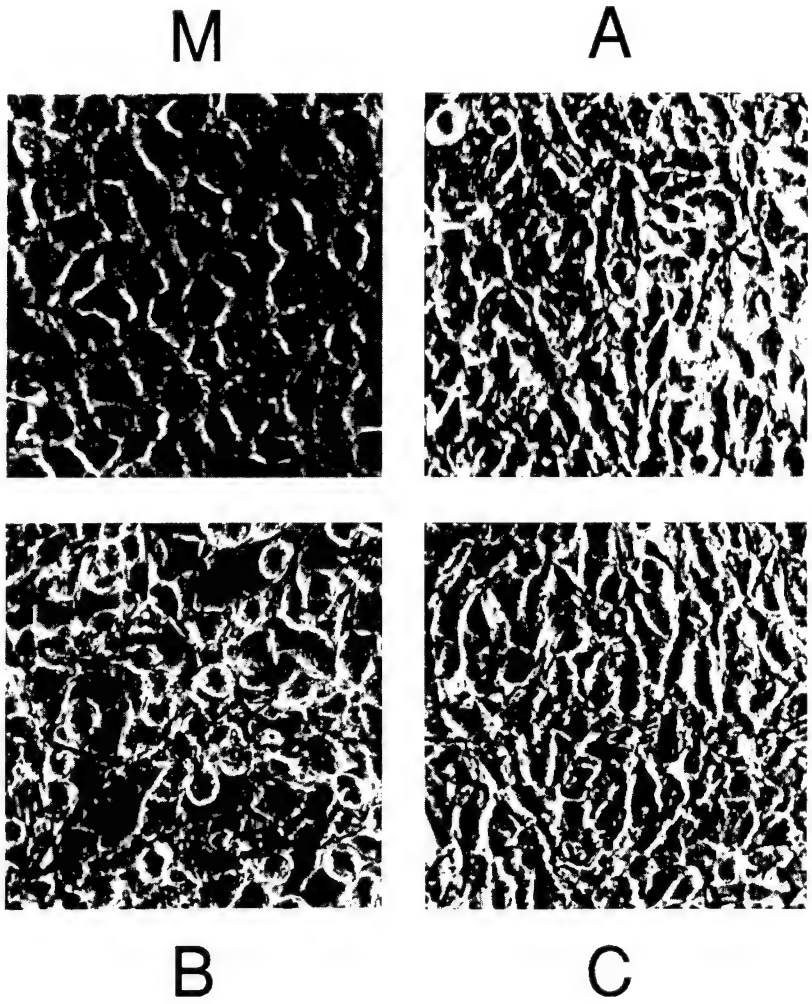

Fig. 2. NIH3T3 cells transfected with different *Fgf-8* isoform cDNAs display different morphologies. Pooled G418^r NIH3T3 cells, transfected with pMIRB only (*M*), pMIRB containing the *Fgf-8a* cDNA (*A*), pMIRB containing the *Fgf-8b* cDNA (*B*), or pMIRB containing the *Fgf-8c* cDNA (*C*) were grown as described in "Materials and Methods."

fixed cell lines using a biotin-avidin-labeled secondary antibody system with HRP staining. The 8A, 8B, and 8C cell lines show positive staining using the affinity-purified, anti-FGF-8 polyclonal antibody described above, although the control MIRB cells do not (Fig. 5). These results confirm that the 8A, 8B, and 8C cell lines produce detectable amounts of FGF-8 isoform protein and suggest that the morphological differences in the transfected cells are not due to absence of the protein but rather are due to differences in the potency of FGF-8 isoforms to transform NIH3T3 cells.

NIH3T3 Cells Producing Different FGF-8 Protein Isoforms Display Different *in Vitro* and *in Vivo* Properties. The pooled G418^r cells from each isoform transfection were compared in several biological assays. The doubling times of the cells lines were examined, and the 8A, 8B, and 8C cell lines displayed slightly shorter doubling times when compared to the MIRB cells (16 h *versus* 18 h), but the difference was not statistically significant (Table 1). In conditions of lower serum (2% FCS and 8% newborn serum), the MIRB and 8A cells died, while the 8C cells stopped growing but did not die (Table 1). 8B cells continued to grow and displayed the same transformed morphology (Table 1 and data not shown), suggesting that it was the more potent FGF-8 transforming protein.

We examined the saturation densities of the FGF-8-expressing cell lines and found clear differences. At confluence, the number of 8A, 8B, and 8C cells was two, five, and four times the number of MIRB cells, respectively (Table 1). In soft agar clonagenicity assays, only 8B cells were able to form soft agar colonies at an average frequency of 5% (Table 1). These *in vitro* assays of proliferation and transformation all suggest that FGF-8b is the more potent transforming protein isoform.

In nude mice tumorigenicity assays (Table 1), tumors formed rapidly when 10^6 8B cells were injected into nude mice, with all 10 animals possessing fibrosarcomas 2 cm or larger after 1 week. No tumors were seen in animals injected with 10^6 MIRB cells, even after 4 months of observation. Tumors were observed in two of four animals injected with 10^6 8A cells and three of four animals injected with 10^6 8C cells, but the tumors in both groups of animals took 4–6 weeks to attain a size of 2 cm and were not detected in the first 3 weeks after the injection of the cells.

Tumors were isolated from all animals, and G418^r cells from tumors from each of the FGF-8 isoform groups were reselected in culture. The morphology of the cells after passage as tumor in the animals was identical to the morphology of the cells prior to passage as tumor, *i.e.,* 8B cells were the most transformed morphologically, and the 8A and 8C cells were less transformed (data not shown). Furthermore, Northern blot analysis of RNA from 8A, 8B, and 8C cell lines after passage as tumors in nude mice show

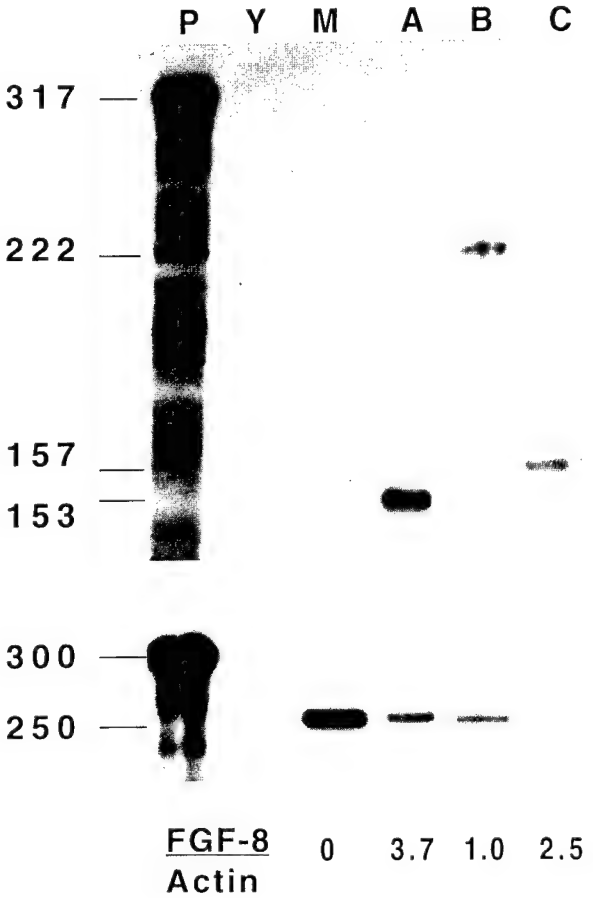

Fig. 3. Pooled G418^r NIH3T3 cells correctly express the transfected *Fgf-8* cDNAs at comparable levels. *Upper panel,* RNase protection assays of RNA from yeast (*Y*), or NIH3T3 cells transfected with pMIRB (*M*), *Fgf-8a* cDNA (*A*), *Fgf-8b* cDNA (*B*), or *Fgf-8c* cDNA (*C*), using an anti-sense *Fgf-8b* riboprobe (*P*) that is 317 nucleotides in length. *Fgf-8a* RNA protects a 153-nt fragment, *Fgf-8b* RNA protects a 222-nt fragment, and *Fgf-8c* RNA protects a 157-nt fragment. *Lower panel,* RNase protection assay of the same RNAs in the *upper panel,* using an anti-sense β-actin riboprobe that is 300 nt in length. β-actin RNA protects 250 nt of the probe. Fragment sizes are indicated at *left* in nt. The relative steady-state quantities of the various *Fgf-8* RNAs are indicated below the *lower panel.* They were corrected for size differences and RNA loading as described in the text and expressed as the FGF-8:actin signal ratio.

that RNA for the FGF-8 isoforms was present (data not shown). These results indicate that the morphology and expression of the transfected *Fgf-8* cDNAs are stable and not altered by passage as tumors in nude mice and suggest that the production of the FGF-8 protein isoform is responsible for the observed phenotypes.

Recombinant FGF-8 Isoforms Morphologically Alter NIH3T3 Cells. To begin to understand the mechanism of the differences observed in the preceding transfection experiments, we added rFGF-8 isoforms, carboxy-terminal histidine-tagged (10 nM), and heparin (3 μg/ml), to the culture medium of NIH3T3 cells. After 3 days in culture, the cells developed the same morphological changes observed with transfection of the cDNAs (Fig. 6). Specifically, the NIH3T3 cells cultured with rFGF-8b were elongated and spindle shaped. The NIH3T3 cells cultured with rFGF-8a or rFGF-8c grew to a higher density and were less contact inhibited than untreated NIH3T3 cells. The cells treated with rFGF-8a or rFGF-8c did not develop the elongated spindle shape of cells treated with rFGF-8b, even when 100 nM concentrations were tried (Fig. 6 and data not shown). These results indicate that the morphological differences observed in the stably transfected NIH3T3 cells are likely due to biological differences in the secreted forms of these FGF-8 proteins.

Discussion

The existence of several FGF-8 isoforms suggests the possibility that they possess different biological functions. We now show that three FGF-8 isoforms have different potencies for transformation of NIH3T3 cells. In agreement with prior results (31), 8B cells are morphologically transformed (Fig. 2), clonagenic in soft agar (Table 1), and rapidly form tumors in nude mice (Table 1). 8A and 8C cells show modest morphological transformation (Fig. 2), are not clonagenic in soft agar (Table 1), and are weakly tumorigenic in nude mice (Table 1). RNase protection analyses indicate that the cell lines produce the correct FGF-8 isoform RNA (Fig. 3) and suggest that the correct FGF-8 isoform protein is produced by the cell lines. The observed differences in potency of NIH3T3 cell transformation shown here are not due to differences in amounts of FGF-8 isoform RNA in the cell lines (Fig. 3) or to the absence of FGF-8 isoform protein (Fig. 5). We show that recombinant FGF-8 isoforms added to the culture medium of NIH3T3 cells leads to the same morphological changes observed when the cells are transfected with the appropriate cDNA (Fig. 6). Although subtle quantitative differences in the production of FGF-8 isoform proteins cannot be excluded, these results suggest that these FGF-8 isoforms possess different potencies for transformation of NIH3T3 cells.

Alternative isoforms of FGF-2 and FGF-3 exist due to different translation initiation sites (20–23), which results in the targeting of these isoforms to different cellular locations (extracellular *versus* nuclear). In contrast, the three FGF-8 isoforms examined in this work have identical signal peptides, are presumably secreted, and differ only at the amino termini of the mature secreted isoform (4). Assuming that the three FGF-8 isoforms are secreted, we would predict that their biological effects would relate to binding of FGFRs. Hence, the differences observed in NIH3T3 cell transformation potency between the FGF-8 isoforms suggest that the amino terminal differences in the FGF-8 isoforms result in the differential ability of FGF-8 isoforms to bind to, or induce signals through, the FGFRs present on NIH3T3 cells.

The FGF-8b isoform has been shown to bind to a mutated FGFR1 that was isolated from the same SC-3 mammary carcinoma cell line from which FGF-8 was originally purified (31). Whether FGF-8b binds normal FGFR1, or other FGFRs, is unknown. No information is available concerning the ability of the other FGF-8 isoforms to bind the various FGFRs. This information is important in order to understand the role of *Fgf-8* in mammalian development, as well the potential tissue specificity of *Fgf-8*-induced oncogenesis.

Additional evidence has been reported for the idea that differences in the amino terminal portion of FGF proteins can alter their interactions with FGFRs. A recombinant amino-truncated FGF-4 is more active than the full-length FGF-4 in an *in vitro* FGFR-binding assay (32). In contrast, a recombinant amino-truncated FGF-7 shows equivalent binding when compared to full-length FGF-7, but the trun-

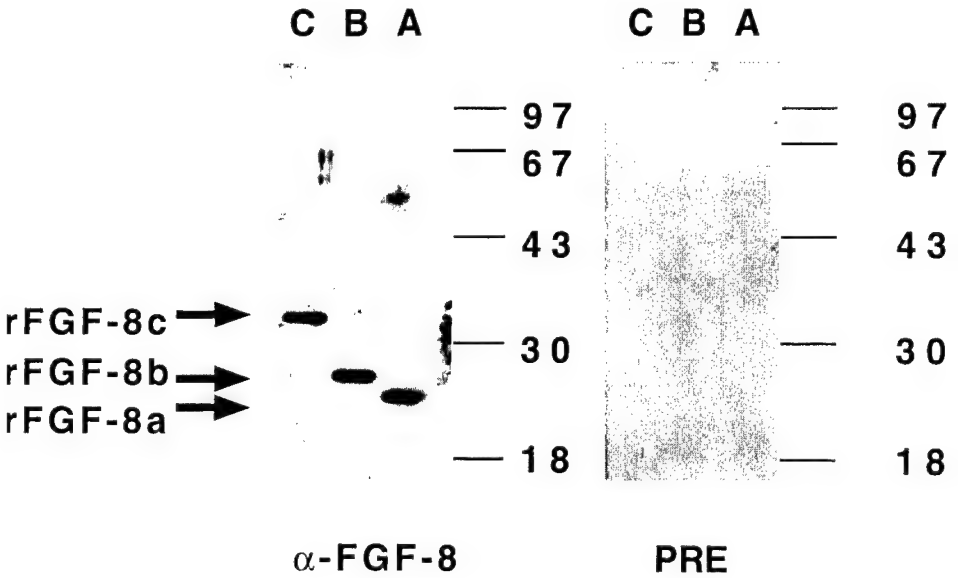

Fig. 4. Affinity-purified polyclonal rabbit anti-mouse FGF-8 antibody recognizes the three recombinant FGF-8 isoforms. Western blots of recombinant FGF-8 isoforms, prepared by histidine-tagging and Ni^{2+} chromatography. *Left panel,* primary antibody is an affinity-purified, polyclonal rabbit anti-mouse FGF-8, which recognizes all three rFGF-8 isoforms. *Right panel,* primary antibody is preimmune rabbit sera. Western blots were prepared using Amersham's ECL reagents and a donkey anti-rabbit IgG secondary antibody from Amersham. The rFGF-8 isoforms are indicated at *left,* and the molecular weight markers in kilodaltons are indicated at *right.*

cated FGF-7 is unable to induce the intracellular tyrosine phosphorylation observed with the full-length FGF-7 (33). Amino-truncated forms of FGF-4 and FGF-7 are not known to exist *in vivo.* However, their *in vitro* properties confirm that amino terminal differences in FGFs can alter the ability of FGFs to bind FGFRs or to transduce a signal following FGFR binding. These findings support the hypothesis that the amino terminal differences observed in natural FGF-8 isoforms are involved in differential interactions of FGF-8 isoforms with FGFRs. Whether the observed phenotypic differences are due to differences in FGF-8 isoform affinity for the various FGFRs and/or differences in the ability of FGF-8 isoforms to lead to signal transduction following receptor occupation remains to be determined.

We and others have recently characterized the temporal and spatial expression of *Fgf-8* during postgastrulation mouse development (24–26). We observed *Fgf-8* expression in the ectoderm of the first branchial arch, nasal pits, and limb buds, as well as in the neuroectoderm of the telencephalon, diencephalon, mesencephalon-metencephalon junction, and infundibulum from days 9 to 13 of development. Isoform-specific localizations were not performed, but preliminary results with an *Fgf-8c*-specific probe indicate that *Fgf-8c* RNA is present in all of the above locations.[4] RNA for the three FGF-8 isoforms was detected by RNase protection assays at days 10–12 of mouse development (25). These results suggest that the splicing of the *Fgf-8* transcript is not regulated during development. If this is the case, then the specific interactions of FGF-8 isoforms with FGFRs during development would depend on the FGFRs present in the local environment of *Fgf-8* expression. FGF signaling pathways have been implicated in the genetic dysmorphology syndromes of achondroplasia (FGFR3 transmembrane mutation; Refs. 34 and 35), Jackson-Weiss and Crouzon Syndromes (FGFR2 bek exon mutations; Refs. 36 and 37), and Pfeiffer Syndrome (FGFR1 mutations; Ref. 38). Therefore, characterization of FGF-8 isoform/FGFR interactions may provide a clearer molecular understanding of these and other rare craniofacial and/or limb dysmorphogenesis syndromes.

Similarly, whether *Fgf-8* has any role in human malignancy will depend on at least three factors: (*a*) whether *Fgf-8* can be transcriptionally activated by a carcinogenic event in a target tissue; (*b*) whether the target tissue has one or more FGFRs that bind one or more FGF-8 isoforms; and (*c*) whether the FGF-8 isoform/FGFR interaction leads to an oncogenic (presumably mitogenic) signal. Since *Fgf-8* is a developmentally silenced gene, it seems likely that oncogenic events could transcriptionally activate the gene in a target tissue, as was observed for metallothioneins in thymic lymphoma cells (39, 40). Therefore, understanding the tissue distribution of FGFRs, their ability to bind the FGF-8 isoforms, and their ability to transduce a mitogenic signal in the target tissue in response to FGF-8 isoform binding will help elucidate the role of *Fgf-8* in cancer.

Materials and Methods

Cell Lines, Vectors, and Transfection. NIH3T3 cells (gift of R. Weinberg, Whitehead Institute, Cambridge, MA) were grown in DMEM-FCS in humidified incubators with 5% CO_2 at 37°C. Cells were passaged at subconfluence to avoid selecting for spontaneous transformants; any cultures with such variants were discarded.

We used an expression vector, pMIRB (generous gift of D. M. Ornitz, Washington University, St. Louis, MO), that generates a bicistronic mRNA that has an internal ribosome entry site for the downstream neomycin phosphoribosyltransferase gene, allowing both transcription units in the mRNA to be translated (Fig. 1). Previously isolated cDNAs with full coding potential for three FGF-8 protein isoforms (4) were cloned into the upstream position of pMIRB (Fig. 1) using the *Eco*RI and blunted *Spe*I sites. The cDNAs were sequenced with *Fgf-8* primers to confirm authenticity. The resulting expression vectors were used to transfect NIH3T3 cells using OptiMEM and Lipofectamine (GIBCO-BRL). Briefly, 6×10^4 cells were cultured on 6-well dishes (Falcon). The next day, the cells were washed with OptiMEM and then placed in 1 ml of OptiMEM. Expression vector

[4] M. Heikinheimo and C. A. MacArthur, unpublished results.

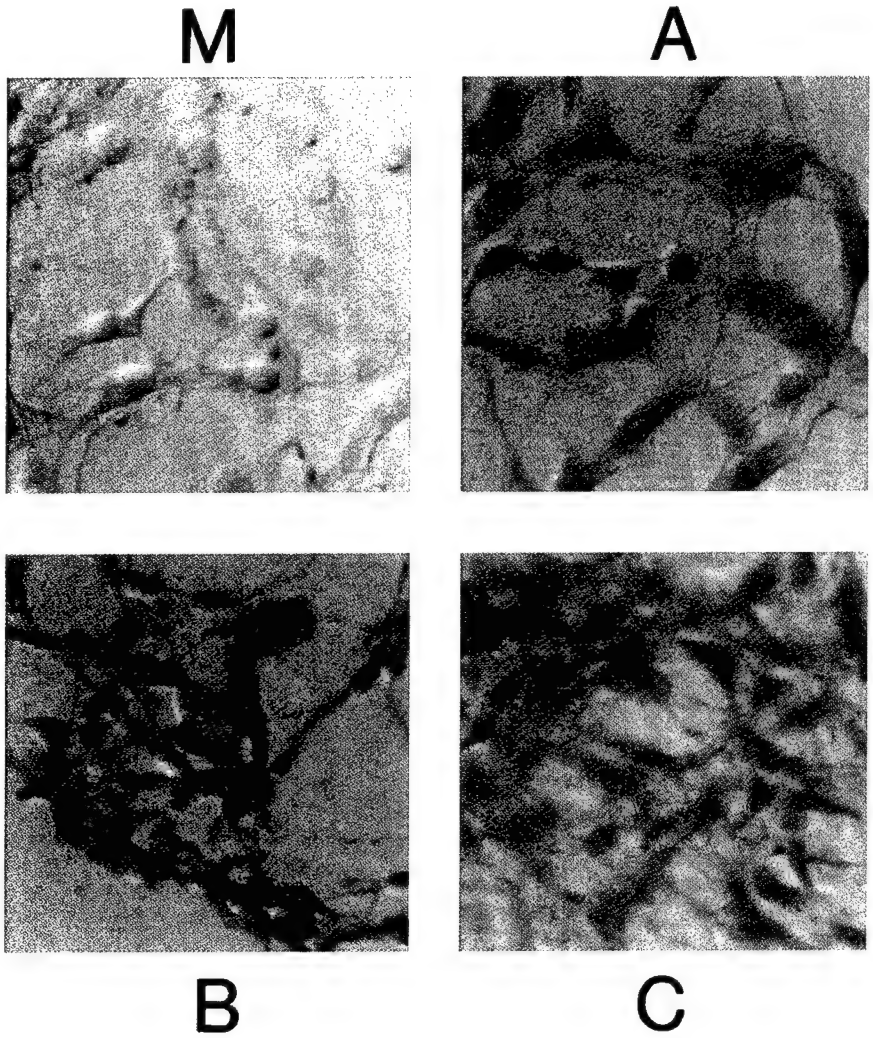

Fig. 5. NIH-3T3 cells transfected with *Fgf-8* isoform cDNAs produce FGF-8 protein. Immunohistochemical staining of pooled G418^r cells expressing the transfected *Fgf-8a* cDNA (*A*), *Fgf-8b* cDNA (*B*), *Fgf-8c* cDNA (*C*), or transfected with pMIRB (*M*). The primary antibody is the common FGF-8 polyclonal antibody (see Fig. 4). The stain is HRP activity on the diaminobenzidine tetrahydrochloride substrate.

(with or without an *Fgf-8* cDNA; 5 μg) was combined with Lipofectamine (10 μl) in 200 μl of OptiMEM per GIBCO-BRL directions. The DNA-Lipofectamine mixture was placed on the cells, and the cells were incubated for 6–8 h at 37°C and 5% CO_2. One ml of DMEM-FCS was added to the transfected cells, and they were incubated overnight. Twenty-four h after transfection, the cells were transferred to new plates, and the cells were selected for stable transfection with DMEM-FCS containing 500 μg/ml Geneticin (G418; GIBCO-BRL). These cells were grown for 10–14 days. The G418^r colonies were pooled from each transfection to create the stable cell lines used in the biochemical and transformation assays.

Transformation Assays. At least 50 G418^r colonies (above) were pooled from each transfection/selection. This pooling of clones was done to minimize the possibility that a single clone that was morphologically transformed by an event unrelated to expression of the FGF-8 isoform would bias our results. The initial transformation assay was a simple morphological examination of the transfected and selected cells. The morphology was documented by photomicroscopy.

The second transformation assay was soft agar clonagenicity. Five thousand G418^r cells from each transfection/selection were placed in 2 ml of DMEM-FCS with 0.5% Low Melt Agarose (GIBCO-BRL). They were overlaid on 100-mm plates containing 10 ml of bottom agar (DMEM-FCS with 0.5% Bacto Agar; Difco) and incubated at 37°C and 5% CO_2 for 14 days. The visible colonies were counted at 14 days, and the colony-forming unit was calculated by dividing the number of soft agar colonies observed at 14 days by the number of cells plated (5000) and multiplying by 100 to convert to percentages.

The third transformation assay was *in vivo* tumorigenesis in nude mice. Five-week-old nude mice (*nu/nu*; The Jackson Laboratory) were injected with 1×10^6 G418^r cells in 0.1 ml of PBS s.c. into the flank. The animals were maintained in laminar cages (4–5 mice/cage) and provided rodent chow (Purina) and water *ad libitum* in the Pediatric Animal Facility at Washington University School of Medicine, in accordance with the NIH Guide to animal welfare. Following injection, the animals were observed every 2 days for the development of tumors. Animals were sacrificed when the tumor became 2 cm in its largest diameter or when the tumor interfered with the animals' daily tasks. Animals were euthanized in accordance with NIH and Washington University School of Medicine Animal Study Committee guidelines. The tumors were used to establish posttumor cell lines by mincing tumor tissue in DMEM-FCS

Table 1 Properties of G418^r NIH3T3 cell lines expressing *Fgf-8* isoform cDNAs

Cell line	Transfected plasmid	Reduced serum growth[a]	Doubling time (h)[b]	Saturation density (10^3 cells/cm^2)[c]	Colony-forming units (%)[d]	Tumorigenicity[e]
MIRB	pMIRB	No	18 ± 2	12 ± 2	0	0/4
8A	pMIRB-Fgf-8a cDNA	No	16 ± 2	27 ± 2	0	2/4[f]
8B	pMIRB-Fgf-8b cDNA	Yes	16 ± 2	67 ± 3	5 ± 2	10/10[g]
8C	pMIRB-Fgf-8c cDNA	No	16 ± 2	48 ± 3	0	3/4[h]

[a] Ability of cells to grow in 2% FCS and 8% newborn serum.
[b] Doubling time, measured while the cells were in log phase in 10% FCS, and presented as the mean of four experiments ± the SE.
[c] Saturation density, measured as the number of cells on the plate at confluence divided by the surface area of the plate and presented as the mean of four experiments ± the SE.
[d] Colony-forming units in soft agar, expressed as a percentage of the plated cells, presented as the mean of four experiments ± the SE.
[e] Presented as the number of animals with tumors divided by the number of animals receiving injections.
[f] Tumor latency was 6 weeks.
[g] Tumor latency was 1 week.
[h] Tumor latency was 4–6 weeks.

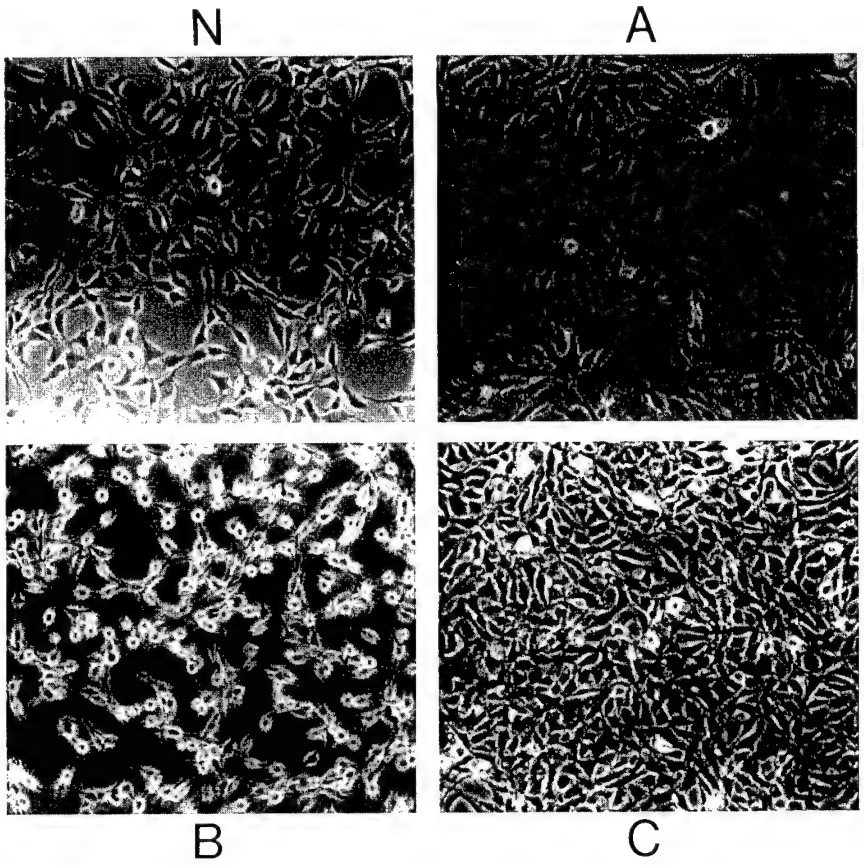

Fig. 6. Recombinant FGF-8 isoforms alter the morphology of NIH3T3 cells. Cells were grown for 3 days in DMEM-FCS, supplemented with 3 μg/ml of heparin and 0 nM rFGF-8 (*N*), 10 nM rFGF-8a (*A*), 10 nM rFGF-8b (*B*), or 10 nM rFGF-8c (*C*).

with 500 μg/ml Geneticin. The resulting suspensions were incubated at 37°C and 5% CO_2.

Cell Proliferation Assays. Multiple platings of G418^r Cells (1000) from each transfection were plated in wells of 6-well dishes and grown at 37°C and 5% CO_2 in DMEM-FCS. The cells from each transfected/selected cell line were removed from the wells with trypsin and counted using a hemocytometer each day. The doubling time was determined for cells in log phase growth. The saturation density for each cell line was determined when the cells reached confluence (8–10 days). The data was collected on four occasions, both at the initial development of the cell lines and after several months in cryopreservation. Results are presented as the mean ± SE.

Isolation of RNA, Northern Blot, and RNase Protection Assays. Total RNA from cells and from tumors was isolated by the guanidinium isothiocyanate/acid phenol method (41). RNase protection assays (Ambion; RPA II kit) were performed on 10 μg of total RNA using antisense riboprobes derived from the *Fgf-8b* 5′ cDNA and β-actin cDNA, as described previously (25). The radioactive signals in the gels were quantitated by phosphor imaging (Molecular Dynamics). The raw data was corrected for differences in *Fgf-8* fragment size (29 UTP residues for *Fgf-8a* protected fragment, 46 UTP residues for *Fgf-8b* protected fragment, and 30 UTP residues for *Fgf-8c* protected fragment) and RNA loading (by dividing by the β-actin signal). The corrected data, expressed as a *Fgf-8*:β-actin signal ratio, was normal-

ized so that the value of the least expressed isoform was one.

Production of Recombinant FGF-8 Isoforms. The cDNAs for the mature forms (*i.e.,* signal peptide removed) of the FGF-8 isoforms were obtained by PCR methods and cloned into the pQE30 (for amino-tagged isoforms) or pQE16 (for carboxy-tagged isoforms) bacterial expression vectors (Qiagen). The histidine-tagged recombinant FGF-8 (rFGF-8) isoforms were purified using the denaturing protocol [6 M guanidinium hydrochloride, 100 mM sodium phosphate, and 10 mM Tris-chloride (pH 8.0)] of Qiagen and Ni-NTA agarose chromatography. The denatured purified rFGF-8 isoforms were eluted with 8 M urea, 100 mM sodium phosphate, and 10 mM Tris-chloride (pH 5.9). The purified rFGF-8 isoforms were renatured by successive dialysis, first against 1 M urea, 100 mM sodium phosphate, 10 mM Tris-chloride, and 5 mM reduced glutathione (pH 8.0), and then against PBS with 5 mM reduced glutathione. The rFGF-8 isoforms were obtained as a powder by lyophilization and quantitated by amino acid analysis.

Since the differences in the FGF-8 isoforms is at the mature amino terminus, the carboxy-tagged rFGF-8 isoforms were used in NIH3T3 culture experiments. NIH3T3 cells were split 1:20 and allowed to attach for 4 h. The medium was replaced with fresh medium containing heparin (final concentration, 3 μg/ml). The rFGF-8 isoform proteins were reconstituted in sterile PBS and added to the cells at various final concentrations (1 nM to 1 μM). The cells were grown as usual for 3 days and photographed.

Generation of FGF-8 Antibody, Western Blot, and Immunohistochemical Analyses. The purified rFGF-8a (amino-tagged) was submitted to Cocalico Biologicals (Reamstown, PA) for immunization of rabbits and antisera production. The antisera produced was further purified, initially by protein A chromatography (42) and subsequently by FGF-8 affinity chromatography, using cyanogen bromide-charged Sepharose and rFGF-8a (42). The affinity-purified, anti-mouse FGF-8 antibody, at a concentration of 0.2–0.5 μg/ml, was used as the primary antibody in Western blots of rFGF-8a, rFGF-8b, and rFGF-8c. Chemiluminescence methods, including a secondary donkey anti-rabbit IgG antibody conjugated with HRP, were used in Western blots (Amersham ECL). The recombinant proteins were separated by SDS-PAGE and transferred by electrophoretic methods to nitrocellulose (Amersham ECL) as described (42). Blocking, incubating the blots with antibodies, washing the blots, and development of the chemiluminescent signal were done according to manufacturer's instructions. The blots were exposed to film (Amersham's Hyperfilm-ECL) for appropriate times.

Immunohistochemical analyses of FGF-8 protein expression were performed on the transfected/selected G418^r cell lines. The cells were grown as above, washed in PBS, fixed with 4% paraformaldehyde in PBS-Ca for 20 min, bleached with 0.3% v/v H_2O_2, and permeabilized in 1% Triton X-100 as described (42, 43). The fixed and permeabilized cells were blocked with 10% goat serum in PBS-Ca and then incubated with the affinity-purified, rabbit anti-mouse FGF-8 antibody described above at a concentration of 0.2 μg/ml in PBS-Ca for 30 min at 37°C. The secondary antibody (biotinylated anti-rabbit IgG) and avidin-HRP detection reagents were part of the Vectastain Elite ABC kit (Vector Labs, Burlingame, CA), and the manufacturer's procedure was used. HRP staining with diaminobenzidine tetrahydrochloride/nickel chloride and H_2O_2 were performed as described (42).

Acknowledgments

We thank David M. Ornitz for the gift of the pMIRB expression vector and David B. Wilson for assistance with photography.

References

1. Fearon, E. R., and Vogelstein, B. A genetic model for colorectal tumorigenesis. Cell, *61:* 759–767, 1990.

2. Tsukamoto, A. S., Grosschedl, R., Guman, R. C., Parslow, T., and Varmus, H. E. Expression of the *int-1* gene in transgenic mice is associated with mammary gland hyperplasia and adenocarcinomas in male and female mice. Cell, *55:* 619–625, 1988.

3. Shackleford, G. M., MacArthur, C. A., Kwan, H. C., and Varmus, H. E. Mouse mammary tumor virus infection accelerates mammary carcinogenesis in *Wnt-1* transgenic mice by insertional activation of *int-2/Fgf-3* and *hst/Fgf-4.* Proc. Natl. Acad. Sci. USA, *90:* 740–744, 1993.

4. MacArthur, C. A., Shankar, D. B., and Shackleford, G. M. *Fgf-8,* activated by proviral insertion, cooperates with the *Wnt-1* transgene in murine mammary tumorigenesis. J. Virol., *69:* 2501–2507, 1995.

5. Tanaka, A., Miyamoto, K., Minamino, N., Takeda, M., Sato, B., Matsuo, H., and Matsumoto, K. Cloning and characterization of an androgen-induced growth factor essential for the androgen-dependent growth of mouse mammary carcinoma cells. Proc. Natl. Acad. Sci. USA, *89:* 8928–8932, 1992.

6. Basilico, C., and Moscatelli, D. The FGF family of growth factors and oncogenes. Adv. Cancer Res., *59:* 115–165, 1992.

7. Miyamoto, M., Naruo, K-I., Seko, C., Matsumoto, S., Kondo, T., and Kurokawa, T. Molecular cloning of a novel cytokine cDNA encoding the ninth member of the fibroblast growth factor family, which has a unique secretion property. Mol. Cell. Biol., *13:* 4251–4259, 1993.

8. Mason, I. J. The ins and outs of fibroblast growth factors. Cell, *78:* 546–552, 1994.

9. Chellaiah, A., McEwen, D. G., Werner, S., Xu, J., and Ornitz, D. M. Fibroblast growth factor receptor 3: alternative splicing in immunoglobulin-like domain III creates a receptor highly specific for acidic FGF/FGF-1. J. Biol. Chem., *269:* 11620–11627, 1994.

10. Dionne, C. A., Crumley, G., Bellot, F., Kaplow, J. M., Searfoss, G., Ruta, M., Burgess, W. H., Jaye, M., and Schlessinger, J. Cloning and expression of two distinct high-affinity receptors cross-reacting with acidic and basic fibroblast growth factors. EMBO J., *9:* 2685–2692, 1990.

11. Lee, P. L., Johnson, D. E., Cousens, L. S., Fried, V. A., and Williams, L. T. Purification and complementary DNA cloning of a receptor for basic fibroblast growth factor. Science (Washington DC), *245:* 57–60, 1989.

12. Miki, T., Fleming, T. P., Bottaro, D. P., Rubin, J. S., Ron, D., and Aaronson, S. A. Expression cDNA cloning of the KGF receptor by creation of a transforming autocrine loop. Science (Washington DC), *251:* 72–75, 1991.

13. Mansukhani, A., Moscatelli, D., Talarico, D., Levytska, V., and Basilico, C. A murine fibroblast growth factor receptor expressed in CHO cells is activated by basic FGF and Kaposi FGF. Proc. Natl. Acad. Sci. USA, *87:* 4378–4382, 1990.

14. Partanen, J., Mäkelä, T. P., Eerola, E., Korhonen, J., Hirvonen, H., Claesson-Welsh, L., and Alitalo, K. FGFR-4, a novel acidic fibroblast growth factor receptor with a distinct expression pattern. EMBO J., *10:* 1347–1354, 1991.

15. Pasquale, E. B. A distinctive family of embryonic protein-tyrosine kinase receptors. Proc. Natl. Acad. Sci. USA, *87:* 5812–5816, 1990.

16. Klagsbrun, M., and Baird, A. A dual receptor system is required for basic fibroblast growth factor activity. Cell, *67:* 229–231, 1991.

17. Yayon, A., Klagsbrun, M., Esko, J. D., Leder, P., and Ornitz, D. M. Cell surface, heparin-like molecules are required for binding of basic fibroblast growth factor to its high affinity receptor. Cell, *64:* 841–848, 1991.

18. Ornitz, D. M., Yayon, A., Flanagan, J. G., Svahn, C. M., Levi, E., and Leder, P. Heparin is required for cell-free binding of basic fibroblast growth factor to a soluble receptor and for mitogenesis in whole cells. Mol. Cell. Biol., *12:* 240–247, 1992.

19. Burrus, L. W., Zuber, M. E., Lueddecke, B. A., and Olwin, B. B. Identification of a cysteine-rich receptor for fibroblast growth factors. Mol. Cell. Biol., *12:* 5600–5609, 1992.

20. Florkiewicz, R. Z., and Sommer, A. Human basic fibroblast growth factor gene encodes four polypeptides: three initiate translation from non-AUG codons. Proc. Natl. Acad. Sci. USA, *86:* 3978–3981, 1989.

21. Acland, P., Dixon, M., Peters, G., and Dickson, C. Subcellular fate of the Int-2 oncoprotein is determined by choice of initiation codon. Nature (Lond.), *343:* 662–665, 1990.

22. Bugler, B., Amalric, E., and Prats, H. Alternative initiation of translation determines cytoplasmic or nuclear localization of basic fibroblast growth factor. Mol. Cell. Biol., *11:* 573–577, 1991.

23. Florkiewicz, R. Z., Baird, A., and Gonzalez, A. M. Multiple forms of bFGF: differential nuclear and cell surface localization. Growth Factors, *4:* 265–275, 1991.

24. Crossley, P. H., and Martin, G. R. The mouse *Fgf8* gene encodes a family of polypeptides and is expressed in regions that direct outgrowth and patterning in the developing embryo. Development (Camb.), *121:* 439–451, 1995.

25. Heikinheimo, M., Lawshé, A., Shackleford, G. M., Wilson, D. B., and MacArthur, C. A. Fgf-8 expression in the post-gastrulation mouse is localized to the developing face, limbs, and central nervous system. Mech. Dev., *48:* 129–138, 1994.

26. Ohuchi, H., Yoshioka, H., Tanaka, A., Kawakami, Y., Nohno, T., and Noji, S. Involvement of androgen-induced growth factor (FGF-8) gene in mouse embryogenesis and morphogenesis. Biochem. Biophys. Res. Commun., *204:* 882–888, 1994.

27. Goldfarb, M., Deed, R., MacAllan, D., Walther, W., Dickson, C., and Peters, G. Cell transformation by Int-2—a member of the fibroblast growth factor family. Oncogene, *6:* 65–71, 1991.

28. Delli Bovi, P., Curatola, A. M., Kern, F. G., Greco, A., Ittman, A., and Basilico, C. An oncogene isolated by transfection of Kaposi's sarcoma DNA encodes a growth factor that is a member of the FGF family. Cell, *50:* 729–737, 1987.

29. Zhan, X., Bates, B., Hu, X., and Goldfarb, M. The human FGF-5 oncogene encodes a novel protein related to fibroblast growth factors. Mol. Cell. Biol., *8:* 3487–3495, 1988.

30. de Lapeyiere, O., Rosnet, O., Benharroch, D., Raybaud, F., Marchetto, S., Planche, J., Galland, F., Mattei, M-G., Copeland, N. G., Jenkins, N. A., Coulier, F., and Birnbaum, D. Structure, chromosome mapping and expression of the murine *Fgf-6* gene. Oncogene, *5:* 823–831, 1990.

31. Kouhara, H., Koga, M., Kasayama, S., Tanaka, A., Kishimoto, T., and Sato, B. Transforming activity of a newly cloned androgen-induced growth factor. Oncogene, *9:* 455–462, 1994.

32. Bellosta, P., Talarico, D., Rogers, D., and Basilico, C. Cleavage of K-FGF produces a truncated molecule with increased biological activity and receptor binding affinity. J. Cell Biol., *121:* 705–713, 1993.

33. Ron, D., Bottaro, D. P., Finch, P. W., Morris, D., Rubin, J. S., and Aaronson, S. A. Expression of biologically active recombinant keratinocyte growth factor. J. Biol. Chem., *268:* 2984–2988, 1993.

34. Rousseau, F., Bonaventure, J., Legeai-Mallet, L., Pelet, A., Rozet, J-M., Maroteaux, P., Le Merrer, L., and Munnich, A. Mutations in the gene encoding fibroblast growth factor receptor-3 in achondroplasia. Nature (Lond.), *371:* 252–254, 1994.

35. Shiang, R., Thompson, L. M., Zhu, Y-Z., Church, D. M., Fielder, T. J., Bocian, M., Winokur, S. T., and Wasmuth, J. J. Mutations in the transmembrane domain of FGFR3 cause the most common genetic form of dwarfism, achondroplasia. Cell, *78:* 335–342, 1994.

36. Reardon, W., Winter, R. M., Rutland, P., Pulleyn, L. J., Jones, B. M., and Malcolm, S. Mutations in the fibroblast growth factor receptor 2 gene cause Crouzon syndrome. Nat. Genet., *8:* 98–103, 1994.

37. Jabs, E. W., Li, X., Scott, A. F., Meyers, G., Chen, W., Eccles, M., Mao, J-i., Charnes, L. R., Jackson, C. E., and Jaye, M. Jackson-Weiss and Crouzon syndromes are allelic with mutations in fibroblast growth factor receptor 2. Nat. Genet., *8:* 275–281, 1994.

38. Muenke, M., Schell, U., Hehr, A., Robin, N. H., Losken, H. W., Schinzel, A., Pulleyn, L. J., Rutland, P., Reardon, W., Malcolm, S., and Winter, R. M. A common mutation in the fibroblast growth factor receptor 1 gene in Pfeiffer syndrome. Nat. Genet., *8:* 269–274, 1994.

39. MacArthur, C. A., Hawley, T., and Lieberman, M. W. Coordinate activation and regulation of quiescent metallothionein I and II genes in carcinogen-treated mouse thymic lymphoma cells. Carcinogenesis (Lond.), *7:* 1487–1495, 1986.

40. MacArthur, C. A., and Lieberman, M. W. Different types of hypersensitive sites in the mouse metallothionein gene region. J. Biol Chem., *262:* 2161–2165, 1987.

41. Chomczynski, P., and Sacchi, N. Single-step method of RNA isolation by acid guanidinium thiocyanate-phenol-chloroform extraction. Anal. Biochem., *162:* 156–159, 1987.

42. Harlow, E., and Lane, D., Antibodies: A Laboratory Manual. Cold Spring Harbor, NY: Cold Spring Harbor Laboratory, 1988.

43. Trausch, J. S., Grenfell, S. J., Handley-Gearhart, P. M., Ciechanover, A., and Schwartz, A. L. Immunofluorescent localization of the ubiquitin-activating enzyme, E1, to the nucleus and cytoskeleton. Am. J. Physiol., *264:* C93–C102, 1993.

JOURNAL OF VIROLOGY, Apr. 1995, p. 2501–2507
0022-538X/95/$04.00+0
Copyright © 1995, American Society for Microbiology
Vol. 69, No. 4

Fgf-8, Activated by Proviral Insertion, Cooperates with the *Wnt-1* Transgene in Murine Mammary Tumorigenesis

CRAIG A. MACARTHUR,[1]† DEEPA B. SHANKAR,[2] AND GREGORY M. SHACKLEFORD[1,2]*

Departments of Pediatrics[1] and Molecular Microbiology and Immunology,[2] University of Southern California School of Medicine and Children's Hospital Los Angeles, Los Angeles, California 90027

Received 1 August 1994/Accepted 28 December 1994

We have used mouse mammary tumor virus (MMTV) infection of *Wnt-1* transgenic mice to accelerate mammary tumorigenesis and to molecularly tag insertionally activated proto-oncogenes that cooperate oncogenically with *Wnt-1* (G. M. Shackleford, C. A. MacArthur, H. C. Kwan, and H. E. Varmus, Proc. Natl. Acad. Sci. USA 90:740–744, 1993). Here we report the identification and characterization of a 31-kb genomic locus that contains clonal MMTV integrations in 8 of 80 mammary tumors from MMTV-infected *Wnt-1* transgenic mice. Two genes were identified within this locus, one of which was transcriptionally activated by MMTV insertions. This activated gene is identical to androgen-induced growth factor (AIGF/*Fgf-8*) (A. Tanaka, K. Miyamoto, N. Minamino, M. Takeda, B. Sato, H. Matsuo, and K. Matsumoto, Proc. Natl. Acad. Sci. USA 89:8928–8932, 1992), the eighth member of the fibroblast growth factor (FGF) family. Transcriptional activation of *Fgf-8* was found in all tumors with MMTV insertions in this locus. *Fgf-8* mRNA was absent in normal mammary glands and was detected only in adult testis and ovary and in midgestational embryos. The sequences of *Fgf-8* genomic and cDNA clones revealed five coding exons, in contrast to the three coding exons found in other FGF genes. cDNAs encoding three isoforms of the FGF-8 protein were isolated. The three corresponding mRNAs resulted from the alternative use of two 5′ splice sites and two 3′ splice sites for the second and third exons, respectively. These results implicate *Fgf-8* as the third FGF gene found to cooperate with *Wnt-1* in MMTV-induced murine mammary tumorigenesis, suggesting that FGFs and Wnts are strong collaborators in this process.

Ectopic expression of the *Wnt-1* proto-oncogene in the mammary glands of transgenic mice causes a diffuse mammary gland hyperplasia, followed by the stochastic development of adenocarcinomas in both males and females after a minimum latency of several months (44). These findings indicate that activation of *Wnt-1* is but one step in the multistep process of mammary tumorigenesis. Early evidence that fibroblast growth factors (FGFs) may be involved in cooperating steps comes from the finding that mouse mammary tumor virus (MMTV) insertionally activates both *Wnt-1* and *Fgf-3* in some tumors of infected nontransgenic mice (35). The cooperation of *Wnt-1* and *Fgf-3* was confirmed with the generation of bitransgenic *Wnt-1*/*Fgf-3* mice, which develop tumors earlier than either of the monotransgenic mice (26).

We have studied multistep murine mammary tumorigenesis by infecting *Wnt-1* transgenic mice with MMTV, expecting that infection would hasten tumor formation in these mice by insertional activation of proto-oncogenes that oncogenically cooperate with *Wnt-1* (37). As a result, activated proto-oncogenes are "tagged" by the nearby provirus, allowing their identification or isolation. Previous studies using murine leukemia virus infection of Eμ-*myc* transgenic mice have uncovered at least five distinct genetic loci that appear to collaborate with c-*myc* in lymphomagenesis (20, 45). MMTV infection of *Wnt-1* transgenic mice results in accelerated mammary tumorigenesis and increased numbers of tumors per animal (37). Approximately 45% of the resulting tumors with clonal, tumor-specific MMTV integrations contain insertionally activated *Fgf-3* or *Fgf-4*, suggesting that the *Wnt-1* gene product can cooperate with at least two members of the FGF family (37).

Despite being able to detect clonal, tumor-specific MMTV proviruses in the remaining 55% of the tumors, we did not detect insertional activation of any previously identified targets for MMTV insertion mutations (*Fgf-3*, *Fgf-4*, *int-3*, or *Wnt-3*) in this group (37). To determine the identity of proto-oncogenes that may be activated in these tumors, we have analyzed the DNAs surrounding proviral integration sites. We report here on the cloning of a new common integration locus for MMTV that contains insertions in 10% of our mammary tumors that have clonal, tumor-specific MMTV proviruses. Of the two genes located in this region, only one is activated by MMTV insertion mutations. This activated gene was found to encode androgen-induced growth factor (42), the eighth member of the FGF family. Thus, the selective activation in this system of a third FGF gene by MMTV proviral insertion suggests that FGFs and Wnts are potent collaborators in murine mammary tumorigenesis.

MATERIALS AND METHODS

Tumor samples. All mammary tumors were derived from a previous study (37) in which we infected female *Wnt-1* transgenic mice (44) at 3 to 4 weeks of age with MMTV produced from EH-2 cells (39).

Preparation of nucleic acids. Tumor DNAs were isolated as described before (39) except that serum separation tubes were used in the extractions (43). The majority of tumor RNAs were isolated by the urea-lithium chloride method (3) as described before (38). The normal tissue RNAs and some tumor RNAs were isolated by the guanidinium isothiocyanate-acid-phenol method (9). Polyadenylated [poly(A)$^+$] RNAs were purified by oligo(dT) chromatography (4). RNAs were stored as isopropanol precipitates at −20 or −80°C.

Southern and Northern (RNA) blot analyses. DNAs (10 μg) were digested with restriction endonucleases, electrophoresed, and capillary blotted to nylon membranes (Amersham Hybond-N) as previously described (39). The blots were

* Corresponding author. Mailing address: Division of Hematology-Oncology, Mailstop 57, Children's Hospital Los Angeles, 4650 Sunset Blvd., Los Angeles, CA 90027-6016. Phone: (213) 669-5661. Fax: (213) 664-9455. Electronic mail address: shacklef@hsc.usc.edu.

† Present address: Department of Pediatrics, Division of Hematology-Oncology, Washington University School of Medicine, St. Louis, MO 63110.

UV cross-linked (11), prehybridized for 1 to 2 h at 65°C, and hybridized overnight at 65°C with ^{32}P-labeled DNA probes. The hybridization buffer contained 0.5 M sodium phosphate (pH 7.2), 1 mM EDTA, 1% bovine serum albumin (fraction V), 7% sodium dodecyl sulfate (SDS), and 15% (vol/vol) formamide. Blots were washed in 40 mM sodium phosphate (pH 7.2)–1% SDS–1 mM EDTA at 65°C. Blots were exposed to Kodak XAR-5 film with intensifying screens at −80°C.

For Northern blots, RNAs were resuspended in a solution containing 50 mM *N*-2-hydroxyethylpiperazine-*N'*-2-ethanesulfonic acid (HEPES, pH 7.0), 10 mM sodium acetate, 1 mM EDTA, 0.25 μg of ethidium bromide per ml, 0.66 M formaldehyde, and 50% (vol/vol) formamide, denatured at 65°C for 5 min, and electrophoresed in 0.8% agarose gels with the same running buffer minus ethidium bromide and formamide at 30 to 45 V for 6 to 14 h (38). Following photography, the gel was capillary blotted overnight to nylon. Cross-linking, prehybridization, hybridization, washing, and exposure were the same as for DNA except that the hybridization buffer contained 30% (vol/vol) formamide for Northern blots. Blots were stripped of probes by incubation in boiling 0.1% SDS for 3 to 5 min and rehybridized as above.

Preparation and screening of genomic libraries. Following identification of a proviral-cellular junction fragment by Southern blotting, the fragment was size-selected by agarose electrophoresis and purified by using either glass beads (Gene Clean II; Bio 101) or agarose digestion (β-Agarase; New England Biolabs) and isopropanol precipitation. The junction fragments were ligated into appropriate lambda phage vectors, depending on the size of the insert (λDash II for inserts of 10 to 20 kb, and λZap II for inserts of less than 10 kb [both from Stratagene]). Phage were prepared by using packaging extracts (Gigapack II Plus; Stratagene) and then titered and screened on appropriate *Escherichia coli* hosts (XL-1 Blue for λZap libraries and P2392 for λDash libraries). Plaque lifts were performed as described before (36), UV cross-linked, hybridized, washed, and exposed as above for Southern blots. Putative positive clones were subjected to two to three rounds of screening to isolate clones. The inserts were obtained in Bluescript (Stratagene) plasmids, either by subcloning or by in vivo excision of λZap clones.

Growth and transfection of Cos-7 cells. A 6-kb *Sst*II fragment containing most of *Fgf-8* (see Fig. 5A) was subcloned into the "exon trap" vector pML53In (gift of M. Reth) (2), in both orientations. The resulting plasmids were transiently expressed in Cos-7 cells (American Type Culture Collection) by lipofectin-mediated transfection (BRL-Gibco). Cos-7 cells were grown in Dulbecco's modified Eagle's medium (DMEM) with 10% fetal calf serum (Sigma), penicillin, and streptomycin. When the cells reached 70% confluence, the medium was changed to DMEM without serum, and the DNA-lipofectin mixture was added according to the manufacturer's directions (BRL-Gibco). After 12 h of incubation of the lipofectin-DNA with the cells, serum was added back, and the cells were grown in DMEM with 10% fetal calf serum for an additional 48 h. The cells were harvested, and total cellular RNA was prepared (9). The RNA was used to generate an *Fgf-8* cDNA, using an exon trap protocol (2).

Generation of cDNAs by RT-PCR. Reverse transcription (RT) of total cellular RNA from transiently transfected Cos-7 cells was done in a buffer containing 50 mM Tris-HCl (pH 8.3), 75 mM KCl, 3 mM $MgCl_2$, 10 μg of random hexamer primers per ml, and avian myeloblastosis virus reverse transcriptase (Stratagene) by incubating at room temperature for 10 min, followed by 37°C for 20 min, and then 42°C for 90 min. The resulting cDNA was amplified by nested PCR with Amplitaq (Perkin-Elmer Cetus), with an initial forward primer (5'-AAGC TCTCTACCTGGTGTGTGG-3') in the 5' insulin exon and an initial reverse primer (5'-CAGTGCCAAGGTCTGAAGGTCA-3') in the 3' insulin exon, followed by a nested forward primer in the 5' insulin exon (5'-GCGAAGTGGAG GATCCACAAG-3') and a nested reverse primer in the 3' insulin exon (5'-ACCCGGATCCAGTTGTGCCA-3'). Initial PCR conditions were 50 mM KCl–1.5 mM $MgCl_2$ and 40 cycles of denaturing at 94°C for 1 min, annealing at 59°C for 1 min, and extending at 72°C for 1 min. Nested PCR conditions were the same except that the annealing temperature was 50°C. The resulting *Fgf-8* cDNA product, obtained only from the plasmid with *Fgf-8* in the correct orientation, was isolated from an agarose gel, cloned into a pBluescript "T-vector" (27), sequenced, and found to contain exons 2A, 3A, 4, and 5 up to the *Sst*II site. The portion of the coding region downstream of the *Sst*II site in exon 5 was added by ligating a 160-bp *Sst*II-*Sst*I fragment.

We obtained cDNAs containing all of the known *Fgf-8* coding region (42) in two subsequent steps. First, upstream cDNAs (exons 1, 2A, and 3A; exons 1, 2A, and 3B; and exons 1, 2B, and 3A) were obtained by nested RT-PCR from murine testis RNA. The RNA was reverse transcribed as above. The first PCR was carried out with a forward primer in *Fgf-8* exon 1 (5'-CGCACCCCGACCTC CCTC-3') and a reverse primer in *Fgf-8* exon 3 (5'-GAGCTGATCCGTCAC CAGGCT-3'). A nested *Fgf-8* exon 1 forward primer (5'-CGCACCTTCGGCT TGTCC-3') was used with the reverse *Fgf-8* exon 3 primer above or with a reverse primer that spans exons 2B and 3A (5'-CTGCTCCCTCACATGT CGCTG-3') in the nested PCR. PCR conditions with recombinant *Pfu* DNA polymerase (Stratagene) for both the initial and nested steps were 10 mM KCl–2 mM $MgCl_2$ and 40 cycles of denaturing at 94°C for 1 min, annealing at 58°C for 1 min, and extending at 72°C for 1 min. Next, these 5' cDNA fragments (189 bp for exons 1, 2A, and 3A; 222 bp for exons 1, 2A, and 3B; and 360 bp for exons 1, 2B, and 3A) were annealed with the exon trap fragment and amplified by *Pfu* DNA polymerase with the forward primer (5'-CGCACCTTCGGCTTGTCC-3') in exon 1 and a reverse primer in exon 5 (5'-CGACTCCCGCTGGATTCCT-3') to give cDNAs containing the entire coding sequence of the three isoforms of *Fgf-8*. The conditions for this step were 10 mM KCl–2 mM $MgCl_2$ and 25 cycles of denaturing at 94°C for 1 min, annealing at 55°C for 1 min, and extending at 72°C for 1 min. These cDNAs were cloned into pBluescript T-vectors (27). Sequencing of two of these fragments showed that they correspond to the previously described clones pSC17 (exons 1, 2A, 3B, 4, and 5) and pSC15 (exons 1, 2B, 3A, 4, and 5) (42). The third fragment is a novel isoform derived from exons 1, 2A, 3A, 4, and 5 (see Results).

Probes and sequencing. The DNA probes used for hybridization were isolated from plasmids by digestion with restriction endonucleases, agarose gel electrophoresis, and glass bead binding. Potential probes were tested for repetitive elements by blotting to nylon and hybridizing with ^{32}P-labeled mouse genomic DNA (41). Unique probes were used on Southern and Northern blots. In addition to the probes generated from the genomic clones and from PCRs described above, the following probes were used on blots: a 1.9-kb *Pst*I-*Xho*I fragment (MMTV *gag* probe) and a 1.2-kb *Bam*HI fragment (MMTV *env* probe) (39); a 475-bp murine acidic FGF/*Fgf-1* cDNA, a 475-bp murine basic FGF/*Fgf-2* cDNA, a full-length 800-bp murine *Fgf-5* cDNA, and a 600-bp murine *Fgf-6* cDNA (21); a 560-bp murine *Fgf-6* cDNA and a 1.6-kb *Xba*I-*Xho*I murine 5' genomic *Fgf-6* fragment (14); a 693-bp rat KGF/*Fgf-7* cDNA (48); a 0.85-kb murine *Fgf-9* cDNA (gift of D. Ornitz); and a 1.3-kb *Pst*I fragment containing rat glyceraldehyde-3-phosphate dehydrogenase cDNA (18).

Double-stranded plasmids containing inserts were sequenced with Sequenase version 2.0 (US Biochemicals). Both strands were sequenced with a combination of deletion subclones and *Fgf-8*-specific primers.

Nucleotide sequence accession number. The GenBank accession number of the cDNA encoding FGF-8a is U18673.

RESULTS

Detection and cloning of a new tumor-specific common insertion site for MMTV. In previous work, we showed that MMTV infection of *Wnt-1* transgenic mice accelerates mammary tumorigenesis by insertional activation of *Fgf-3* and *Fgf-4* (37). However, approximately half of the tumors that we examined did not exhibit activation of any of the proto-oncogenes known to be affected by MMTV in tumors of normal mice (including *int-3* and *Wnt-3*), despite the presence of clonal proviral insertions in these tumors (37). We reasoned that these tumors were likely to harbor unpredicted or novel proto-oncogenes activated by proviral insertion. To isolate such genes, we first sought to clone the proviral-cellular junction fragments from tumors that contained only one or two clonally integrated proviruses. Southern blot analysis of tumor DNAs with an MMTV *gag* probe identified several candidate junction fragments (Fig. 1 and data not shown).

The *Xho*I-cleaved junction fragments from tumors 95 and 111 (Fig. 1) were cloned into lambda vectors and isolated by screening with an MMTV *gag* probe. Unique cellular DNAs flanking the MMTV proviruses in these clones were isolated and used as probes on Southern blots of DNAs from 80 tumors with clonal insertions to determine if other tumors had rearrangements due to proviral insertions in these loci. Data from these experiments suggested that the insertions in tumors 95 and 111 were actually in the same locus and, furthermore, that six other tumors also contained proviruses in this region (Fig. 2 and 3 and data not shown). Hybridization of these blots with MMTV probes confirmed that the rearrangements of this locus in affected tumors were due to proviral integrations (Fig. 2 and 3 and data not shown). The apparent presence of two insertions in tumor 135 is discussed below.

Detection of expressed genes in the common insertion region. In a search for active genes in this locus, we made probes from the cloned cellular DNAs described above as well as from adjacent regions cloned subsequently for use in Northern blot analyses of tumor RNAs. Two genes were identified. A genomic clone that detected RNA from one of these genes was sequenced and found to be identical with the cDNA of androgen-induced growth factor (42), the eighth member of the FGF family. We will hereafter refer to this gene as *Fgf-8*. The second

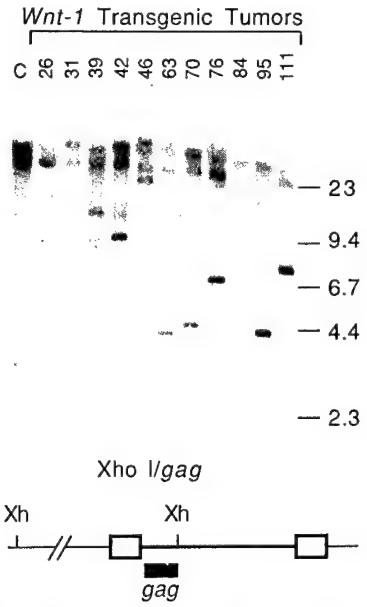

FIG. 1. MMTV proviruses in tumors of *Wnt-1* transgenic mice. Genomic DNAs were isolated from normal mammary gland (lane C) or from mammary tumors (designated by tumor number) of MMTV-infected *Wnt-1* transgenic mice. DNAs were digested with *Xho*I, separated by agarose gel electrophoresis, capillary blotted to nylon membranes, and hybridized with a ^{32}P-labeled MMTV *gag* probe. All DNAs have large *gag* fragments, indicative of endogenous retroviruses in these animals. Most of the tumor samples have an additional fragment(s), indicating the presence of clonal, tumor-specific MMTV proviruses. The positions of DNA size markers (in kilobases) are indicated at the right. A diagram showing the origin of the *gag* probe used and the 5′ proviral-cellular junction fragment it detects is shown below the gel. MMTV DNA is represented with bold lines. Open boxes, MMTV LTRs. Xh, *Xho*I.

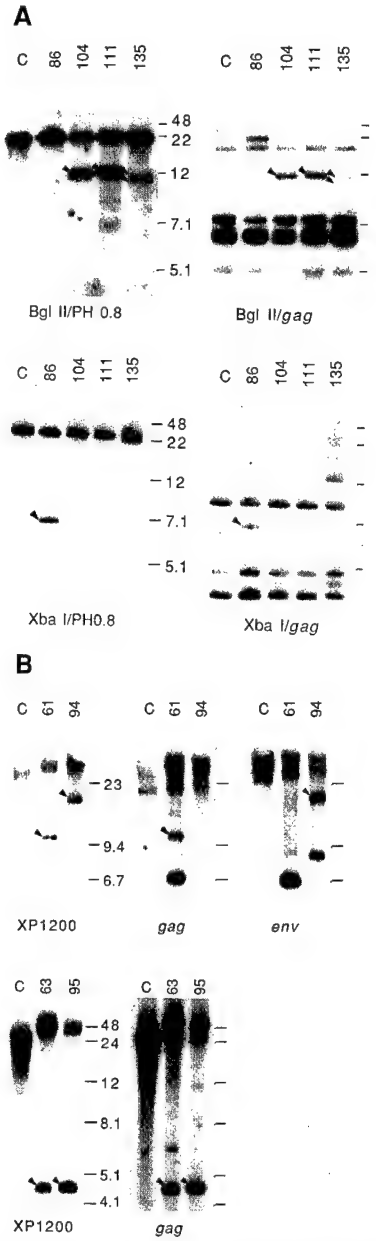

FIG. 2. MMTV proviral insertions into a new common integration locus. (A) Southern blots of DNAs from kidney as a control (lanes C) and from mammary tumors 86, 104, 111, and 135. Rearrangements of this locus in tumors were detected following digestion of the DNAs with either *Bgl*II or *Xba*I (which cut within MMTV) and hybridization of the resulting blots with the cellular probe PH 0.8 (see Fig. 3). Arrowheads identify fragments that anneal to both cellular (left panels) and MMTV *gag* (right panels) probes, demonstrating the location and orientation of the inserted provirus. (B) Southern blots of DNAs from normal mammary gland as a control (lanes C) and from mammary tumors 61, 63, 94, and 95. Rearrangements of this locus in tumors were detected following digestion of the DNAs with *Xho*I and hybridization of the resulting blots with the cellular probe XP1200 (see Fig. 3). The orientation of the MMTV provirus was determined as for panel A but with XP1200, *gag*, and *env* probes.

gene in this locus, which we have designated *Nub-1*, is novel. The deduced *Nub-1* product is unrelated to any oncoproteins, but it has sequence similarities to two nucleolar chaparone proteins, nucleoplasmin and B23/nucleophosmin (6, 16). A description of *Nub-1*, beyond the RNA data below, will be presented elsewhere.

When small amounts of total cellular RNAs available from tumors were examined by Northern blotting for expression of these genes, we found evidence for transcriptional activation of *Fgf-8* in all tumors with insertions in this locus except tumor 104; *Fgf-8* RNA was undetectable in tumors without insertions and in normal mammary gland (Fig. 4 and data not shown). RT-PCR experiments confirmed the presence of *Fgf-8* RNA in tumor 104 and its absence in normal mammary gland (data not shown). In contrast, the RNA levels of the constitutively active *Nub-1* gene do not appear to be significantly affected by the surrounding MMTV insertions (Fig. 4). Thus, the activated expression of *Fgf-8* in multiple tumors by clonal proviral insertions suggests that this gene is causally related to tumor formation.

***Fgf-8* exon structure and alternative splicing.** To determine the physical relationship of the proviral insertions to the *Fgf-8* gene, we established its exon structure by sequencing portions of our genomic clones and comparing these with the *Fgf-8* cDNA sequences reported earlier (42). This revealed that *Fgf-8*, as represented by these cDNAs, is approximately 6.5 kb in length and has at least five coding exons (Fig. 5A), unlike other analyzed FGF genes, which have only three coding exons (1, 14, 19, 24, 28, 49, 50). All of the insertions detected were mapped upstream of *Fgf-8*, and all, except those in tumors 61 and 86, were in the opposite transcriptional orientation to *Fgf-8* (Fig. 3 and 5A and data not shown). Two of the insertions (tumors 63 and 95) disrupted the *Nub-1* gene, which is located approximately 5 kb upstream of *Fgf-8* in the same orientation, and two insertions (tumors 61 and 94) were upstream of both genes (Fig. 3 and data not shown).

The comparison of *Fgf-8* genomic and cDNA sequences also

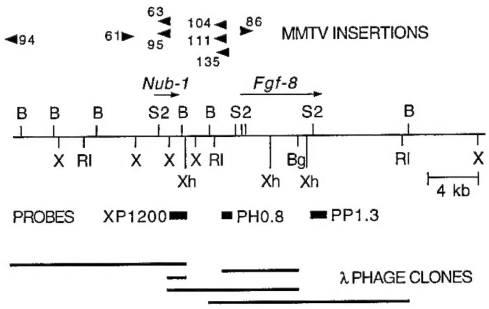

FIG. 3. Map of proviral insertions in the new common integration locus. This locus was mapped with restriction digests of lambda phage clones and plasmid subclones containing inserts from this locus, and by Southern blotting of genomic DNAs with probes from the locus. The lambda phage clones are indicated at the bottom of the figure. MMTV proviral insertions were mapped by Southern blotting with probes from this locus (XP1200, PH 0.8, and PP 1.3) and from MMTV, as described in the legend to Fig. 2. In some cases, the MMTV proviral insertion site was sequenced following amplification by PCR. Arrowheads denote the locations and transcriptional orientations of the MMTV proviruses. B, *Bam*HI; Bg, *Bgl*II; RI, *Eco*RI; S2, *Sst*II; X, *Xba*I; Xh, *Xho*I.

showed the existence of at least two 5′ splice sites in exon 2 and two 3′ splice sites in exon 3. Alternative splicing between these sites could potentially produce RNAs encoding four isoforms of the protein (Fig. 5A to C). In exon trap experiments with an *Sst*II genomic fragment containing most of *Fgf-8* (see Materials and Methods) and in nested RT-PCR experiments with RNA from adult murine testis and from tumor 61, we amplified and cloned cDNAs of alternatively spliced mRNAs encoding three different isoforms: FGF-8a, FGF-8b, and FGF-8c (Fig. 5A to C). We did not obtain a cDNA containing both exons 2B and 3B, which would encode the fourth potential isoform (data not shown). All three cloned versions have the same predicted signal peptide sequence and code for the same protein downstream of the alternative splice, but differ in the amino-terminal regions of the putative secreted products (Fig. 5C).

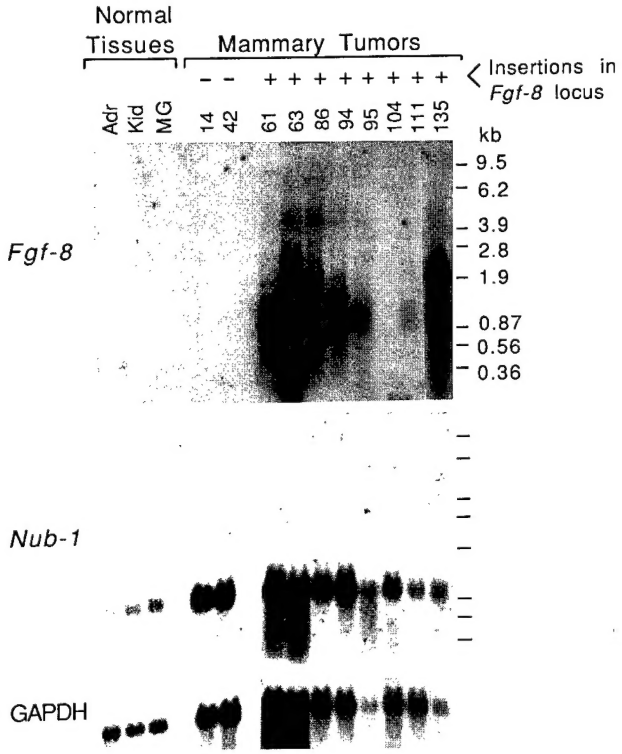

FIG. 4. Transcriptional activation of *Fgf-8* by MMTV insertion in tumors from infected *Wnt-1* transgenic mice. Northern blot of total cellular RNA (5 μg) from three normal tissues (adrenal gland, kidney, and mammary gland), two tumors without MMTV proviruses near *Fgf-8* (tumors 14 and 42), and eight tumors with MMTV insertions near *Fgf-8*. The blot was initially probed with a full-length *Fgf-8b* cDNA (upper panel), then with a *Nub-1* cDNA (middle panel), and finally with a glyceraldehyde-3-phosphate dehydrogenase (GAPDH) cDNA (lower panel). The locations of RNA size markers are shown at right.

Expression of *Fgf-8* in murine tissues. We performed Northern blots of poly(A)$^+$ RNA from normal murine tissues to determine the normal expression patterns of *Fgf-8* (Fig. 6). Weak expression was detected in ovary and testis, but we did not detect *Fgf-8* RNA in normal mammary gland or in any of 10 other tissues (Fig. 6). These data suggest that MMTV insertions in tumors activate this gene from a transcriptionally silent state.

Since FGFs are frequently expressed during embryogenesis (5), we looked for expression of *Fgf-8* during murine development by Northern blot analysis of total cellular RNA from whole embryos staged by gestational age. We found high expression of *Fgf-8* at 10.5 days postconception, the earliest time tested, which decreased to nearly undetectable levels by 14.5 days (Fig. 6). We did not observe *Fgf-8* expression at 16.5 or 17.5 days postconception (data not shown).

DISCUSSION

We previously showed that infection of *Wnt-1* transgenic mice with MMTV accelerates mammary tumorigenesis by insertionally activating *Fgf-3* and/or *Fgf-4*, indicating that these two members of the FGF family can cooperate with *Wnt-1* in murine mammary tumorigenesis (37). By cloning and analyzing proviral insertion sites from several tumors that lack these activations, we show here that 8 of 80 tumors with clonal, tumor-specific MMTV proviruses had MMTV insertions in a genomic region that contains *Fgf-8* (Fig. 2 and 3). Elevated levels of *Fgf-8* RNA were detected in affected tumors but not in other tumors or in normal mammary gland (Fig. 4). Analysis of the normal gene and its expression showed that *Fgf-8* contains at least five coding exons and can encode at least three different protein isoforms by alternative splicing and that RNA was present in the testes and ovaries of adults and in midgestational embryos. Together, these findings suggest that the overexpression of *Fgf-8* which accompanies MMTV insertion into this locus contributes to the formation of these tumors.

Proviral insertions. Studies of MMTV insertion sites in mammary tumors indicate that MMTV can transcriptionally activate an adjacent proto-oncogene from upstream or downstream locations in either transcriptional orientation relative to the gene, although the vast majority are classical "enhancer insertions," in which the 5′ long terminal repeat (LTR) of the provirus is situated closest to the activated gene (12, 30, 33). All of the insertions described here are located upstream of *Fgf-8*; two of these (in tumors 61 and 86) were in the same orientation as *Fgf-8* (and *Nub-1*). The location of the provirus in tumor 61 might predict a large fusion transcript with *Nub-1*, starting from an MMTV LTR, but no aberrant *Nub-1* (or *Fgf-8*) RNAs were observed in this tumor. Thus, it appears that the *Fgf-8* gene is activated by an enhancer insertion mechanism in tumor 61, despite the "promoter insertion" orientation of the provirus. The identities of the additional sequences in the *Fgf-8* transcripts larger than 1.9 kb observed in several tumors (e.g., tumors 63, 86, and 135 in Fig. 4) are unknown.

Tumors 61 and 94 are unusual in that a second gene, *Nub-1*,

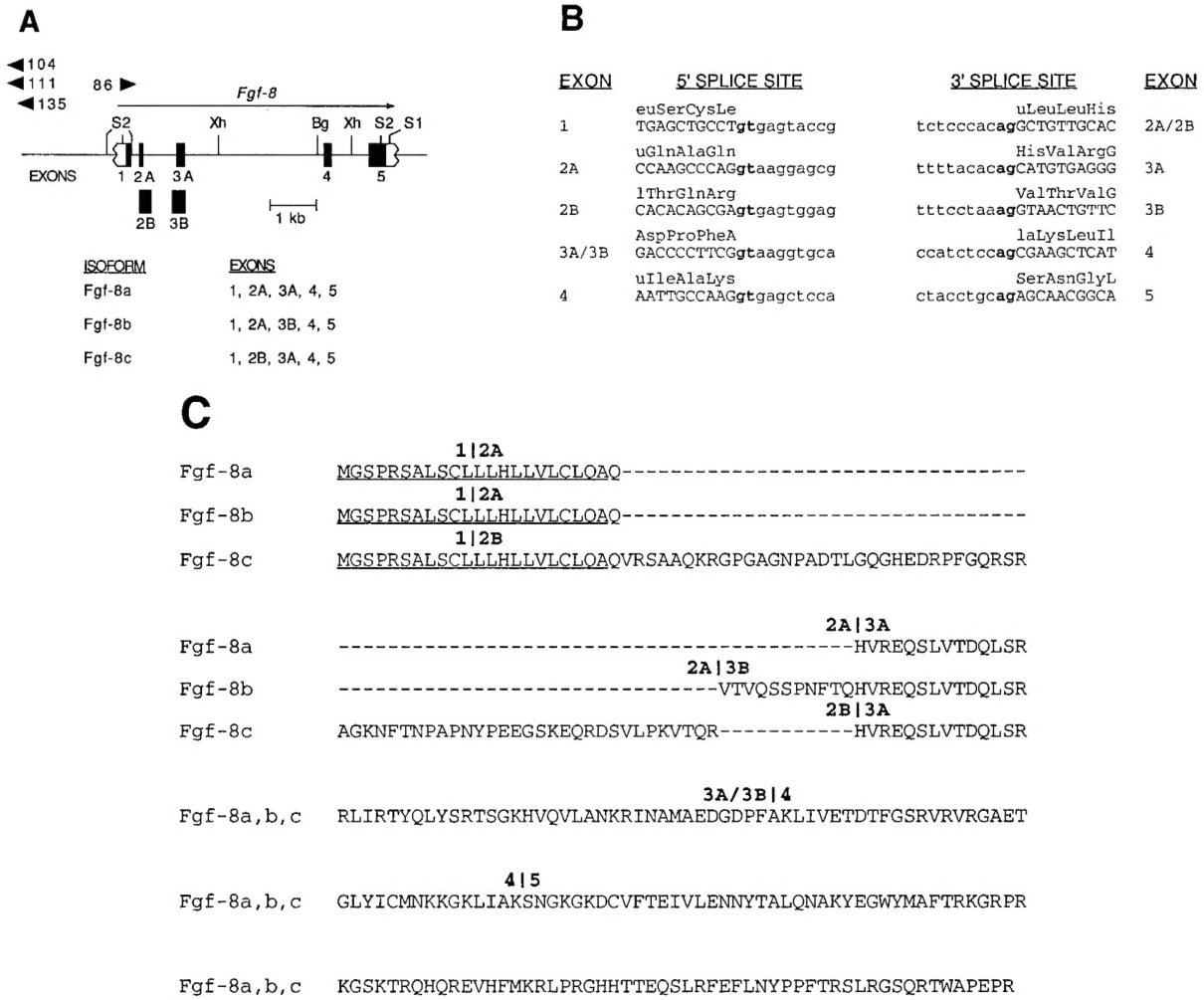

FIG. 5. *Fgf-8* gene structure and protein sequences. (A) *Fgf-8* gene structure. The five exons of *Fgf-8* are depicted as boxes, with filled areas indicating the coding domains. Exons 2A and 2B differ in their 3′ termini, and exons 3A and 3B have different 5′ termini. Note that there are at least four potential alternatively spliced forms of *Fgf-8* mRNA (containing exons 2A and 3A, exons 2A and 3B, exons 2B and 3A, or exons 2B and 3B), all of which would maintain the same reading frame. The exon contents of cDNAs encoding three FGF-8 protein isoforms are indicated below the gene structure. *Fgf-8* sequences outside the jagged boundaries of exons 1 and 5 have not been determined. (B) Sequences of *Fgf-8* exon-intron junctions. Exon sequences are indicated by uppercase letters, and intron sequences are shown in lowercase letters. Highly conserved nucleotides at the ends of introns are in boldface. Three-letter amino acid abbreviations are given above each codon. (C) Amino acid sequences of three FGF-8 isoforms. The predicted signal peptide sequence (46) is underlined. Exon splice sites are indicated by vertical bars. Note that the three isoforms differ only at the amino termini of the secreted forms.

is found between the proviral insertions and the activated *Fgf-8* gene. The basal activity of *Nub-1* does not seem to be significantly affected by the insertions, while *Fgf-8* is activated from an apparently quiescent state. Although proviral enhancers are known to activate genes from significant distances, to our knowledge, MMTV activation of the distal, but not the proximal, gene of a linked pair has not previously been observed. The apparent selective mechanism involved is unclear but may be explained in part by the relatively high basal level of *Nub-1* expression, by possible toxicity of higher levels of Nub-1 protein, or by a discriminating compatibility of MMTV enhancers with the *Fgf-8* promoter.

Tumor 135 appears to contain two separate MMTV proviral insertions at similar locations in this locus, but not both insertions on a single chromosome (Fig. 2B). It seems unlikely that a selective advantage for tumor cell growth would result from both copies of the gene being activated by proviral insertion, since, for example, we have never seen insertional activation of the endogenous *Wnt-1* gene in MMTV-infected *Wnt-1* trans-

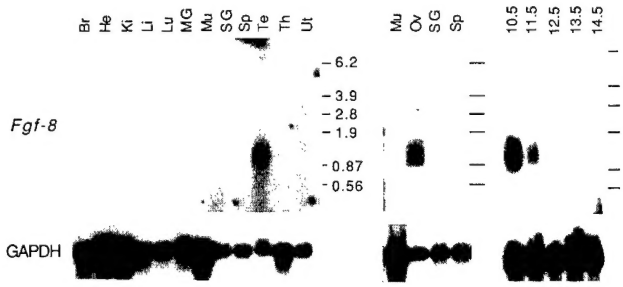

FIG. 6. *Fgf-8* is normally expressed during embryogenesis and in adult ovaries and testes. Northern blots were made of normal adult tissue poly(A)$^+$ RNAs (Br, brain; He, heart; Ki, kidney; Li, liver; Lu, lung; MG, mammary gland; Mu, muscle; Ov, ovaries; SG, salivary gland; Sp, spleen; Te, testis; Th, thymus; Ut, uterus) and murine embryonic total cellular RNAs (embryo lanes labeled in days postconception). The *Fgf-8* and glyceraldehyde-3-phosphate dehydrogenase (GAPDH) probes are the same as in Fig. 4. The positions of RNA size markers (in kilobases) are shown at the right of each blot.

genic mice (37). Although a requirement for a threshold level of *Fgf-8* expression might explain the two insertions, alternative interpretations are that tumor 135 is oligoclonal, with tumor cells possessing one or the other insertion, or that a single insertion exists with a rearranged form present in some tumor cells. In addition, tumor 135 has an insertion in the *Fgf-3/Fgf-4* locus (37). This finding reintroduces the notion of possible cooperation among FGF family members (37), but oligoclonality could also explain the data.

Gene activation by MMTV insertions. Almost all tumors with insertions in this locus displayed readily discernable activation of *Fgf-8* with small amounts of total RNA by Northern analysis. Only tumor 104 required RT-PCR for detection. The cause for the wide variation in MMTV-activated *Fgf-8* gene expression is unknown, but such variation is common for genes activated by MMTV insertions (15, 31, 34, 37). Because of the lack of obvious changes in *Nub-1* RNA levels in affected tumors and the interruption of its coding domain in two tumors, alterations in *Nub-1* expression by proviral insertions do not appear to contribute to tumorigenesis. The relationship of *Nub-1* to the nucleolar proteins nucleoplasmin and B23/nucleophosmin, two abundant and well-studied molecular chaperones with no known oncogenic potential (6, 16), also does not immediately point to a role for *Nub-1* in tumorigenesis. Although the recently described fusion of nucleophosmin to the cytoplasmic tyrosine kinase domain of a transmembrane receptor in chromosomal translocations in some lymphomas is intriguing in this regard, nucleophosmin's proposed role is to provide an active promoter for the kinase (7, 29). Together with the activated expression of *Fgf-8* shown here and the reported transforming potential of *Fgf-8b* cDNA in NIH 3T3 cells (25, 26a), it is likely that *Fgf-8*, and not *Nub-1*, is the gene pertinent to oncogenesis in this locus.

Alternative splicing and gene expression. The transcribed portion of the *Fgf-8* gene is divided into at least five coding exons (Fig. 5A), two more than are found in the other FGF genes examined (1, 14, 19, 24, 28, 49, 50). The first three exons of *Fgf-8* described here correspond to the first exon of other FGF genes. *Fgf-8* is also unusual in that it can be alternatively spliced between exons 2 and 3 to yield at least three protein isoforms which differ only in the amino-terminal portion of the secreted mature protein. We isolated the two previously described cDNAs (42), which code for the isoforms FGF-8b and FGF-8c, and a third cDNA that encodes the previously undescribed isoform FGF-8a (Fig. 5A to C). All three mRNA species were detected in both testis and tumor 61. We have not detected a fourth possible splice variant which would contain exons 2B and 3B in either testis or mammary tumor RNA (data not shown). These cDNA clones will allow a comparison of the three isoforms for possible differences in, for example, their transforming potentials, tissue expression patterns, half-lives, or affinities for the various FGF receptors.

We found expression of *Fgf-8* in adult testis and ovary (Fig. 6), but this expression is much lower than in the tumors with MMTV insertions near *Fgf-8* (Fig. 4). The expression of *Fgf-8* during murine embryogenesis (Fig. 6) suggests that this gene may be important in embryonic development. Recent studies using in situ analysis of whole-mount embryos and embryo sections confirm the expression of *Fgf-8* during murine embryogenesis (22). Definitive proof that *Fgf-8* expression is important in murine development will require the creation and analysis of mice lacking a functional *Fgf-8* gene.

The MMTV LTR contains androgen-responsive enhancer elements which can place nearby promoters under androgen regulation (8, 13, 32). In light of our finding that *Fgf-8* is active only in mammary tumors with MMTV proviruses in this locus, and given that androgen induction of *Fgf-8* has only been demonstrated in cells from a mouse mammary tumor (Shionogi carcinoma 115) and a derivative cell line (SC-3) (42), it seems possible that the androgen-inducible nature of *Fgf-8* in these cells might be attributed to MMTV insertional activation of *Fgf-8* rather than to any inherent feature of the gene. Consistent with this idea is the finding that glucocorticoids—well known for their stimulatory effects on transcription from the MMTV LTR—can also induce *Fgf-8* activity in these cells (47).

***Wnt-1* and *Fgf-8* cooperation.** *Fgf-8* is the third member of the FGF family to be identified as a *Wnt-1* collaborator in mammary carcinogenesis. Surprisingly, only FGF genes have been found to be activated by MMTV in this transgenic model system (37). Assuming that many proto-oncogenes are potential targets for activating insertion mutations, this selectively suggests that FGFs cooperate oncogenically with *Wnt-1* in an especially potent manner. It is possible that the signaling pathways of these two families function in a highly complementary fashion to deregulate mammary epithelial cell growth and proliferation. Alternatively, activated FGFs could contribute to neoplasia in a less direct manner, for example, by stimulating angiogenesis (17, 23). However, it is notable that genes of the *Wnt* and FGF families can evidently collaborate in an experimental model of mesoderm induction (10), suggesting that cooperation in tumorigenesis may derive from the normal interactions of these genes.

The detection of a third activated FGF gene in these tumors prompted us to survey all other known FGF loci for insertions by Southern blot analysis, but no rearrangements in other FGF genes have been found thus far (40). Given the propensity of this model system to activate FGF genes, we speculate that analyses of other common insertion loci in the remaining tumors from this collection may reveal new members of this gene family or identify important downstream components in the FGF signal transduction pathway.

ACKNOWLEDGMENTS

C.A.M. and D.B.S. contributed equally to this work; the order of these authors is arbitrary.

We thank H. Varmus for discussions and the generous gift of tumor samples; O. de Lapeyriere, J. Hébert, G. Martin, W. McKeehan, and D. Ornitz for providing FGF DNA probes; M. Reth for providing the exon trap vector; J. Wang for technical assistance; and E. Bogenmann and A. Erdreich-Epstein for critical reading of the manuscript.

This work was supported by grants from the University of Southern California Zumberge Research and Innovation Fund and the National Institutes of Health (CA58412) to G.M.S. C.A.M. is a recipient of a Howard Hughes Medical Institute Postdoctoral Fellowship for Physicians. D.B.S. is supported by a predoctoral fellowship (DAMD 17-94-J-4319) from the Department of the Army. G.M.S. is a recipient of a Junior Faculty Research Award from the American Cancer Society.

REFERENCES

1. **Abraham, J. A., J. L. Whang, A. Tumolo, A. Mergia, and J. Friedman.** 1986. Human basic fibroblast growth factor: nucleotide sequence and genomic organization. EMBO J. **5:**2523–2528.
2. **Auch, D., and M. Reth.** 1990. Exon trap cloning: using PCR to rapidly detect and clone exons from genomic DNA fragments. Nucleic Acids Res. **18:**6743–6744.
3. **Auffray, C., and F. Rougeon.** 1980. Purification of mouse immunoglobulin heavy-chain messenger RNAs from total myeloma tumor RNA. Eur. J. Biochem. **107:**303–314.
4. **Aviv, H., and P. Leder.** 1973. Purification of biologically active globin messenger RNA by chromotography on oligothymidylic acid-cellulose. Proc. Natl. Acad. Sci. USA **69:**1408–1412.
5. **Basilico, C., and D. Moscatelli.** 1992. The FGF family of growth factors and oncogenes. Adv. Cancer Res. **59:**115–165.
6. **Borer, R. A., C. F. Lehner, H. M. Eppenberger, and E. A. Nigg.** 1989. Major nucleolar proteins shuttle between nucleus and cytoplasm. Cell **56:**379–390.
7. **Bullrich, F., S. W. Morris, M. Hummel, S. Pileri, H. Stein, and C. M. Croce.**

1994. Nucleophosmin (*NPM*) gene rearrangements in Ki-1-positive lymphomas. Cancer Res. **54:**2873–2877.

8. **Cato, A., D. Henderson, and H. Ponta.** 1987. The hormone response element of the mouse mammary tumour virus DNA mediates the progestin and androgen induction of transcription in the proviral long terminal repeat region. EMBO J. **6:**363–368.
9. **Chomczynski, P., and N. Sacchi.** 1987. Single-step method of RNA isolation by acid guanidinium thiocyanate-phenol-chloroform extraction. Anal. Biochem. **162:**156–159.
10. **Christian, J. L., D. J. Olsen, and R. T. Moon.** 1992. XWnt-8 modifies the character of mesoderm induced by bFGF in isolated *Xenopus* ectoderm. EMBO J. **11:**33–41.
11. **Church, G. M., and W. Gilbert.** 1984. Genomic sequencing. Proc. Natl. Acad. Sci. USA **81:**1991–1995.
12. **Clausse, N., D. Baines, R. Moore, S. Brookes, C. Dickson, and G. Peters.** 1993. Activation of both *Wnt-1* and *Fgf-3* by insertion of mouse mammary tumor virus downstream in the reverse orientation: a reappraisal of the enhancer insertion model. Virology **194:**157–165.
13. **Darbre, P., M. Page, and R. King.** 1986. Androgen regulation by the long terminal repeat of mouse mammary tumor virus. Mol. Cell. Biol. **6:**2847–2854.
14. **de Lapeyriere, O., O. Rosnet, D. Benharroch, F. Raybaud, S. Marchetto, J. Planche, F. Galland, M.-G. Mattei, N. G. Copeland, N. A. Jenkins, F. Coulier, and D. Birnbaum.** 1990. Structure, chromosome mapping and expression of the murine *Fgf-6* gene. Oncogene **5:**823–831.
15. **Dickson, C., R. Smith, S. Brookes, and G. Peters.** 1984. Tumorigenesis by mouse mammary tumor virus: proviral activation of a cellular gene in the common integration region *int-2*. Cell **37:**529–536.
16. **Dingwall, C., and R. A. Laskey.** 1990. Nucleoplasmin: the archetypal molecular chaperone. Semin. Cell Biol. **1:**11–17.
17. **Folkman, J., K. Watson, D. Ingber, and D. Hanahan.** 1989. Induction of angiogenesis during the transition from hyperplasia to neoplasia. Nature (London) **339:**58–61.
18. **Fort, P., L. Marty, M. Piechaczyk, S. El Sabrouty, C. Dani, P. Jeanteur, and J. M. Blanchard.** 1985. Various rat adult tissues express only one major mRNA species from the glyceraldehyde-3-phosphate-dehydrogenase multigenic family. Nucleic Acids Res. **13:**1431–1442.
19. **Gospodarowicz, D., G. Neufeld, and L. Schweigerer.** 1987. Fibroblast growth factor: structural and biological properties. J. Cell. Physiol. Suppl. **5:**15–26.
20. **Haupt, Y., W. S. Alexander, G. Barri, L. P. Klinken, and J. M. Adams.** 1991. Novel zinc finger gene implicated as *myc* collaborator by retrovirally accelerated lymphomagenesis in Eμ-*myc* transgenic mice. Cell **65:**753–763.
21. **Hébert, J. M., C. Basilico, M. Goldfarb, O. Haub, and G. Martin.** 1990. Isolation of cDNAs encoding four mouse FGF family members and characterization of their expression patterns during embryogenesis. Dev. Biol. **138:**454–463.
22. **Heikinheimo, M., A. Lawshé, G. M. Shackleford, D. B. Wilson, and C. A. MacArthur.** 1994. *Fgf-8* expression in the post-gastrulation mouse is localized to the developing face, limbs and central nervous system. Mech. Dev. **48:**129–138.
23. **Kandel, J., E. Bossy-Wetzel, F. Radvanyi, M. Klagsbrun, J. Folkman, and D. Hanahan.** 1991. Neovascularization is associated with a switch to the export of bFGF in the multistep development of fibrosarcoma. Cell **66:**1095–1104.
24. **Kelley, M. J., M. Pech, H. N. Seuanez, J. S. Rubin, S. J. OBrien, and S. A. Aaronson.** 1992. Emergence of the keratinocyte growth factor multigene family during the great ape radiation. Proc. Natl. Acad. Sci. USA **89:**9287–9291.
25. **Kouhara, H., M. Koga, S. Kasayama, A. Tanaka, T. Kishimoto, and B. Sato.** 1994. Transforming activity of a newly cloned androgen-induced growth factor. Oncogene **9:**455–462.
26. **Kwan, H. C., V. Pecenka, A. S. Tsukamoto, T. G. Parslow, R. Guzman, T. P. Lin, W. J. Muller, F. S. Lee, P. Leder, and H. E. Varmus.** 1992. Transgenes expressing the *Wnt-1* and *int-2* proto-oncogenes cooperate during mammary carcinogenesis in doubly transgenic mice. Mol. Cell. Biol. **12:**147–154.

26a. **MacArthur, C. A., A. Lawshé, D. B. Shankar, M. Heikinheimo, and G. M. Shackleford.** FGF-8 isoforms cause differential transformation of NIH 3T3 cells. Submitted for publication.

27. **Marchuk, D., M. Drumm, A. Saulino, and F. S. Collins.** 1991. Construction of T-vectors, a rapid and general system for direct cloning of unmodified PCR products. Nucleic Acids Res. **19:**1154.
28. **Moore, R., G. Casey, S. Brookes, M. Dixon, G. Peters, and C. Dickson.** 1986. Sequence, topography and protein coding potential of mouse *int-2*: a putative oncogene activated by mouse mammary tumour virus. EMBO J. **5:**919–924.
29. **Morris, S. W., M. N. Kirstein, M. B. Valentine, K. G. Dittmer, D. N. Shapiro, D. L. Saltman, and A. T. Look.** 1994. Fusion of a kinase gene, *ALK*, to a nucleolar protein gene, *NPM*, in non-Hodgkin's lymphoma. Science **263:**1281–1284.
30. **Nusse, R.** 1991. Insertional mutagenesis in mouse mammary tumorigenesis, p. 43–65. *In* H. J. Kung and P. K. Vogt (ed.), Retroviral insertion and oncogene activation. Springer-Verlag, New York.
31. **Nusse, R., A. van Ooyen, D. Cox, Y. K. T. Fung, and H. E. Varmus.** 1984. Mode of proviral activation of a putative mammary oncogene (*int-1*) on mouse chromosome 15. Nature (London) **307:**131–136.
32. **Parker, M. G., P. Webb, M. Needham, R. White, and J. Ham.** 1987. Identification of androgen response elements in mouse mammary tumour virus and the rat prostate C3 gene. J. Cell. Biol. **35:**285–292.
33. **Peters, G.** 1990. Oncogenes at viral integration sites. Cell Growth Differ. **1:**503–510.
34. **Peters, G., S. Brookes, R. Smith, M. Placzek, and C. Dickson.** 1989. The mouse homolog of the *hst/k-FGF* gene is adjacent to *int-2* and is activated by proviral insertion in some virally induced mammary tumors. Proc. Natl. Acad. Sci. USA **86:**5678–5682.
35. **Peters, G., A. E. Lee, and C. Dickson.** 1986. Concerted activation of two potential proto-oncogenes in carcinomas induced by mouse mammary tumour virus. Nature (London) **320:**628–631.
36. **Sambrook, J., E. F. Fritsch, and T. Maniatis.** 1989. Molecular cloning: a laboratory manual, 2nd ed. Cold Spring Harbor Laboratory Press, Cold Spring Harbor, N.Y.
37. **Shackleford, G. M., C. A. MacArthur, H. C. Kwan, and H. E. Varmus.** 1993. Mouse mammary tumor virus infection accelerates mammary carcinogenesis in *Wnt-1* transgenic mice by insertional activation of *int-2/Fgf-3* and *hst/Fgf-4*. Proc. Natl. Acad. Sci. USA **90:**740–744.
38. **Shackleford, G. M., and H. E. Varmus.** 1987. Expression of the proto-oncogene *int*-1 is restricted to postmeiotic male germ cells and the neural tube of mid-gestational embryos. Cell **50:**89–95.
39. **Shackleford, G. M., and H. E. Varmus.** 1988. Construction of a clonable, infectious, and tumorigenic mouse mammary tumor virus provirus and a derivative genetic vector. Proc. Natl. Acad. Sci. USA **85:**9655–9659.
40. **Shankar, D. B., and G. M. Shackleford.** Unpublished results.
41. **Steinmetz, M., J. Hocht, H. Schnell, W. Gebhard, and H. Zachau.** 1980. Cloning of V region fragments from mouse liver DNA and localization of repetitive DNA sequences in the vicinity of immunoglobulin gene segments. Nucleic Acids Res. **8:**1721–1729.
42. **Tanaka, A., K. Miyamoto, N. Minamino, M. Takeda, B. Sato, H. Matsuo, and K. Matsumoto.** 1992. Cloning and characterization of an androgen-induced growth factor essential for the androgen-dependent growth of mouse mammary carcinoma cells. Proc. Natl. Acad. Sci. USA **89:**8928–8932.
43. **Thomas, S. M., R. F. Moreno, and L. L. Tilzer.** 1989. DNA extraction with organic solvents in gel barrier tubes. Nucleic Acids Res. **17:**5411.
44. **Tsukamoto, A. S., R. Grosschedl, R. C. Guman, T. Parslow, and H. E. Varmus.** 1988. Expression of the *int-1* gene in transgenic mice is associated with mammary gland hyperplasia and adenocarcinomas in male and female mice. Cell **55:**619–625.
45. **van Lohuizen, M., S. Verbeek, B. Scheijen, E. Wientjens, H. van der Gulden, and A. Berns.** 1991. Identification of cooperating oncogenes in Eμ-*myc* transgenic mice by provirus tagging. Cell **65:**737–752.
46. **von Heijne, G.** 1986. A new method for predicting signal sequence cleavage sites. Nucleic Acids Res. **14:**4683–4690.
47. **Yamanishi, H., N. Nonomura, A. Tanaka, Y. Nishizawa, N. Terada, K. Matsumoto, and B. Sato.** 1991. Proliferation of Shionogi carcinoma 115 cells by glucocorticoid-induced autocrine heparin-binding growth factor(s) in serum-free medium. Cancer Res. **51:**3006–3010.
48. **Yan, G., S. Nikolanopoulos, F. Wang, and W. L. McKeehan.** 1991. Sequence of rat keratinocyte growth factor (heparin-binding growth factor type 7). In Vitro Cell. Dev. Biol. **27A:**437–438.
49. **Yoshida, T., K. Miyagawa, H. Odagiri, H. Sakamoto, P. F. Little, M. Terada, and T. Sugimura.** 1988. Genomic sequence of *hst*, a transforming gene encoding a protein homologous to fibroblast growth factors and the *int-2*-encoded protein. Proc. Natl. Acad. Sci. USA **84:**7305–7309.
50. **Zhan, X., B. Bates, X. G. Hu, and M. Goldfarb.** 1988. The human *FGF-5* oncogene encodes a novel protein related to fibroblast growth factors. Mol. Cell. Biol. **8:**3487–3495.